2018

RATIONAL DESIGN OF PEPTIDES BINDING TOWARDS HUMAN PD-L1 USING KNOB-SOCKET MODEL

Xingchen Zha
University of the Pacific, x_zha1@u.pacific.edu

RATIONAL DESIGN OF PEPTIDES BINDING TOWARDS HUMAN PD-L1 USING KNOB-SOCKET MODEL

by

Xingchen Zha

A Thesis Submitted to the

Graduate School

In Partial Fulfillment of the

Requirements for the Degree of

MASTER OF SCIENCE

Thomas J. Long School of Pharmacy and Health Sciences
Pharmaceutical and Chemical Sciences

University of the Pacific
Stockton, CA

2018

RATIONAL DESIGN OF PEPTIDES BINDING TOWARDS HUMAN PD-L1 USING KNOB-SOCKET MODEL

by

Xingchen Zha

APPROVED BY:

Thesis Advisor: Bhaskara R. Jasti, Ph.D.

Thesis Co-Advisor: Xiaoling Li, Ph.D.

Committee Member: Jerry Tsai, Ph.D.

Department Chair: William K. Chan, Ph.D.

Dean of Graduate School: Thomas H Naehr, Ph.D.

RATIONAL DESIGN OF PEPTIDES BINDING TOWARDS HUMAN PD-L1 USING KNOB-SOCKET MODEL

by

Xingchen Zha

DEDICATION

This thesis is dedicated to my family, teachers, and friends.

ACKNOWLEDGMENTS

I would like to thank my advisor Dr. Bhaskara Jasti for offering me the opportunity to work with him and guiding me through my research with his expertise, patience, and kindness. I greatly appreciate Dr. Xiaoling Li for his valuable guidance, help, and suggestions on my research and for serving on my committee as well. I would like to thank Dr. Jerry Tsai for his great help in designing peptides for the study and for serving on my committee. I greatly appreciate Dr. Liang Xue and Dr. Lisa Wrischnik for all their help, guidance and for letting me work in their laboratory. I also thank Dr. Hyun Joo and Jerome for patiently guiding me through the Knob-Socket model. I am grateful to Ms. Kathy Kassab and Ms. Lynda Davis for all their support throughout my graduate studies.

I would like to thank Jerome, Zahir, Poonam, Jingda, Lavanya, Ryan, Chao, Bob, Shen, Hank and Yan for their support and friendship. Finally, I would like to thank my parents for their love, support, and encouragement that make all this possible.

Rational Design of Peptides Binding towards Human PD-L1 Using Knob-Socket Model

Abstract

by Xingchen Zha

University of the Pacific
2018

Programmed death-ligand 1 (PD-L1) is a type 1 transmembrane protein that has been reported to play a vital role in mediating suppressed immunity. The interaction between PD-L1 and PD-1 delivers a negative signal that reduces the proliferation of these T cells and induces apoptosis at the same time. Antibodies that can block the Programmed death-ligand 1 (PD-L1) on tumor cells have been shown to alleviate cancer-induced immunosuppression. While antibodies have a great potential in various therapeutic uses, many drawbacks such as the high cost of production, huge molecular size, and poor permeability impose restrictions on the extensive use of full-length antibodies. These limitations have necessitated research for finding alternatives to antibodies, such as peptides, that have lower molecular weight and similar properties as antibodies but do not have the lengthy and complicated approach of producing antibodies.

In this study, a novel approach based on molecular interactions of the PD1-PD-L1 complex was developed to design peptides against PD-L1 using Knob-Socket model as basis. Three generations of peptides, α-helix, over-packed and salt bridge function peptides, were designed. All designed peptides were docked in the Molecular Operating Environment (MOE) and the AutoDock Vina software for the docking energy and the detail interaction information. Synthesis and characterization of selected peptides were performed after simulation studies. Surface Plasmon Resonance (SPR) studies showed that α-helix and over-packed peptides can't bind to the PD-L1 protein with no response on sensorgrams, while peptides with salt bridge function had a higher binding response than those two generations of peptides. In confocal microscopic studies, PD-L1 positive breast cancer cell line MDA-MB-231 was used to determine the binding specificity of the salt bridge function peptides to PD-L1 in vitro, while another breast cancer cell line (MCF-7, without PD-L1) was used as a control. After incubation with peptides, significant fluorescence intensities were detected on the MDA-MB-231 cells, while only background fluorescence was observed on MCF-7 cells.

In conclusion, this study demonstrated that peptides against PD-L1 designed using the Knob-Socket model and molecular interaction between PD-L1-PD1 complex showed feasibility to bind specifically with PD-L1 receptors.

TABLE OF CONTENTS

LIST OF TABLES

Table Page

LIST OF FIGURES

Figure Page

Chapter 1: Introduction

Cancer is a category of diseases caused by uncontrolled cell division and growth with the ability to invade and destroy other parts of the body [1,2]. There are many treatment options for cancer such as chemotherapy, radiation therapy, targeted therapy, and immunotherapy. Chemotherapy is the predominant treatment for cancer and usually comes with one or more cytotoxic anti-cancer drugs [3]. Ideally, these traditional antineoplastic drugs such as 5-fluorouracil and cyclophosphamide can kill rapidly dividing cancer cells but not the normal cells. However, the lack of tumor selectivity and low potency impose restrictions on those drugs in chemotherapy. To overcome the potency problem, more effort was put into the discovery of natural sources for efficient drugs such as auristatins. However, the selectivity of these drugs, which could lead to serious toxicity during the treatment, was still the significant problem for chemotherapy [4].

Targeted therapy is a more specific therapy compared to the conventional chemotherapy which has effects on both the fast-dividing cancer cells and normal cells. Currently, targeted therapies are widely performed for breast cancer, melanoma, lymphoma, and other types of cancer [2]. There are two types of targeted therapies, active targeted therapy and passive targeted therapy. Passive targeting therapy was employed in an approach to deliver drugs through capillaries which resulted in less

accumulation on normal cells but selective accumulation on cancer cells. The improvement selectivity was attributed to the increased permeation and retention function [5,6]. Correspondingly, the treatment of drugs used for their interaction specifically with molecular targets associated with cancers is called active targeted therapy. The specific interaction can be used in both the cancer growth and spreading stage.

1.1 Cancer immunotherapy

Cancer immunotherapy uses the immune system itself to treat cancer [7]. In the past few decades, immunotherapy has become a significant way of treating different types of cancer. Similar to targeted therapy, immunotherapies consist of active, passive, and hybrid therapy. The cancer cell surface has molecules called tumor-associated antigens, which can be determined by the immune system. Both active and passive immunotherapies can take advantage of those molecules in guiding the targeted response.

Antibody therapy is one of the most important immunotherapies [8]. The immune system produces specific antibodies after detecting antigens on the cell surface. Antibodies can utilize the cell surface receptors as targets for the treatment of a wide range of cancers. An appropriate antibody could not only prevent the interference from tumor cells but could also induce antibody-dependent cytotoxicity when it binds to a targeting cancer antigen. All these functions could induce cell apoptosis and limit the cancer development. There are many approved antibodies for immunotherapy on the market such as *Rituximab, Alemtuzumab, Nivolumab, and Ipilimumab*. Therefore, the

rational designing of a novel antibody for immunotherapy has a significant impact on cancer study.

1.2 Antibody

Many immunotherapeutic regimens involve antibodies. Antibodies are a key component of the adaptive immune response and play a central role in both recognizing foreign antigens and stimulating an immune response. Antibodies are Y-shaped proteins mostly produced by plasma cells and are composed of two regions: an antigen-binding fragment (Fab), which binds to antigens, and a Fragment crystallizable (Fc) region, which interacts with Fc receptors that are expressed on the surface of different immune cell types including macrophages, neutrophils, and natural killer (NK) cells.

1.2.1 Structure of an antibody. As can be seen in Figure1.1, antibodies consist of three parts that are combined by disulfide bonds. The two arms of the antibodies account for the variable region (V) that is responsible for the binding of the antigen. In the variable region, there are regions called complementarity-determining regions (CDRs) that determine the binding specificity of antibodies. The constant (C) region with less variability is the last part of the antibodies and can bind to other immune molecules in the immune system. Many physiological functions such as lysis of cells and recognition of immune particles need the involvement of the C region of an antibody [9-11].

Antibodies consist of heavy chains and light chains. Heavy chains have the following five isotypes: Immunoglobulin A (IgA), Immunoglobulin D (IgD), Immunoglobulin E (IgE), Immunoglobulin G (IgG), and Immunoglobulin M (IgM).

Immunoglobulin A (IgA) is an antibody that is distributed in mucous membranes and plays a critical role in the immune system. Mucosal membranes produce more of IgA than all the other types of antibodies [12]. More than three grams of IgA are generated in the intestinal lumen, which takes up to 15% of all immunoglobulins [13,14]. Immunoglobulin D (IgD), with molecular weight 185kDa, is an antibody that is found in the plasma membranes of B-lymphocytes and the blood serum. The half-life of IgD is 2.8 days [15]. Additionally, IgD can activate the antimicrobial function which results in an increased immune surveillance [16]. Immunoglobulin E (IgE) is a type of antibody that is secreted by plasma cells. IgE plays a vital role in protecting the immune system from parasites such as helminths [17] (for example, Fasciola hepatica) and Schistosoma mansoni [18-20]. It can also bind to the receptors on platelets and eosinophils resulting in the activation of the immune system [21]. Immunoglobulin M (IgM) is the largest antibody produced by vertebrates. It is the first antibody involved in the response to an antigen [22,23]. Immunoglobulin G (IgG) is also generated by plasma B-lymphocytes. IgG is a type of antibody with a molecular weight around 150kDa, making up approximately 75% of the serum antibodies in humans [24]. IgG is also the most common type of antibody in the human immune system [25]. IgG molecules with two antigen binding sites are synthesized and released by plasma B cells. IgG can protect the body from an infection by recognizing and binding pathogens such as viruses and bacteria. Antibody-dependent cell-mediated cytotoxicity (ADCC) will be performed after IgG binds to pathogens and makes them easy to be attacked [26].

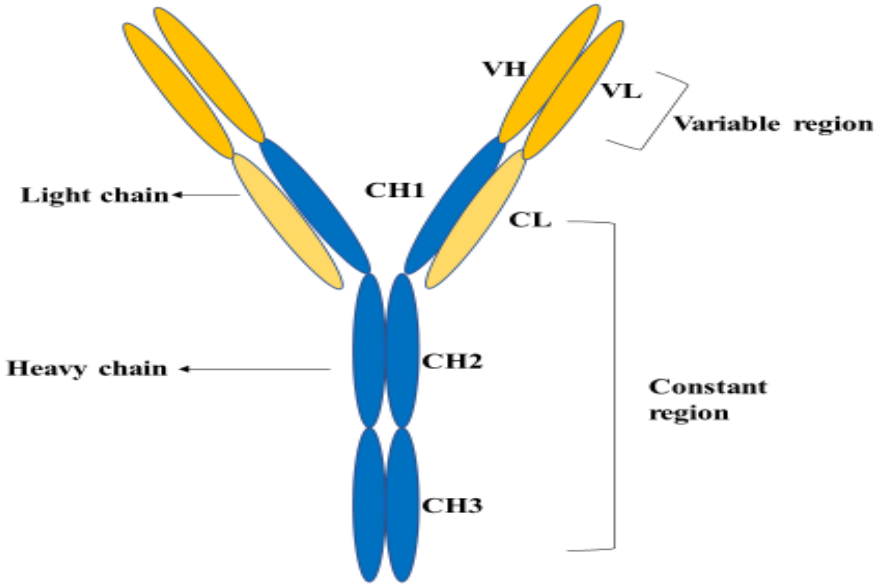

Figure 1.1 Structure of an Antibody

1.2.2 Binding between antibody and antigen. The antigen-antibody interaction mechanisms have been studied by various models for a long time [16, 27]. The body can be protected from harmful foreign molecules, such as pathogens, by the antigen-antibody interaction. Antibodies can bind to antigens with high specificity and affinity in the blood, and then, the antigen-antibody complex is transported for deactivation.

In 1952, Richard J. Goldberg from the University of Wisconsin developed the first correct definition of the antigen-antibody interaction [28,29]. It is also called the "Goldberg's theory" [30].

The flexibility of antibodies has been studied by scientists for a long time. Many different techniques such as fluorescence depolarization and X-ray crystallography have been used to determine the flexibility of the antibodies' conformation [24]. To bind with an antigen, the constant domain of an antibody can change dramatically in the X-ray crystallography studies [26,31,32].

Each antibody can bind to one or multiple specific antigens based on the conformational flexibility. Manivel V et al. proved this mechanism based on the thermodynamic analysis [33]. Additionally, James et al. also determined the conformational flexibility of an antibody based on their research through crystallographic studies and the results showed that an antibody can bind to different antigens [34].

For the antibody-antigen interaction, tyrosine and tryptophan are abundant on the binding interfaces while less charged residues such as glutamate, lysine except for arginine. Tyrosine, with a large hydrophobic surface, could form hydrogen bonds with

antigen for its hydroxyl group. Arginine can build hydrogen bonds and salt bridges based on its guanidinium part and three hydrophobic methylene carbons [35,36].

However, not all the six CDRs have a connection with the antigen on the antigen-antibody interface. It is known that a minimum of four CDRs can bind to antigens [37]. Camelid single-domain antibodies, however, can bind to antigens though it has only two CDRs in its nanomolar ranges [38]. VH CDRs have more extensive interaction with antigen than VL CDRs [39]. Besides, some antigens such as peptides with a grooved contacting surface can bind to special sockets on the antibodies, which are different from the large protein antigens with planar surface [40].

The binding of an antibody to its antigen is determined by affinity and specificity. The binding can be reversed and determined by the reactants concentrations. The antibody-antigen complex has a balance rate between formation and dissociation at the equilibrium phase. An affinity constant (K_D) can be calculated based on the associate and dissociate rate constants. The high affinity of the antibody-antigen complex usually comes with the small K_D. Normally, K_D values of antibodies are in the range of 10^{-6} to 10^{-9}. Antibodies with K_D values in the low nanomolar range (10^{-9}) can be considered as a high affinity. Additionally, the specificity of the binding is attributed to the specific chemical structure of each antibody. Some small residues in the CDR1 and CDR2 of VH determine the binding specificities of the individual antibodies. The principles of specificity of the antigen-antibody interaction are valuable in the clinical laboratory for diagnostic purposes. The most basic application is in the determination of the ABO blood group, useful for blood transfusion [41]. It is also performed as a molecular

technique for infection with different pathogens, such as helminth parasites, HIV, and microbes.

1.2.3 Development and categories of an antibody. In 1890, Emil von Behring and Shibasaburo Kitasato built a theory for antibodies. They found that infected animals suffering from diphtheria can be cured by the transfer of therapeutic serum from immunized animals [42,43]. Behring won the Nobel Prize in 1901 for the work in potential treatment in humans [44]. In 1900, the side-chain theory was developed by Paul Ehrlich, in which he proposed the hypothesis that side-chain receptors on cells can interact with a given pathogen. In his model, he assumed that an antibody can bind to foreign molecules called antigens and activate the complement pathway. The 'lock and key' theory developed by Emil Fischer came to the same conclusion as this model [45,46]. In 1948, Astrid Fagraeus proposed that an antibody was secreted by plasma B cells, and later in 1957, the clonal selection theory was given by Frank Burnet and David Talmage [47]. This theory was different from the model developed by Linus Pauling in 1940 and stated that the antigen acted as a template for the antibody [48].

Gerald Edelman and Rodney Porter won the Nobel Prize jointly in 1972 for their independently publishing of the molecular structure of antibodies in 1959 [49-51]. The first antibody fragment atomic resolution structure was published in 1973 [52]. Furthermore, the modern research of antibodies began based on the discovery of monoclonal antibodies by Georges Köhler and César Milste in 1975 [53].

An antibody can be produced from many different systems such as yeast bacteria and mammalian cell systems. Humans with non-glycosylated proteins can obtain it from

bacteria such as Streptomyces and Escherichia coli. Only simple media was needed for protein growth with a range between 1 to 300 mg/L from the bacteria system [54]. But it is impossible to perform further modifications and collect full-size antibodies from the bacteria system. Additionally, expression levels of protein will reduce due to the loss of plasmid during bacterial culture.

Yeast is another production, but inefficient, system for antibodies. Each liter of yeast medium could only generate few microgram antibodies until the 1980s [55]. Then, the methylotrophic yeast was developed, which produced antibodies with an increased productivity of 100 milligrams per liter yeast [56].

More complicated proteins such as full-size antibodies can only be obtained from the mammalian cells system. However, the high cost of the cell culture media and instruments impose restrictions on the development of mammalian cells system [57,58]. Therefore, it is better to obtain economically complex recombinant proteins from transgenic plants and animals instead of the traditional mammalian cells system.

During the past several decades, great progress has been made in the field of antibody discovery and therapy with a total of over 300 unique monoclonal antibodies investigated in clinical trials.

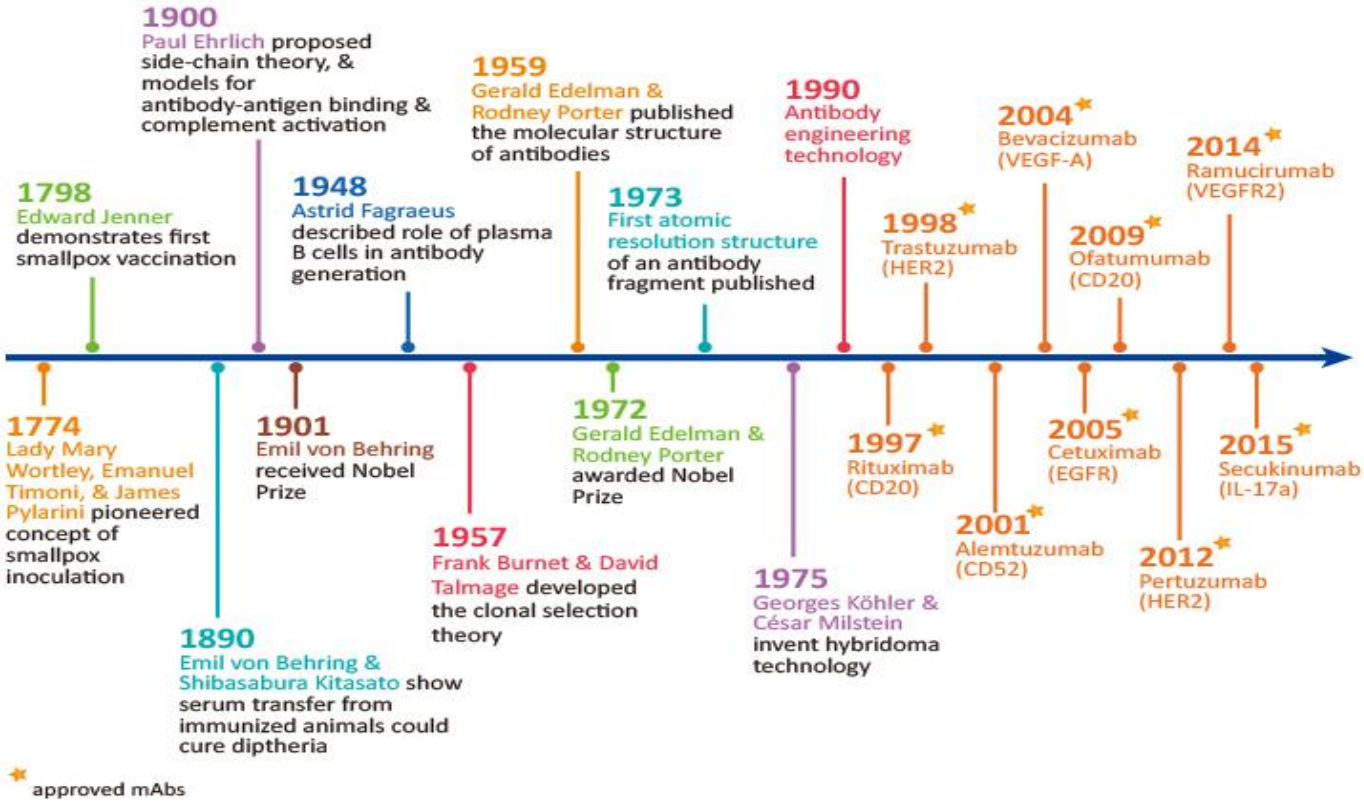

Figure 1.2 History of antibody research [42].

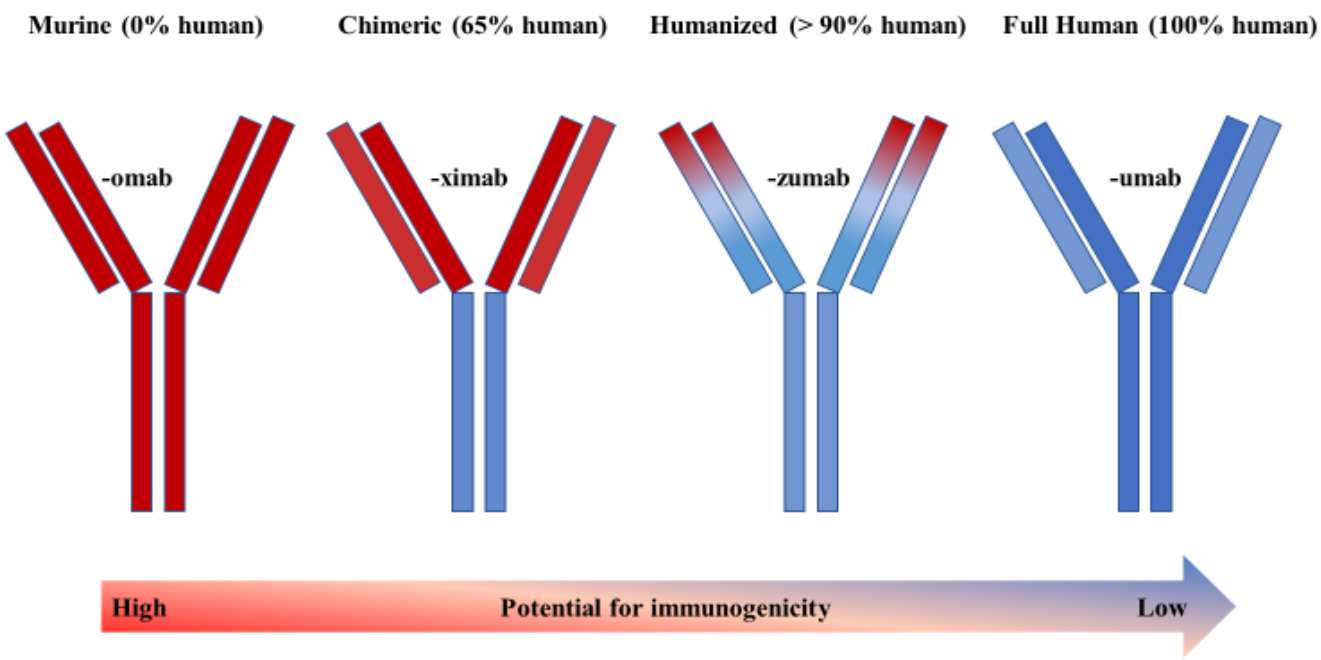

Figure 1.3 Evolution of therapeutic antibody technology.

1.2.4 Polyclonal and monoclonal antibodies

1.2.4.1 Polyclonal antibodies. Polyclonal antibodies (pAbs) are generated by different B cell lineages within the body while monoclonal antibodies (mAb) are only secreted by a single cell lineage. Polyclonal antibodies are a mixture of immunoglobulin molecules that bind to a specific antigen, each identifying a different epitope.

Polyclonal antibodies with different specificities and affinities are stable in a pH and salt concentration range [59]. Compared to other mammals producing polyclonal antibodies, the rabbit is the most significant production source of polyclonal antibodies for its low cost of maintenance and simple handling. Polyclonal antibodies are generally obtained by immunizing animals through intradermal and subcutaneous injections. The immune response was increased by using antigens with adjuvants such as bovine serum albumin [60].

1.2.4.2 Monoclonal antibodies. Monoclonal antibodies (mAb) are made by identical immune cells that are all clones of a unique parent cell. Monoclonal antibodies are homogenous and can bind to the same epitope. These monoclonal antibodies have similar immunochemical function due to the derivation of a single B cell clone of one animal while polyclonal antibodies bind to multiple epitopes and are generated by several different plasma cell lineages. Most monoclonal antibodies are obtained from rabbits and mice. By changing the therapeutic targets of one single monoclonal antibody to two epitopes, bispecific monoclonal antibodies can also be modified and obtained.

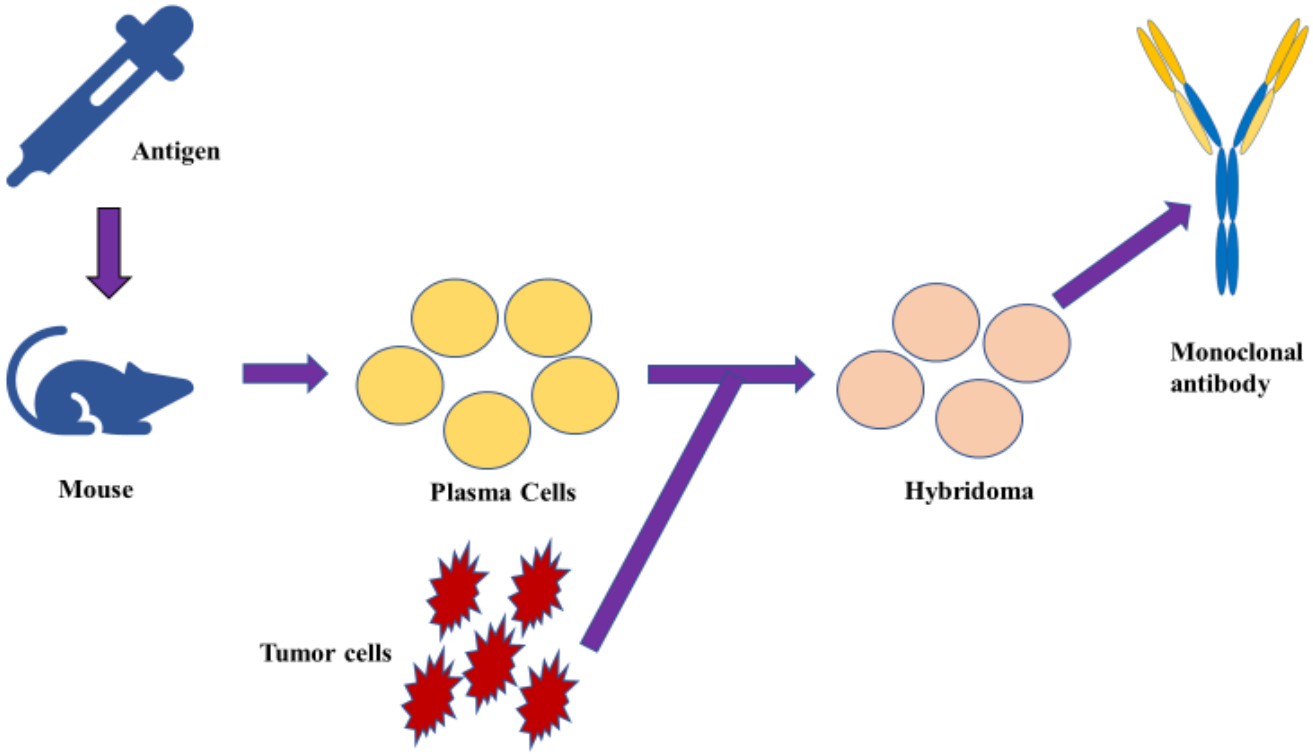

Figure 1.4 Monoclonal antibody production.

1.2.5 Limitations of current antibody. As the pharmaceutical market in the world continues to expand, biopharmaceutical products such as therapeutic mAbs play a more significant role in cancer treatment. Approximately 60% of biopharmaceutical sales is attributed to monoclonal antibody products, and these products have grown to almost $90 billion in the past three years. A worldwide sales of monoclonal antibody products will take place in the future. However, getting treated with mAbs still has side effects such as tumor lysis syndrome and anaphylaxis [61].

Poor tumor permeability is another limitation of antibodies regardless of the adverse effects of mAbs. In the tumor microenvironment, the number of functional lymphatic vessels are not sufficient enough to transport the macromolecules such as mAbs [62]. The potential of an antibody treatment is reduced since it is difficult for mAbs to penetrate deeply into the tumor microenvironment.

Additionally, the mAbs treatment currently available on the market is very expensive. The average annual cost of an mAb treatment was $96,731, and the Herceptin costs for the treatment was $43080 per year [63]. The production cost and development time also determine the application of antibodies. It took about 10 years for a mAbs to come to the market including the discovery and research time. In addition to this, the cost of mAbs development is over $650 million, which is very high.

1.2.6 Antibody alternatives. Since mAbs have many disadvantages as mentioned above, alternatives to antibodies have been created for the market. These molecules, with lower molecular weight, usually have a similar function such as binding specificity, affinity, and tissue penetration. These alternatives include Fab, nanobodies, single chain fragment variable (scFv), antibody mimics [64,65], and so on. Furthermore, the research and screening time of antibody alternatives is shorter than a monoclonal antibody. Compared with the traditional mAbs, these molecules with lower molecular weight can easily penetrate to the tumor site and bind to an antigen.

1.2.6.1 Single chain fragment variable (scFv). Single chain fragment variable is a protein consisting of the variable regions of the heavy and light chains of immunoglobulins [66]. scFv can be employed to build molecules for different purposes due to the retainment of the binding specificity and affinity of a full antibody [67-69]. However, scFv with a molecular weight around 25kDa has a limitation of lower half-life, making it difficult to be used in the market [70]. Two scFvs can be connected by a peptide linker or a disulfide bond [69,71-73]. E. coli bacterial with an ability to generate foreign protein in a large amount can secrete scFv at a high speed [74]. Generally, mRNA is isolated from the hybridoma [75-77] or spleen cells from immunized mice [78,79] or B lymphocytes [80,81] and is reverse transcribed into DNA followed by gene amplification by the PCR technique. The only issue with this approach is that some protein lacks certain conformation due to the limited folding capacity of the E. coli bacterial system. The problem has been studied by many reports [82,83].

1.2.6.2 Antibody mimic. Antibody mimic is a molecule that can bind to a protein with specificity and affinity. The molecular weight of an antibody mimic is less than 10 kDa [84]. Antibody mimic can bind to an antigen with no risk of ADCC and CDC because of the lack of constant region of an antibody. There are many different approaches such as phage display, mRNA display, and yeast two-hybrid system for the development of antibody mimics [85,86].

In 1998, the first antibody mimic was designed to bind to TNF-α by performing a phage display [87]. However, the binding affinities of the isolated peptides were too low for them to be used for treatment. A lot of effort has been put on the discovery and screening for antibody mimics with K_D values in the picomolar to the millimolar range [88,89]. The three-amino-acid motif RGD, developed by a phage display technique, is one of the most promising examples among them. This motif with a K_D of 0.8 nM can bind to the αVβ3 integrin that forms the tumor vascular endothelial cells [90].

Chemical synthesis is another feasible approach to obtain antibody mimics. Before synthesis, a mass of molecular docking should be done between the screening peptides with a random sequence and a library of thousands of human proteins [91]. Rod Balhorn et al. discovered selective high-affinity antibody mimics that target leukemia or lymphoma through molecular docking [92]. However, all docking based on these screenings are tedious and time-consuming due to the trial-and-error principle. Therefore, a rational design of peptides based on the molecular interaction between antibody and antigen can be considered as a viable approach.

1.3 Programmed Death-Ligand 1

Programmed death-ligand 1 (PD-L1) is a 40kDa type 1 transmembrane protein that has been studied to play a critical role in mediating the suppressed immune function during specific events such as tissue allografts and autoimmune diseases. This molecule was named as PD-L1 due to its identification as a ligand of PD-1 after its first characterization by Mayo Clinic as an immune regulatory molecule, B7-H1 [93]. The immune system takes the response to foreign antigens that are relative to both exogenous and endogenous danger signals, which causes an activation and proliferation of the antigen-specific T cells. The interaction between PD-L1 and PD-1 delivers a negative signal to these T cells and results in the reduced proliferation of T cells [94].

Blockade of PD-L1 can limit the growth of tumors in the presence of immune cells while most cancer cells have the ability to express high levels of PD-L1. A conclusion can be made that tumor cells can escape immune attack with PD-L1 [95]. PD-L1 can modulate activation or inhibition upon binding with its receptor PD-1, which is located on activated T cells, B cells, and myeloid cells. Said et al. found that PD-L1 can induce IL-10 production when interacting with PD-1 which is upregulated on activated CD4 T-cells [96].

It is reported that the upregulation of PD-L1 could help cancers to escape attack from the host immune system. Antibodies that can block PD-L1 on tumor cells have shown the ability to alleviate cancer-induced immunosuppression [97]. Many PD-L1 inhibitors such as durvalumab, atezolizumab, and avelumab are in development as immuno-oncology therapies and are showing good results in clinical trials [98,99]. PD-

L1 has been considered as a potential target for a receptor-mediated delivery system of peptides, antibodies, or drugs for cancer treatment.

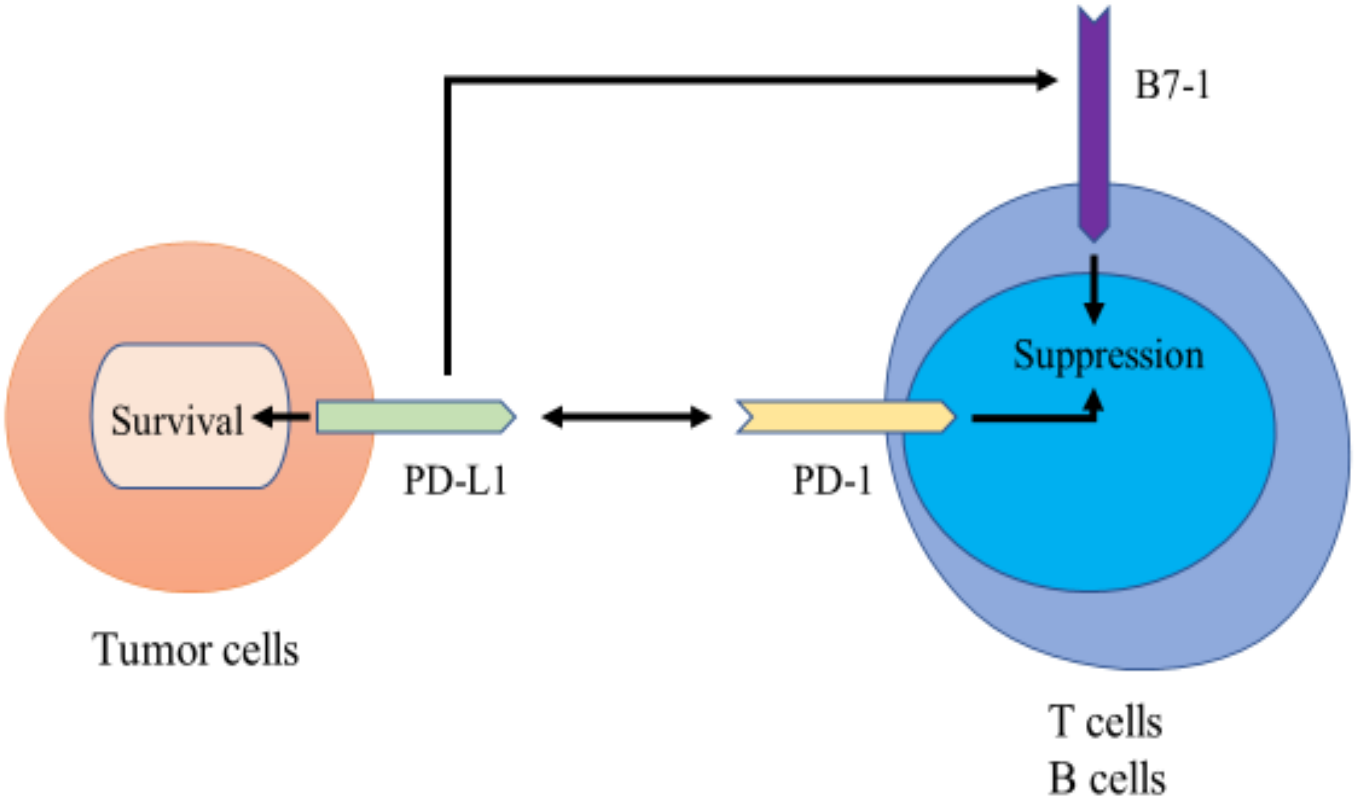

Figure 1.5 Mechanism of PD-L1 delivers T Cell Suppression and Tumor Cell Survival [100].

1.4 Statement of the Problem

Antibodies have been commonly used as reagents to recognize antigens or proteins in life science research due to their binding specificity. Recently, several antibodies have been successfully developed for therapeutic uses. However, extensive uses of antibodies are limited by their high cost of production, long production period, and poor stability. These limitations have necessitated research for finding antibody alternatives with lower molecular weight and similar properties as antibodies but without the limitations of the lengthy and complicated approach of producing antibodies. Some examples of these efforts include fragment antigen binding (Fab) and scFv, or synthetic antibody mimics. Though these molecules have lower molecular weight when compared with antibodies, they still have the disadvantages of tedious and time-consuming processes, the uncertainty of the outcome, and high costs of production. A rational design of molecules that can mimic the antibody-antigen interaction based on the molecular interaction and Knob-Socket model can be considered as a viable approach for antibody alternatives. In this study, we proposed an approach to design peptides against a target without involving massive experimental screening trials.

1.5 Hypothesis

Rationally designed peptides that specifically bind to PD-L1 based on molecular interactions between the ligand-receptor and Knob-Socket model.

1.6 Specific Aims

The objective of this dissertation research is to design, synthesize, and characterize novel peptides for binding PD-L1 based on the PD1-PD-L1 interaction and

Knob-Socket model. To achieve the research objective, the specific aims are described as following:

1. To design peptides based on the Knob-Socket model and protein-protein interaction. Peptides which can specifically bind to the PD-L1 and scrambled (control) sequence peptides are designed.
2. To perform computer simulation studies and to determine the number of interactions, docking energy, and binding position by Molecular Operating Environment (MOE) and AutoDock Vina software. Selected peptides based on these parameters are utilized for future studies in vitro.
3. To synthesize and characterize peptides. Designed peptides and scrambled sequence peptide with and without the FITC conjugation are synthesized using the solid phase synthesis method. The purity and mass to charge ratio will be determined by the high-performance liquid chromatography (HPLC) and mass spectrometer.
4. To study the *in vitro* binding specificity and affinity of peptides to PD-L1. The binding affinity and specificity will be determined by performing the Surface Plasmon Resonance (SPR) technique and cell uptake experiments with confocal microscopy.

Chapter 2: Design and Computational Studies of Peptides

2.1 Introduction

In life sciences, antibodies are commonly performed to bind to different targets with significant affinity and specificity in various areas such as therapeutic agents. When compared with antibodies, peptides are much smaller in mass and size. Peptides can simulate the interaction between antibodies and antigens with a small molecular weight. Additionally, due to their small structure, they can penetrate tumor tissues easily and are unlikely to trigger immunogenicity [101].

Molecular modeling is performed to predict the structure of biological molecules and simulate the binding functions between the receptor and ligand in biological and chemical systems. In this part, peptides are designed against the target based on the molecular interactions between the antibody and antigen instead of complicated experimental screening trials.

Molecular Operation Environment (MOE) is widely used as a drug discovery software in different fields of molecular modeling, protein and antibody modeling, and fragment and structure-based designing. The docking program in MOE can be performed to mimic the interaction between two molecules based on their crystalline structures. The possible orientation of two molecules can be obtained and analyzed in the docking program. MOE can be used to screen the molecules based on the estimated binding energy from the docking program. A stable system usually has a lower binding

energy suggesting a possible interaction between two molecules. Also, a map with detailed interaction on the interface between the two molecules can be determined by the ligand interaction function in MOE. In other words, we can identify and select the specific amino acid sequences in the binding interface that are significant for the receptor to bind ligands.

AutoDock Vina is another screening software for molecular modeling which can perform to determine the average accuracy of the binding mode predictions. It is an important program for molecular docking and virtual screening. Vina performs a sophisticated gradient optimization approach in its local optimization procedure. The calculation of the gradient effectually offers the optimization algorithm a direction from a single evaluation. By using multithreading, multiple CPUs or CPU cores can be employed by Vina to speed up the calculation in screening molecules. After docking in the AutoDock Vina, designed peptides can be screened based on the binding position against the PD-L1 protein. Only peptides bound to the designed binding interface from PD-L1 can be considered as important candidates.

PSIPRED is a precise and simple secondary structure prediction approach, incorporating two feed-forward neural networks which carry out an analysis on output got from PSI-BLAST (Position Specific Iterated - BLAST). The secondary structure of peptides that we designed can be predicted by PSIPRED.

The interaction between PD1 and PD-L1 has been extensively studied by scientists [102,103]. The three-dimensional structures of the different PD1-PD-L1 complex can be observed and identified based on the crystalline structure obtained from

the Protein Data Bank (PDB). Core amino acids from the binding interface of the PD1-PD-L1 complex can be collected and employed to design the peptides for PD-L1 after analyzing the binding details.

The interaction between the novel peptide and PD-L1 was optimized by using the Knob-Socket model developed by Joo et al. [104]. The packing between the interactions of two molecules can be analyzed and explained by this model in a simplified and straightforward approach. When it is compared with the other packing models, the Knob-Socket model can be used to determine and optimize all kinds of packing in the secondary structure [105]. In this model, Knob-Socket is defined as a four-residue tetrahedral: one knob **B** in one secondary structure packed into a three residue **H: YX** socket presented on the other secondary structure (Figure 2.1). The **X** and **Y** are consecutive residues that pack with the covalent peptide bond (continuous black line), where the hydrogen bond (broken red line) connects **X** and **H**. The **H** and **Y** residues only connect by their side-chain interactions. Additionally, three types of sockets were provided in the Knob-Socket model: a free socket with no packing knob, filled socket with a packing knob, and a non-socket. The amino acid propensities determine the packing strategy for choosing the binding peptide sequences in these three types of socket.

A two-dimensioning map can be obtained with the information of sockets formed on PD-L1 and specific binding knobs from PD1 in the principle of the Knob-Socket model. Furthermore, a particular amino acid sequence that has a high frequency to be

filled into sockets on PD-L1 can be determined and can be used for optimizing and designing the peptides against PD-L1.

In this chapter, by using the Knob-Socket model, the interaction between different PD1-PD-L1 complexes was analyzed and studied for the designing of the novel peptide sequences towards PD-L1.

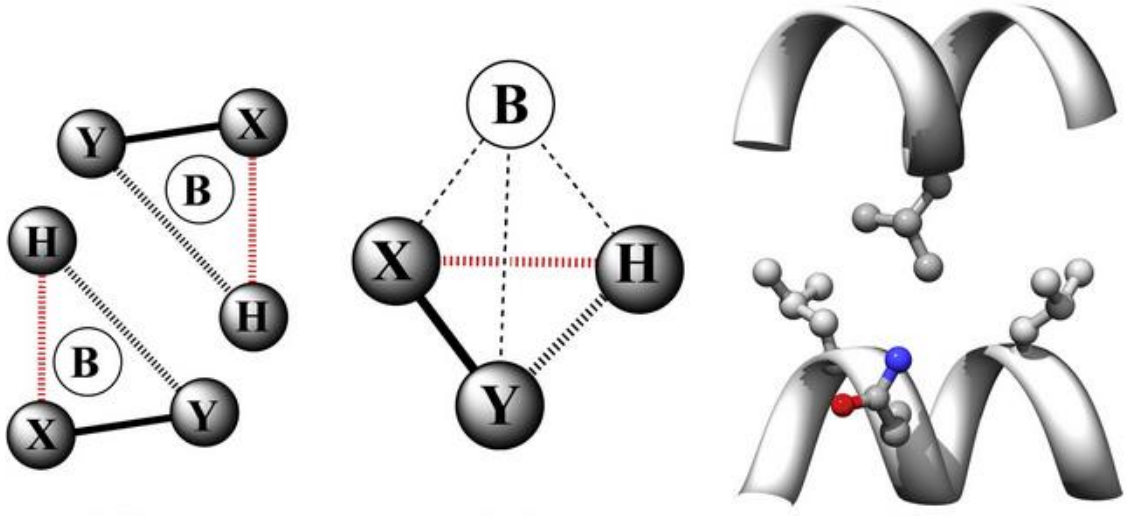

(a) (b) (c)

Figure 2.1 Two-dimensional schematic of Knob-Socket model.

(a) A two-dimensional representation of the Knob-Socket model shows that the three residues X, Y, and H in the socket are all packed against a knob residue B from the other secondary structure.

(b) The four-residue motif is arranged in the tetrahedral structure. All residues are represented by spheres. The knob residue B connects to all the three socket residues only through side-chain interactions.

(c) The Knob-Socket model shown between two α-helices.

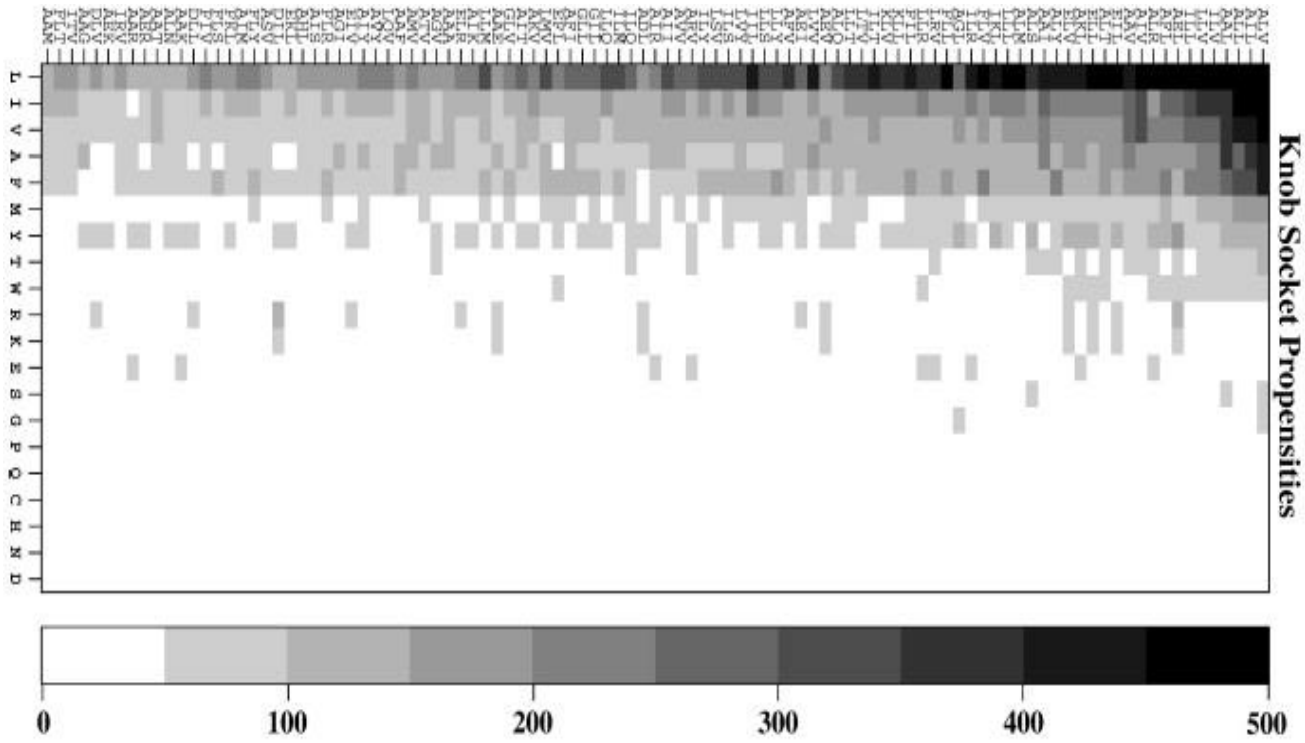

Figure 2.2 Knob-Socket Propensity of various knobs to sockets. Adapted from Hyun Joo et al [114].

2.2 Materials

UCSF-Chimera package (Version 1.10, San Francisco, CA, USA), MOE software (Version 2013.08) from Chemical Computing Group Inc. (Montreal, QC, Canada), AutoDock Vina from Scripps Research Institute (La Jolla, CA, USA). PSIPRED from University College London (London, United Kingdom).

2.3 Method

2.3.1 Design of peptides. Peptides were designed based on the crystal structure of PD1-PD-L1 and the Knob-Socket model. The crystal structures (PDB 3SBW and 5IUS) were analyzed to determine which residues in PD-1 have maximum interaction with the PD-L1 epitopes. For the first and second generations of peptides, the PD-L1 protein surface was identified to provide sockets in the two-dimensional map with binding knobs from PD1 by analyzing the crystal structure PDB 3SBW. Correspondingly, crystal structure PDB 5IUS was used for designing the third generation of peptides. Each amino acid knob residues from the PD-1 is in contact with the socket formed by the three amino acid residues on the PD-L1 surface. Based on the probability of packing the amino acid knob to a different socket, peptides were designed in an approach of linking the identified knob. Franking amino acids can be used to fill the space when the distance between two residues is a lot. Different peptide sequences can be designed by combining the amino acids from the list of possible knobs with various sockets. For the α-helix peptides, 12 different peptide sequences were designed in 25 amino acids length. To increase the stability and build an α-helix structure, several amino acids were added to the start and end of the peptide sequences. The key amino acid knobs from α-helix peptides were used to design the over-packed peptides with a 13 amino acids length. Correspondingly, the third generations of peptides, the peptides with salt bridge function, have 67 peptides sequences including one scrambled sequence peptide as a negative control.

2.3.2 Secondary structure prediction for peptides in alpha helix design. The secondary structure of peptides in alpha helix design was predicted by PSIPRED. Several UCL structure prediction techniques were combined into one location by the PSIPRED Protein Sequence Analysis Workbench. The results of the prediction were received after submitting a protein sequence.

Peptides with high ratio of alpha helical structure and confidence of prediction were then selected for further experiments and were docked in the AutoDock Vina to check whether they could bind to the designed part of the target protein for further screening.

2.3.3 Computer modeling studies. The crystalline structure of the PD-PD-L1 complex that was downloaded from the protein databank with PDB ID:3SBW and 5IUS was analyzed in Chimera and optimized in MOE. Molecular Operating Environment (MOE) was performed to determine the binding interface between the ligand and receptor. The binding socket from PD-L1 and the amino acid knobs from PD1 were assigned for the docking study by the atom selector. We can obtain the detailed interaction map between PD-1 and PD-L1 by ligand interaction simulation. Furthermore, core amino acid sequences for the design of peptides can also be analyzed and determined by the direct interaction sequence from ligand interaction simulation.

Designed peptides were screened by utilizing the Molecular Operating Environment (MOE) and the AutoDock Vina software. After performing energy minimization, the conformation of the peptide with the lowest energy was docked in the

MOE software to calculate the binding energy. The lower (negative) suggests better binding.

Peptides with more number of interactions, preserved interactions, and lower docking energy were then selected for further experiments and were docked in the AutoDock Vina to check whether they could bind to the designed part of the target protein for further screening.

2.4 Results and Discussions

2.4.1 Design of peptides. Peptides were designed based on the PD1-PD-L1 crystal structure and the Knob-Socket model. Taking the frequency data of knob and sockets from Figure 2.2, the design of peptide sequences was determined by the propensity of preferable knobs to sockets. The map and ribbon diagram of the PD-L1 surface bound by PD1 for α-helix and over-packed peptides are shown in Figure 2.3. The knob positions from the ligand are represented as spheres. The pink color represents knobs from PD1 in a covalent bond. Correspondingly, the map and ribbon diagram of the peptides with the salt bridge function is shown in Figure 2.4. The side-chains of the amino acids are also displayed, and the knob positions from the ligand are shown as spheres. The orange color represents knobs from PD-1 in a covalent bond and red represents the salt bridge function.

For the α-helix and over-packed peptide sequences, the packing interface lattice diagram consisting of knobs and sockets is shown in Figure 2.3 (left). The filled sockets are in grey and free sockets with no binding knobs are in yellow. The knobs are presented in the same color as the ribbon diagram.

Based on the mapping data, the key amino acid sequences are designed as shown in Figure 2.5. The α-helix peptide sequences are designed based on these 13 amino acids. To increase the stability and build an α-helix structure, several amino acids are added to the start and end of the peptides. There are 25 α-helix amino acids in total. Furthermore, over-packed peptides are designed by the 13 key amino acids as shown in Figure 2.6.

Additionally, the sequences of third generation peptides are shown in Figure 2.7. Arginine was chosen as the first amino acid for its basic side chain that can bind to the acidic part of the protein shown on coulombic surface coloring; “a double anchor” with glutamic acid and aspartic acid. The second amino acid, lysine, was also chosen because it can bind to glutamic acid. The third, fifth, and seventh amino acids were selected based on the propensity of the Knob-Socket model. Proline was used to give a turn off in the fourth position. For the sixth position, serine was added to increase the hydrophily of the peptide. Glycine was used in the eighth position as a franking amino acid. Glutamine was used for its propensity in socket ADY. Threonine and glutamic acid were used for its salt bridge. Histidine had a connection with aspartic acid. Knobs in pink and red that have high preference such as Leu (L), Glu (E), Phe (F), and Tyr (Y) were filled in the sockets and were connected based on the space between them and the other amino acids.

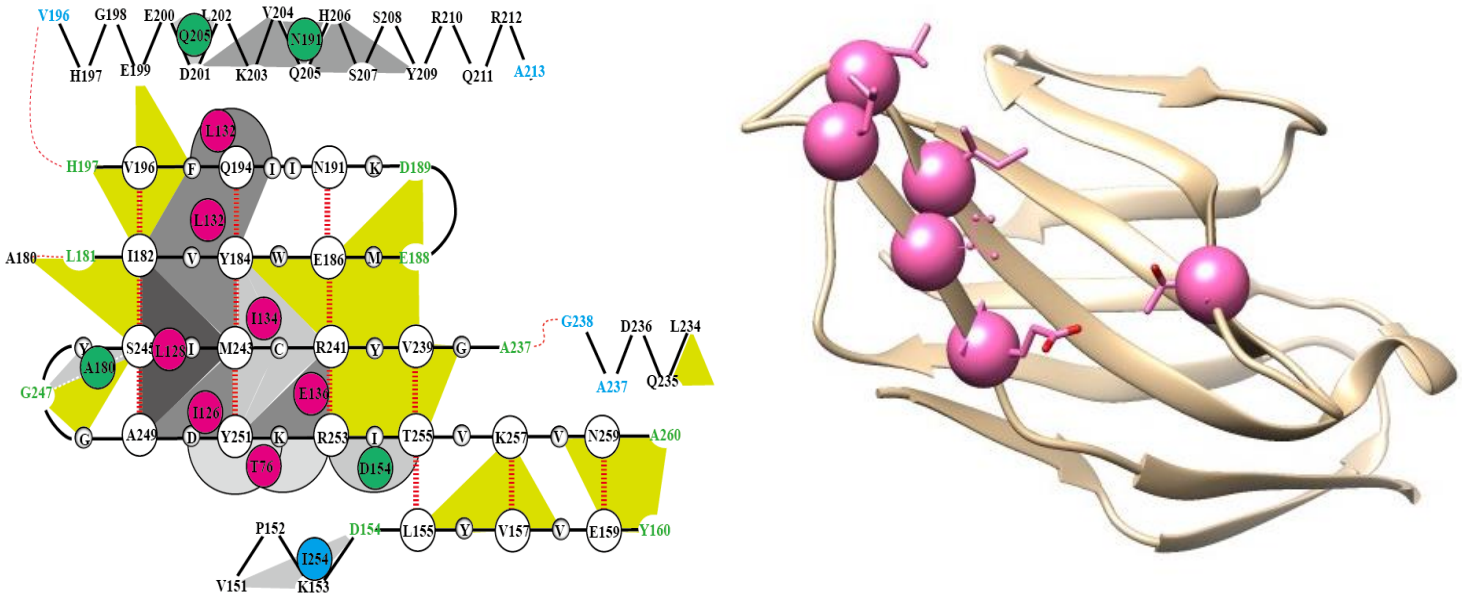

Figure 2.3 Mouse PD-1 mutant and human PD-L1: Ribbon diagram of the PD1-PD-L1 interface (right) and schematic of the interaction map diagram (left).

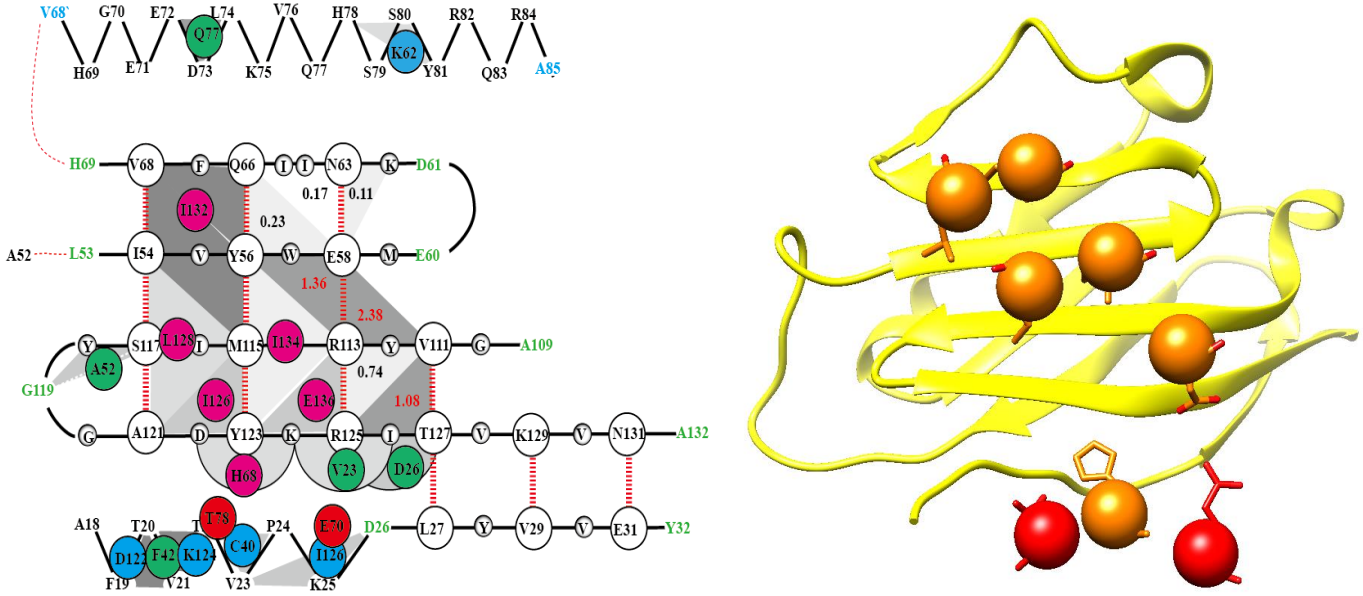

Figure 2.4 High affinity mouse PD-1 and human PD-L1: Ribbon diagram of the PD1-PD-L1 interface (right) and schematic of the interaction map diagram (left).

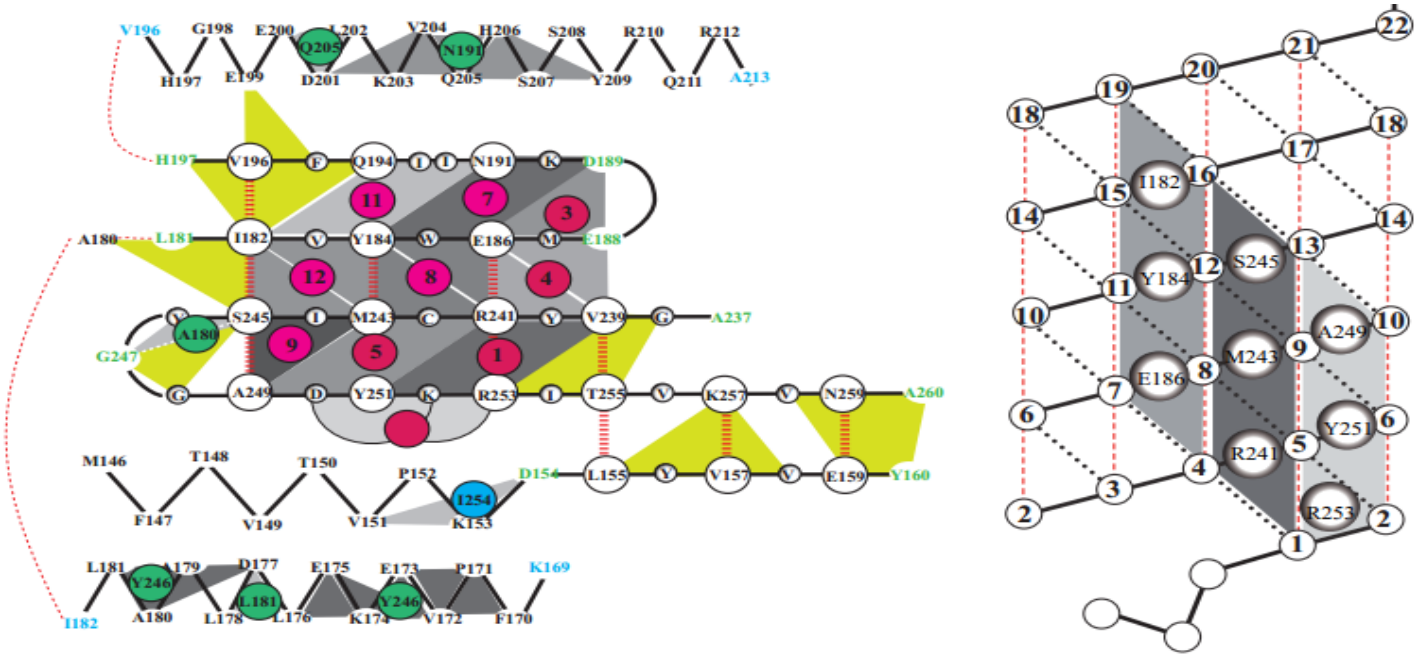

Figure 2.5 Mouse PD-1 mutant and human PD-L1: α-Helix Peptides designed based on the PD1-PD-L1 interaction map diagram.

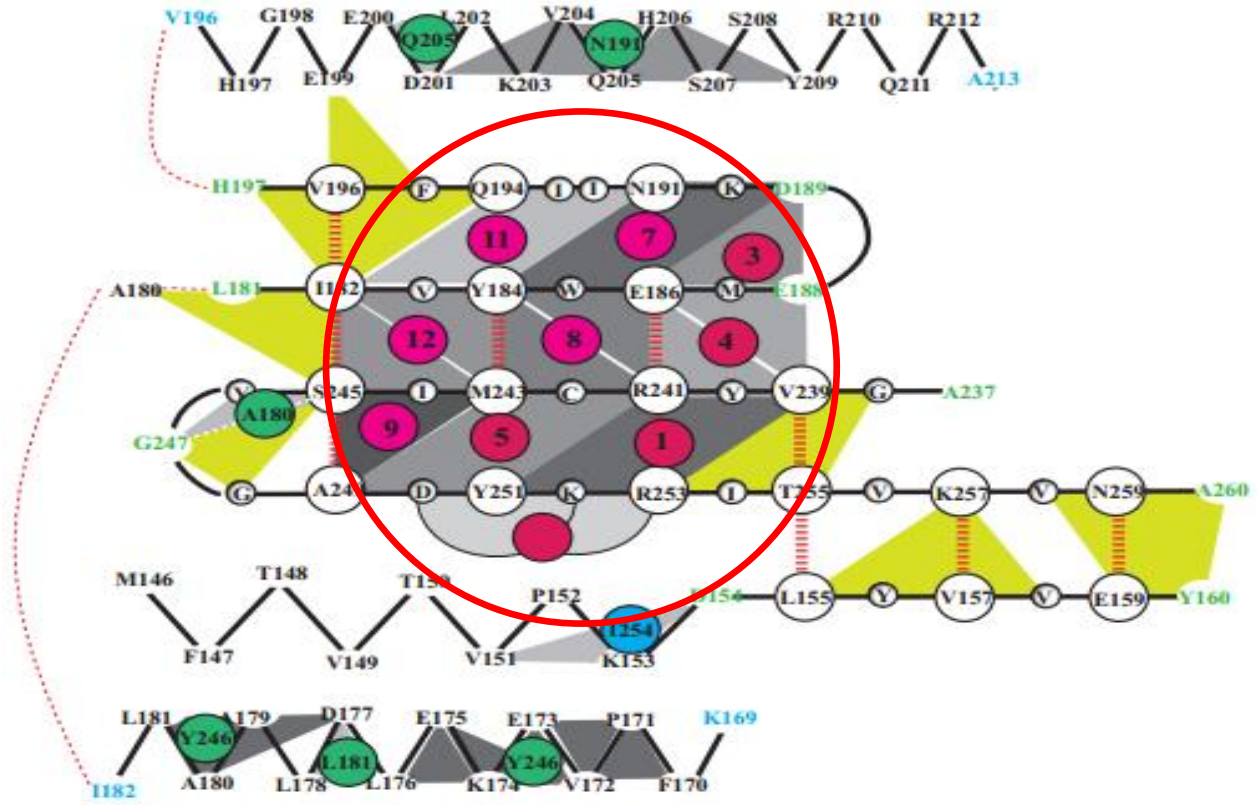

Figure 2.6 Mouse PD-1 mutant and human PD-L1: Over-packed Peptides designed based on the PD1-PD-L1 interaction map diagram.

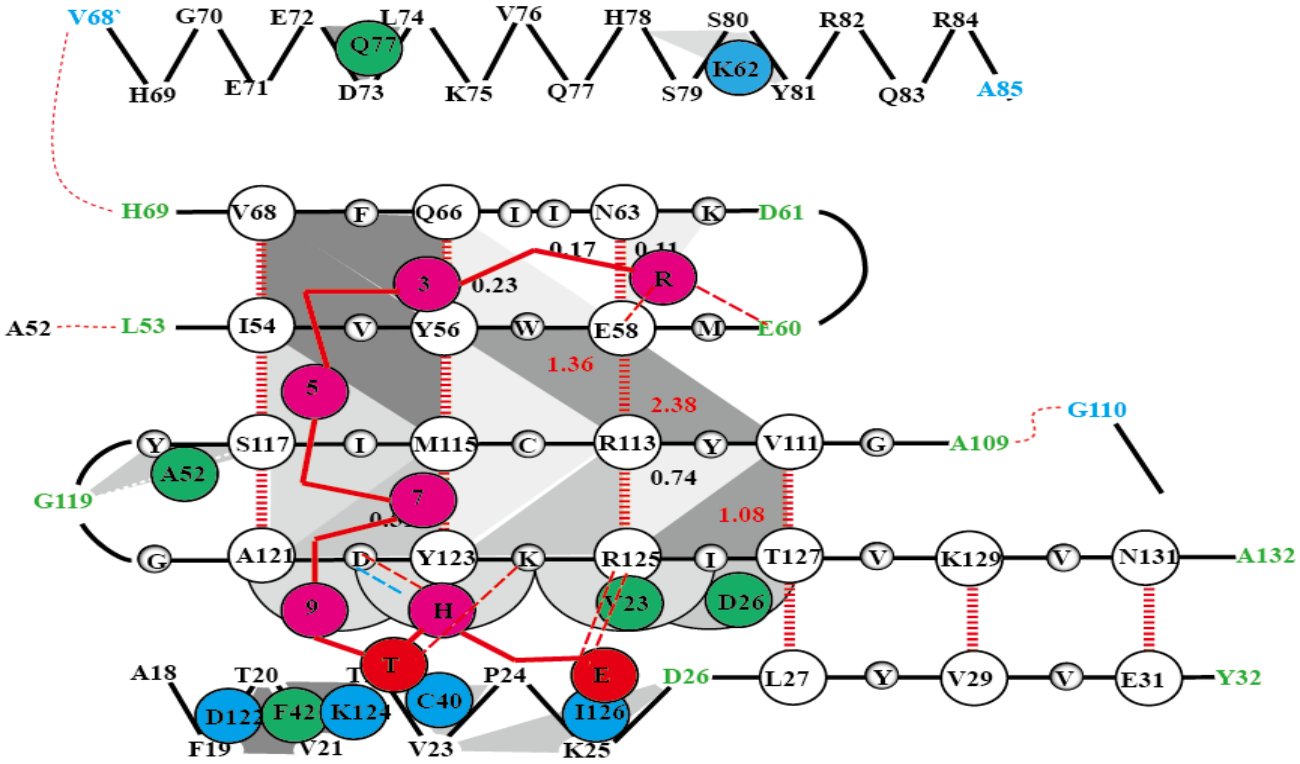

Figure 2.7 High affinity mouse PD-1 and human PD-L1: Peptides with SB function designed based on the PD1-PD-L1 interaction map diagram.

2.4.2 Secondary structure prediction for peptides in alpha helix design.

Peptides were selected based on the result of the ratio of alpha helical structure and confidence of prediction. The sequences and prediction results of α-helix peptides are shown in Figure 2.8. PDL1-01-25MER was chosen based on the high ratio of alpha helical structure and confidence of prediction.

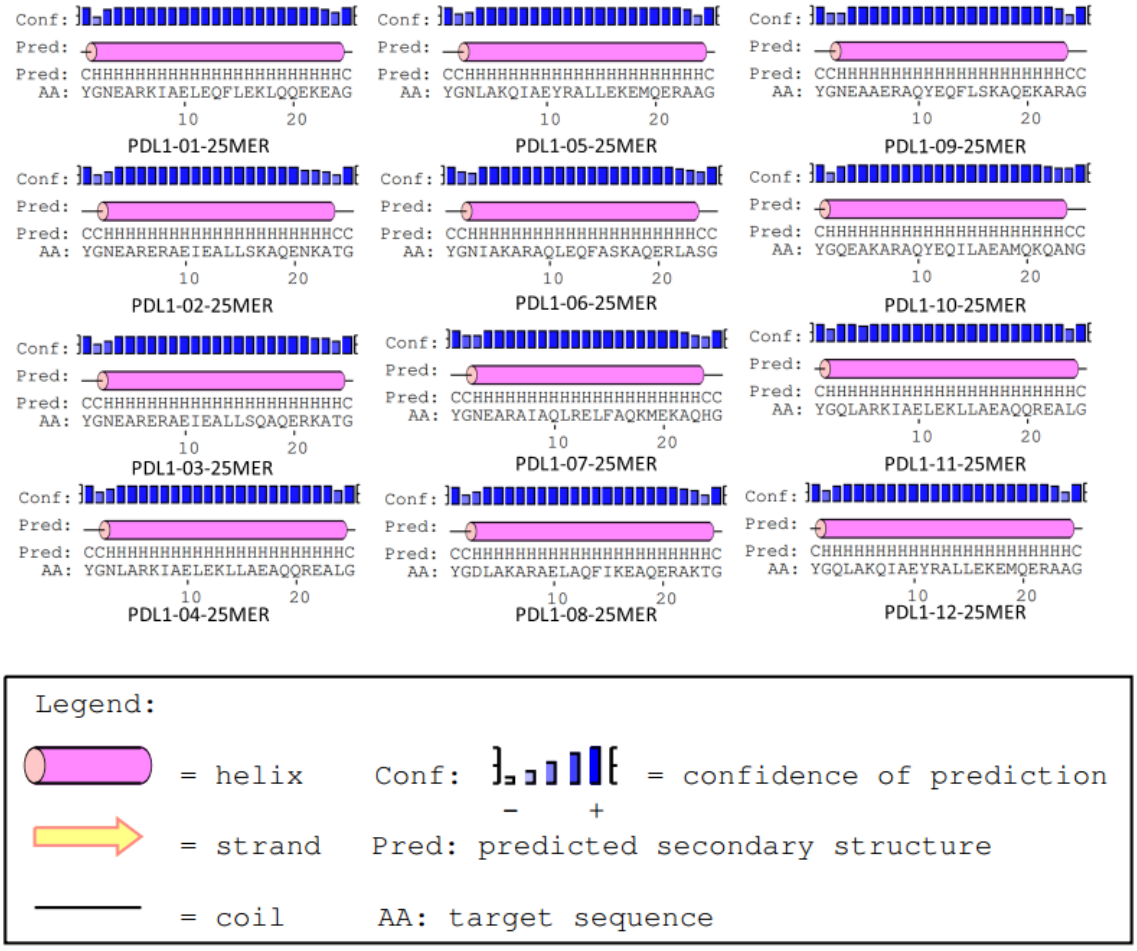

Figure 2.8 Prediction results of peptides in α-helix design.

2.4.3 Computer modeling studies. Peptides were selected based on the result of the total number of interactions, preserved interactions, and docking energy. The sequences and docking results of over-packed peptides are shown in Table 2.1. For over-packed peptides, PDL1-06-13MER was chosen based on the lower docking score. For the peptides with salt bridge, PDL1-P13-01, PDL1-P13-28, PDL1-P13-40, and PDL1-P13-55 were selected based on their lower binding energy as shown in Table 2.2.

A conclusive docking was performed by AutoDock Vina in terms of the total number of interactions, preserved interactions, and docking energy, and the results are shown in Table 2.3. The α-helix and over-packed peptides with a higher binding energy and with a less number of total and preserved interactions suggested poor binding affinity and specificity.

Table 2.1 Docking results of over-packed peptides.

Ranking	Peptide No.	Sequence	Docking Score
1	PDL1-06-13MER	IAKARAQLEQFAS	-11.11
2	PDL1-07-13MER	EARAIAQLRELFA	-11.01
3	PDL1-09-13MER	EAAERAQYEQFLS	-10.93
4	PDL1-12-13MER	LAKQIAEYRALLE	-10.68
5	PDL1-08-13MER	LAKARAELAQFIK	-10.66
6	PDL1-01-13MER	EARKIAELEQFLE	-10.54
7	PDL1-02-13MER	EARERAEIEALLS	-10.43
8	PDL1-10-13MER	EAKARAQYEQILA	-10.36
9	PDL1-11-13MER	LARKIAELEKLLA	-9.98

Table 2.2 Docking results of peptides with salt bridge function.

Top 20%: 13	Ranking	Sequence	Results
	1	PDL1-P13-28	-15.5482
	2	PDL1-P13-14	-15.4521
	3	PDL1-P13-53	-15.4139
4 Run	4	PDL1-P13-31	-15.1848
	5	PDL1-P13-1	-15.1122
	6	PDL1-P13-32	-15.0183
	7	PDL1-P13-45	-14.8636
	8	PDL1-P13-11	-14.7244
	9	PDL1-P13-62	-14.7051
	10	PDL1-P13-55	-14.6899
	11	PDL1-P13-8	-14.5711
	12	PDL1-P13-60	-14.551
	13	PDL1-P13-40	-14.5242
	28	PDL1-P13-33	-14.0458
	37	PDL1-P13-X (Control)	-13.8937

Table 2.3 Peptides sequence with molecular modeling results.

	Name	Sequence	Energy (kcal/mol)	Preserved interactions	Total interactions
α-helix	PDL1-01 25MER	YGNLARKIAELEK-LLAEAQQREALG	-4.1	0	10
Over-packed	PDL1-06-13MER	IAKARAQLEQFAS	-4.0	1	6
Peptides with SB function	PDL1-P13-01	RKIPLSIGQTHSE	-5.6	2	11
	PDL1-P13-28	RKFPLSKGQTHSE	-5.5	3	15
	PDL1-P13-33	RKFPSSFGQTHSE	-4.7	2	10
	PDL1-P13-40	RKIPHSKGQTHSE	-5.4	2	11
	PDL1-P13-55	RKVPHSIGQTHSE	-6.1	6	12
	PDL1-P13-X (control)	RQSKLHPGSKTFE	-4.4	0	7

AutoDock Vina was used to perform a second screening for the selected peptides from the MOE software. From the Figure 2.9, we can determine that only PDL1-P13-55 can bind to the designed part of the target protein.

In this study, a screening approach of potential molecules to a given target was evaluated by using the MOE and AutoDock Vina software. The optimized potential energy was used in docking software instead of the free energy of the protein. Three generations of peptides were designed based on the molecular interaction between PD-L1 and PD-1 and were optimized by utilizing the Knob-Socket model. α-helix and over-packed peptides selected from MOE suggested that these molecules might not bind to PD-L1. Besides, the third generations of peptides showed the binding preference against the PD-L1 protein, based on the docking results from MOE and AutoDock Vina. The binding between the designed peptides and PD-L1 still needed verification in experiments. Based on the docking results from MOE and AutoDock Vina, PDL1-01-25MER, PDL1-06-13MER, PDL1-P13-01, PDL1-P13-33, PDL1-P13-28, PDL1-P13-40, and PDL1-P13-55 were selected for future studies.

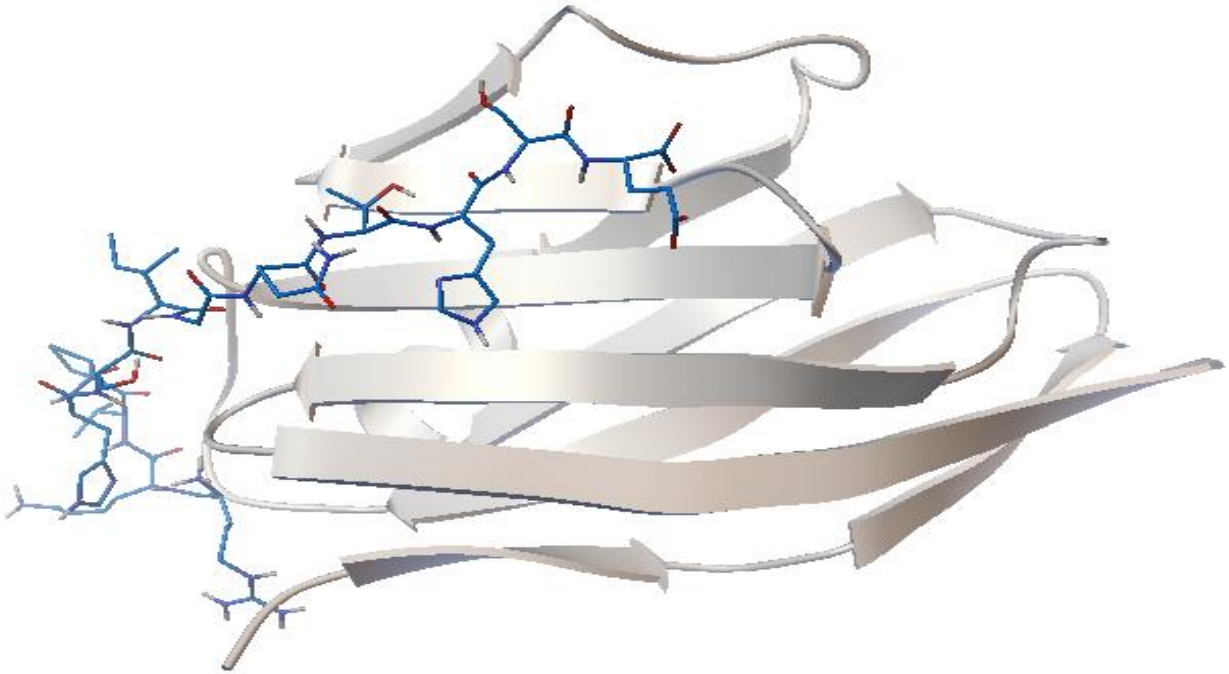

Figure 2.9 Binding position of PDL1-P13-55 in AutoDock Vina.

Chapter 3: Synthesis and Characterization of Peptides for PDL1

3.1 Introduction

The established method for synthesizing peptides in the lab is known as solid-phase peptide synthesis (SPPS) [106]. This method was developed by Robert Bruce Merrifield in 1963 [107,108] and it has frequently been used to synthesize different peptides and proteins. SPPS leads to high yields of pure products and saves more time than traditional synthesis such as liquid-phase peptide synthesis (LPPS). The advantages of this method are very impressive. In the replacement of a complicated isolation procedure, lots of time is saved for each intermediate product with a simple washing step [109]. Additionally, this technique is feasible as well for automatic peptide synthesizers that are commercially available. However, this method has the disadvantages of low output since there are many cycles of coupling and deprotection for each amino acid in the peptides synthesis and the intermediates cannot be purified after each coupling.

The key feature of SPPS is the continuous attachment of amino acids to a solid support bead called resins. The chemical structure of the resin that we will use in the lab is shown in Figure 3.1 (called Wang resin). The hydroxyl group is the place of attachment to the C-terminal amino acid in the peptide chain. The rest of the peptide is then synthesized by coupling one amino acid at a time [106]. Wang resin will keep strong bondage to the peptides until cleaved by trifluoroacetic acid (TFA). These solid

resins build a synthesis environment in which the peptide sequences being attached will not cross a filter in the synthesis vessel.

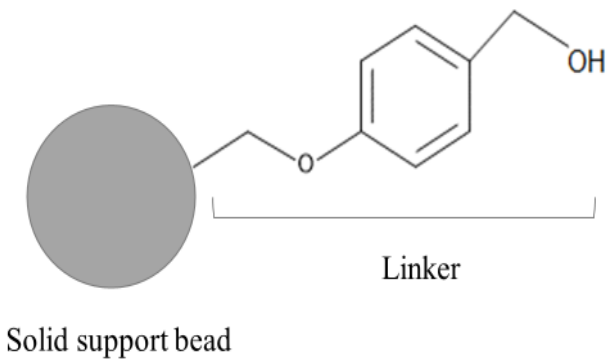

Figure 3.1 Wang resin

Each amino acid has both an amine and carboxylic acid functional group, which would result in side recreation through the synthesis process. Therefore, it is significant to consider the protection strategies. 9-Fluorenylmethoxycarbonyl (Fmoc), used as the protecting group, is commonly used in the peptides synthesis experiment. The N-terminal of each amino acid will be protected with Fmoc, and only the amino acid at the end of C-terminal of the sequence will be attached on to the Wang resin [110,111].

It is necessary to protect the side chain with protecting groups such as tert-butyloxycarbonyl (Boc) and tert-butyl (tBu) to prevent degradation during synthesis. These protecting groups are stable enough in their basic conditions [107]. Additionally, these protecting groups are convenient due to their instability in acid and will be cleaved by the TFA in the final cleavage step.

The first amino acid usually has an attachment to Wang resin. Therefore, the first step is removing the Fmoc group on the C-terminal amino acid by employing a base such as mild basic solution 20% piperidine in DMF. The second Fmoc-protected amino acid is then attached utilizing a coupling reagent such as diisopropylcarbodiimide (DIC) and 1-hydroxybenzotriazole (HOBt) to make the reaction. Besides, several other coupling agents such as 2-(1H-benzotriazol-1-yl)-1,1,3,3-tetramethyluronium hexafluorophosphate (HBTU), and 2-(1H-7-azabenzotriazol-1-yl)-1,1,3,3-tetramethyluronium hexafluorophosphate (HATU) that require a base for activation were employed with N, N-Diisopropylethylamine (DIPEA) in peptide synthesis. The completion of each reaction is analyzed and confirmed by the Kaiser test based on the different colors.

After the final coupling and deprotection of the peptide, trifluoroacetic acid (TFA) can be used to cleave the peptide from the solid support. Peptides were separated by using ice-cold diethyl ether from the cleavage cocktail solution. The peptides can be characterized after lyophilization. Mass spectrophotometric techniques were used to confirm the molecular weight of peptides and high-performance liquid chromatography (HPLC) was used to detect and purify peptides.

Circular dichroism (CD) is dichroism involving circularly polarized light, in other words, the differential absorption of left- and right-handed light. CD spectroscopy has a wide range of applications in many different fields, such as determination of the secondary structure of proteins. The far-UV CD spectrum of proteins can reveal important characteristics of their secondary structure. The typical CD spectrum of alpha-helix, the beta-sheet, and random coil are shown in Figure 3.3. The alpha helix of proteins has CD spectral signatures representative of their structures. The secondary structure of peptides designed in α-helix method can be checked by CD.

A series of peptides to PD-L1 will be synthesized by using the solid phase synthesis method. HPLC will be used for the purification of peptides and ESI-MS will be used for determining the m/z value of peptides.

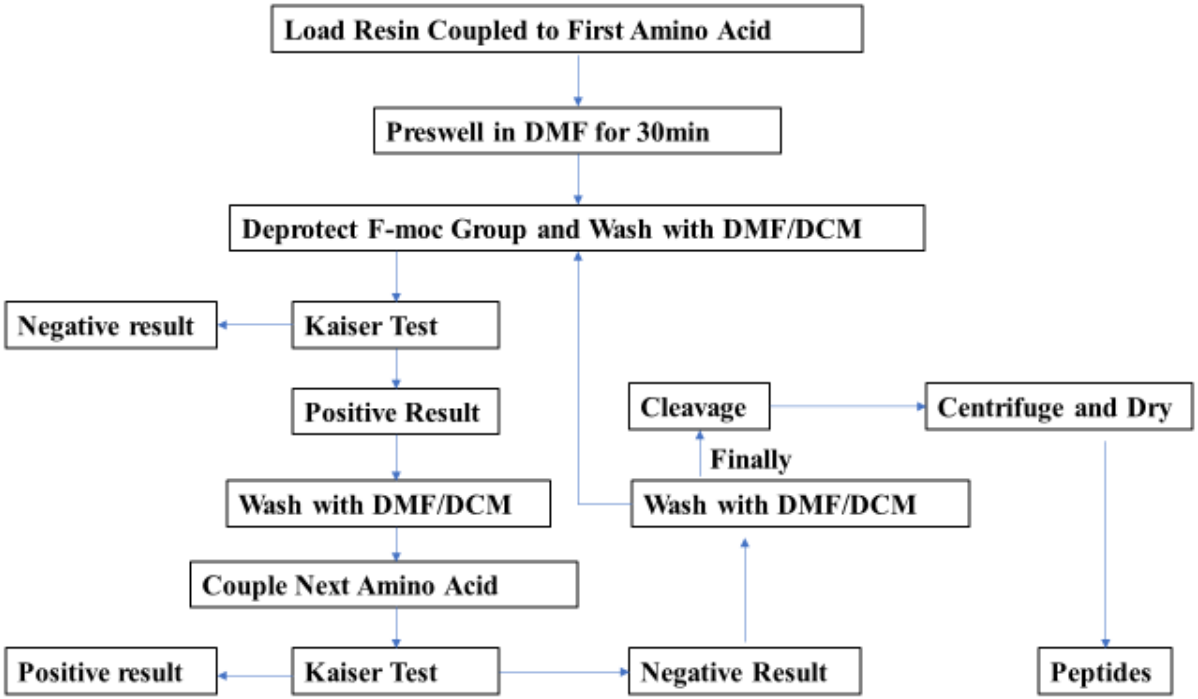

Figure 3.2 Schematic of the Fmoc/tBu peptide synthesis.

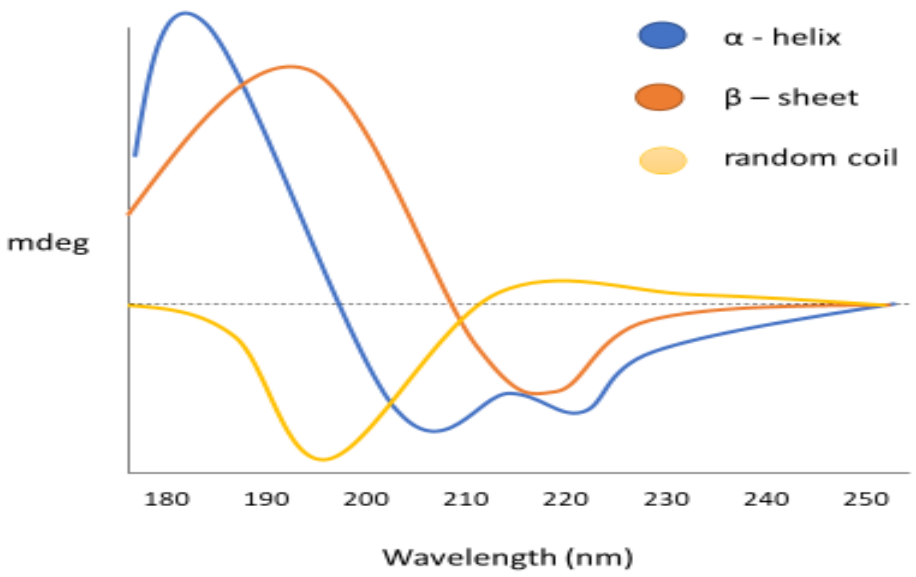

Figure 3.3 The typical spectrum of in an α-helix, β-sheet, and random coil peptide

3.2 Materials

All peptide synthesis reagents including Fmoc-Wang resins, amino acids, N, N'-Diisopropylcarbodiimide (DIC), N, N-Diisopropylethylamine (DIPEA), triisopropylsilane (TIS), N-hydroxybenzotriazole (HOBT), 2-(1H-7-azabenzotriazol-1-yl)-1,1,3,3 tetramethyluronium hexafluorophosphate (HATU), O-(Benzotriazol-1-yl)-N,N,N',N'-tetramethyluronium hexafluorophosphate (HBTU), piperidine, and 6-aminohexanoic acid (Ahx) were purchased from Chem-Impex International Ltd (Wood Dale, IL, USA). Solvents including dichloromethane (DCM), N, N'-dimethyl formamide (DMF), and Acetonitrile (ACN) were of HPLC grade from Fisher Scientific (Pittsburgh, PA, USA). Phenol, diethyl ether, and trifluoroacetic acid (TFA) were obtained from

Acros organics (Pittsburgh, PA, USA). Acetic anhydride was obtained from Mallinckrodt (St. Louis, MO, USA). Fluorescein isothiocyanate (FITC) was purchased from Calbiochem (San Diego, CA, USA). All chemicals and solvents were used without further purification.

3.3 Methods

3.3.1 Synthesis of peptides. The peptides: PDL1-01-25MER, PDL1-06-13MER, PDL1-P13-1, PDL1-P13-28, PDL1-P13-33, PDL1-P13-40, PDL1-P13-55, and PDL1-P13-X were synthesized by the solid phase peptide synthesis method using standard Fmoc chemistry (Table 3.1). First, the Wang resin (0.2 mmol scale) preloaded with the C-terminal end amino acid of these different sequences was preswelled in DMF for 20 minutes, and the amino group of that amino acid was deprotected using 20% piperidine in DMF for 30 minutes. After washing with both DMF and DCM three times, the Fmoc protected amino acid was added with five equivalences of HBTU and HOBT and nine equivalences of DIPEA for three hours. The Kaiser test was performed to estimate the completeness of the coupling by observing the color of resin. The deprotection and coupling procedures were repeated until the last amino acid at the end of N-terminal was attached on to the resin. After every three coupling procedures, capping was performed to block the intermediates that cannot be washed away by using acetic anhydride and DIPEA in the DMF solution. At last, the cleavage of the peptide was conducted by adding the cleavage cocktail of TFA, phenol, deionized water, and TIPS in the ratio 88:5:5:2 and reacting for three hrs. The TFA solution was added into ice-cold diethyl ether to precipitate the peptides. The diethyl ether and peptide mixture were kept at -20˚C overnight to obtain the maximum amounts of products. Ice-cold diethyl ether was used again to collect the precipitate by centrifuging and washing it three times. After that, the peptides were all lyophilized and stored at -80˚C before further using.

3.3.2 Synthesis of FITC-peptide conjugations. In confocal microscopy studies, FITC was commonly used to conjugate onto the N-terminus of the peptides as a fluorescent probe. The Ahx (6-aminohexanoic acid), protected by Fmoc, was used as a linker and was added to the N-terminus of the peptides using the same method as that of amino acids. Three equivalents of FITC were dissolved in anhydrous DMF with 10 equivalents of DIPEA and agitated overnight in the dark. FITC-peptide conjugations were then cleaved from the resin by using the cleavage cocktail containing TFA, phenol, deionized water, and TIPS in the ratio 88:5:5:2 without the deprotection procedure. After three hours of shaking, the mixture was added into ice-cold diethyl ether to form precipitation. Ice-cold diethyl ether was used again to collect the precipitate by centrifuging and washing it three times. After that, the FITC-peptide conjugations were all lyophilized and stored at -80˚C before further using.

3.3.3 Characterization of all peptides and FITC-peptide conjugations.

Peptides were characterized by MALDI-TOF (Shimadzu-Kratos PC Axima CFR V2.2.1) using α-Cyano-4-hydroxycinnamic acid (CHCA) as a matrix or Electro-Spray Ionization Mass Spectrometry (ESI-MS, Varian 320 ESI-triple-quadrupole mass spectrometer). Samples were prepared in methanol and water in a 1:1 ratio. The purity of all compounds was determined by high-performance liquid chromatography (HPLC), Agilent 1100 Series, using Agilent Zorbax SB-C18, 3.5µm, 4.6 × 150 mm, column. Water with 0.1% TFA (A) and acetonitrile with 0.1% TFA (B) were used as the mobile phase. Both analyzation and purification were performed in the same HPLC column by collecting the separated fractions, and then the peptides were lyophilized and stored at -80˚C before further analysis.

3.3.4 Characterization of secondary structure for peptides in alpha helix design. The secondary structure for peptides in alpha helix design were characterized by Spectra Manager Version 2 software in Jasco J-810 spectropolarimeter. Samples were prepared in methanol and water in a 1:1 ratio.

3.4 Results and discussion

All peptides were successfully synthesized by the solid phase peptide synthesis method. In the binding studies, these peptides without FITC will be tested with PD-L1 protein using the Surface Plasmon Resonance (SPR) technique. To build the peptide chain, it is necessary to repeat deprotection and coupling protocols in the synthesis of these peptides. Most of the amino acids were coupled using five folds excess in three hours. However, a certain amino acid such as arginine took double couplings in two

hours. HBTU, a stronger coupling agent with DIPEA, was performed to complete the coupling procedure instead of DIC when the amino acid was not conjugated to the resin. The presence of free primary amino groups was checked by the Kaiser test, which is a useful way to determine the completeness of a coupling step. The peptides were separated from the side products and other impurities by using HPLC with a hydrophobic C18 column after the cleavage step. It was necessary to add 0.1% TFA into the mobile phases since the behavior of some C18 columns greatly relied on strong ion pairing agents that could enhance the shape and resolution of the peak. Additionally, it was easy for TFA to volatilize and it had a low absorption within the detection wavelengths. The desired peaks were finally separated and purified. The final purity of the peptide is shown in Table 3.1 and HPLC peaks of all the peptides are shown from Figures 3.15 to 3.20.

Different peaks were collected to identify and confirm by MS. All the peptides with or without FITC were characterized by ESI MS. The MS results showed the desired molecular weight of the peptides. The desired peptides with right molecular weight were obtained from the analyses of the mass spectrum. The MS spectra are shown from Figure 3.3 to 3.8.

FITC labeled peptides were synthesized as well for cellular uptake studies by using the confocal microscopy technique. During cleavage, N-terminal FITC-labeled peptides undergo a cyclization, resulting in the development of a fluorescein followed by the removal of the last amino acid on the peptide. It is difficult to conjugate FITC onto the N-terminus of the amino acid because of Edman degradation during the reaction

which leads to an unexpected product. An alkyl spacer 6-aminohexanoic acid (Ahx) was added at N-terminus of the peptide, and then the Ahx group provided FITC with space which resulted in the acquiring of the desired product [112]. Additionally, the influence of FITC to the binding/function of peptides can also be reduced by the attachment of the Ahx group [113]. FITC labeled peptides were successfully synthesized based on the analyses of the mass spectrum. The MS spectra of FITC labeled peptides are shown from Figure 3.9 to 3.14. The MS results showed the desired molecular weight of the peptide and were confirmed by the products with their m/z values detected in ESI-MS. For all the FITC conjugated peptides, the final purity was checked by the HPLC analysis using the same methods mentioned before. The final purity of the FITC labeled peptide is shown in Table 3.1, and the HPLC peaks of all the FITC-peptides are shown from Figures 3.21 to 3.26.

The secondary structure for peptides in alpha helix design was determined by Circular Dichroism. The CD spectrum of PDL1-01-25MER is shown in Figure 3.27. The results showed the desired figure but the low ratio of α-helical structure of peptide in alpha helix design.

Peptides and FITC-peptides were successfully synthesized by using the solid phase peptide synthesis and were characterized by MS and HPLC. FITC was successfully conjugated to the N-terminus of the peptides. The binding specificity and affinity towards PD-L1 will be discussed later.

Table 3.1 Sequence of peptides for synthesis

Peptides	**Primary structure**	**MW [M+3H]3+**	**HPLC Purity (%)**
PDL1-01-25MER	YGNLARKIAELEKLL-AEAQQREALG	697.3	98
PDL1-06-13MER	IAKARAQLEQFAS	478.4	94
PDL1-P13-01	RKIPLSIGQTHSE	550.2	99
PDL1-P13-28	RKFPLSKGQTHSE	505.8	99
PDL1-P13-33	RKFPSSFGQTHSE	503.4	95
PDL1-P13-40	RKIPHSKGQTHSE	502.4	95
FITC-PDL1-P13-01	FITC-RKIPLSIGQTHSE	717.7	93
FITC-PDL1-P13-28	FITC-RKFPLSKGQTHSE	673.4	95
FITC-PDL1-P13-33	FITC-RKFPSSFGQTHSE	670.9	94
FITC-PDL1-P13-40	FITC-RKIPHSKGQTHSE	669.9	94
FITC-PDL1-P13-55	FITC-RKVPHSIGQTHSE	660.3	96
FITC-PDL1-P13-X (Control)	FITC-RQSKLHPGSKTFE	673.4	93

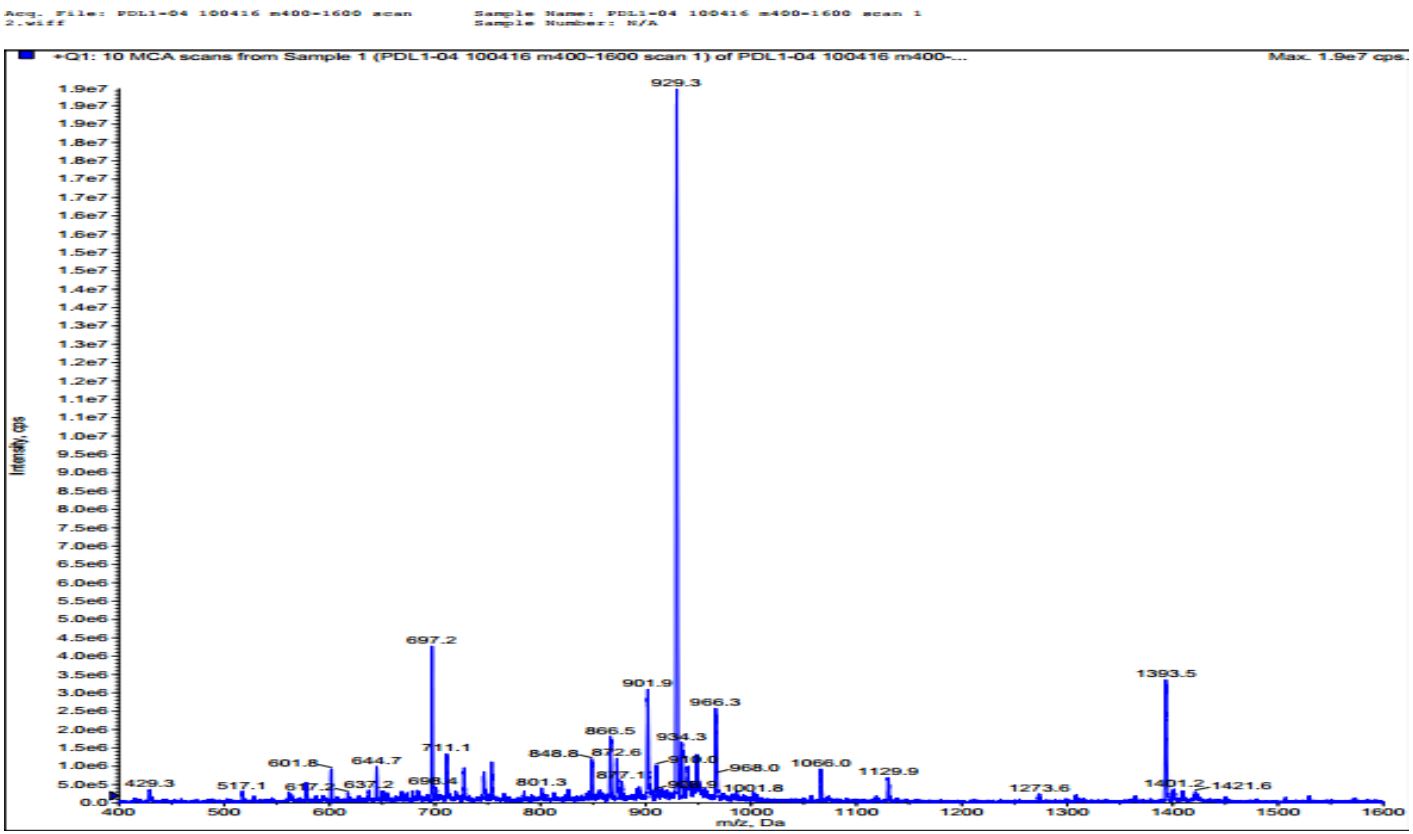

Figure 3.4 ESI-MS spectrum of PDL1-01-25MER, MW: (M+3H)3+ 697.3

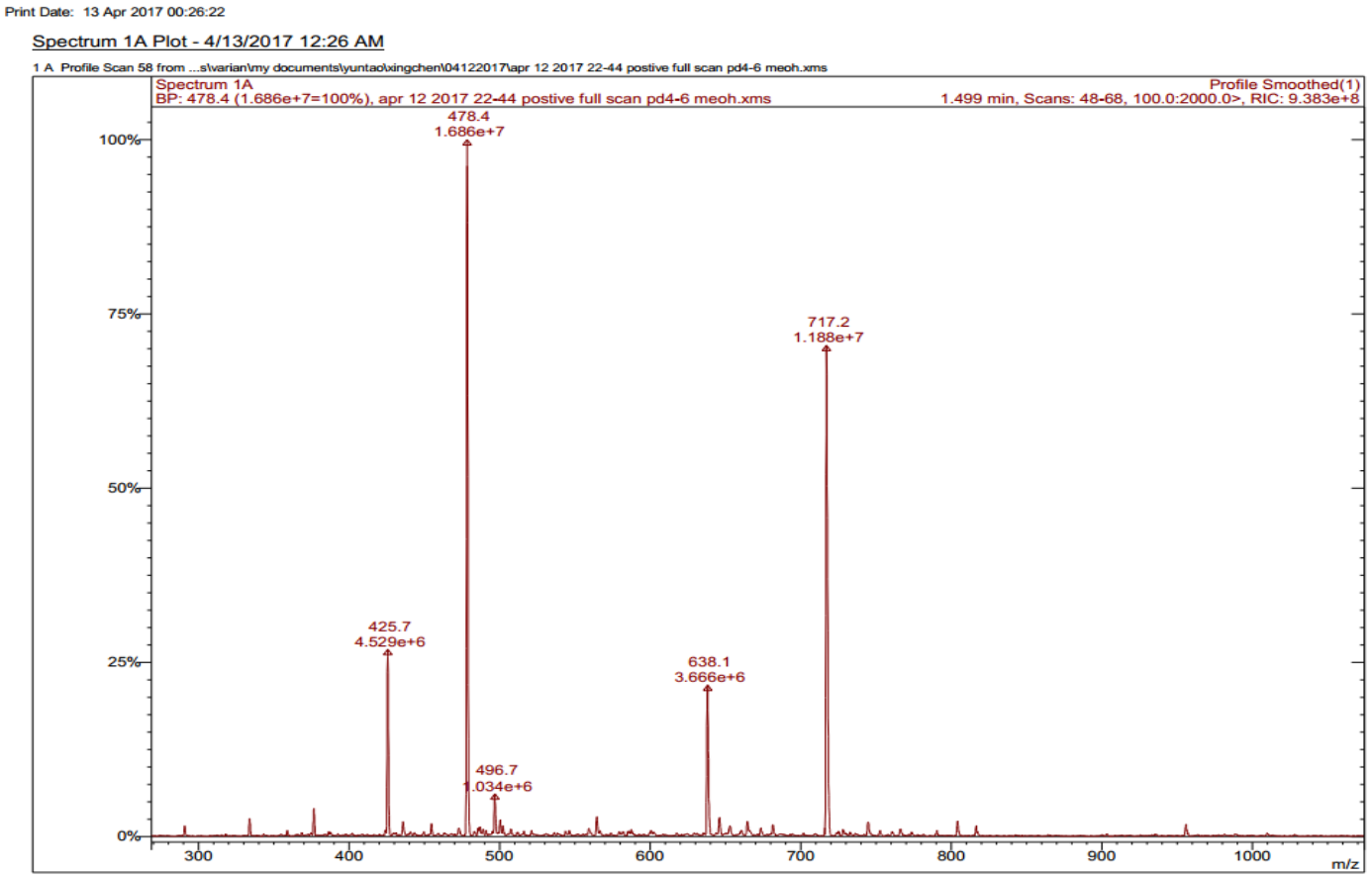

Figure 3.5 ESI-MS spectrum of PDL1-06-13MER, MW: (M+3H)3+ 478.4

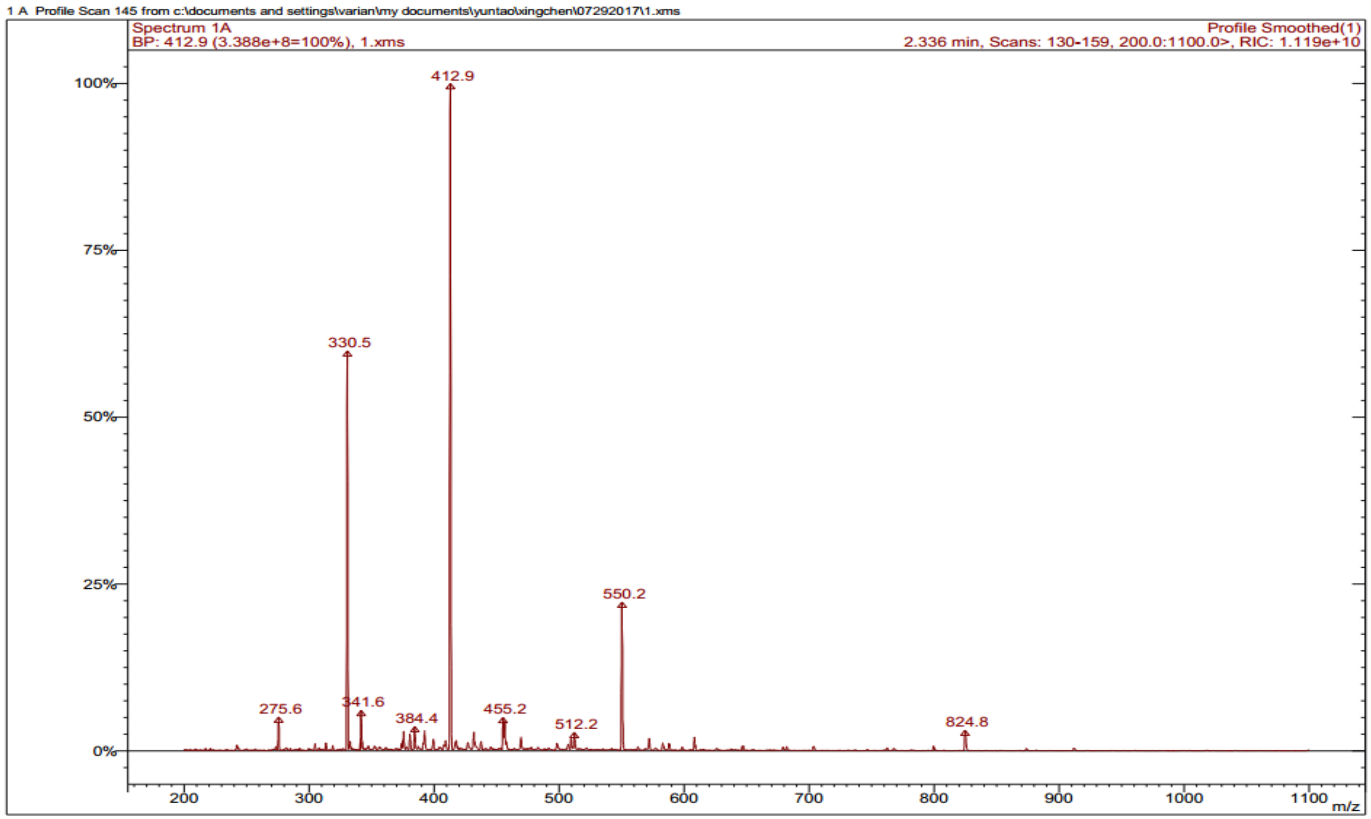

Figure 3.6 ESI-MS spectrum of PDL1-P13-01, MW: (M+3H)3+ 550.2

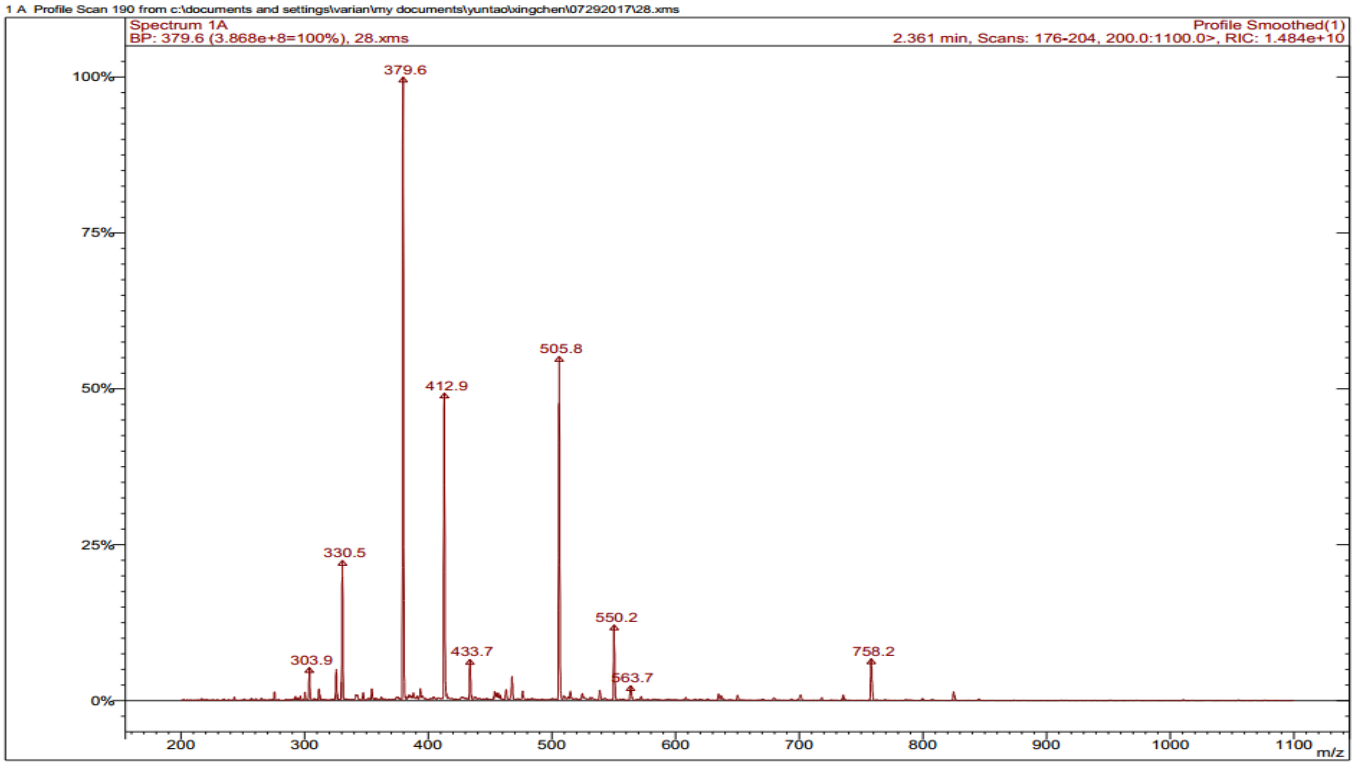

Figure 3.7 ESI-MS spectrum of PDL1-P13-28, MW: (M+3H)3+ 505.8

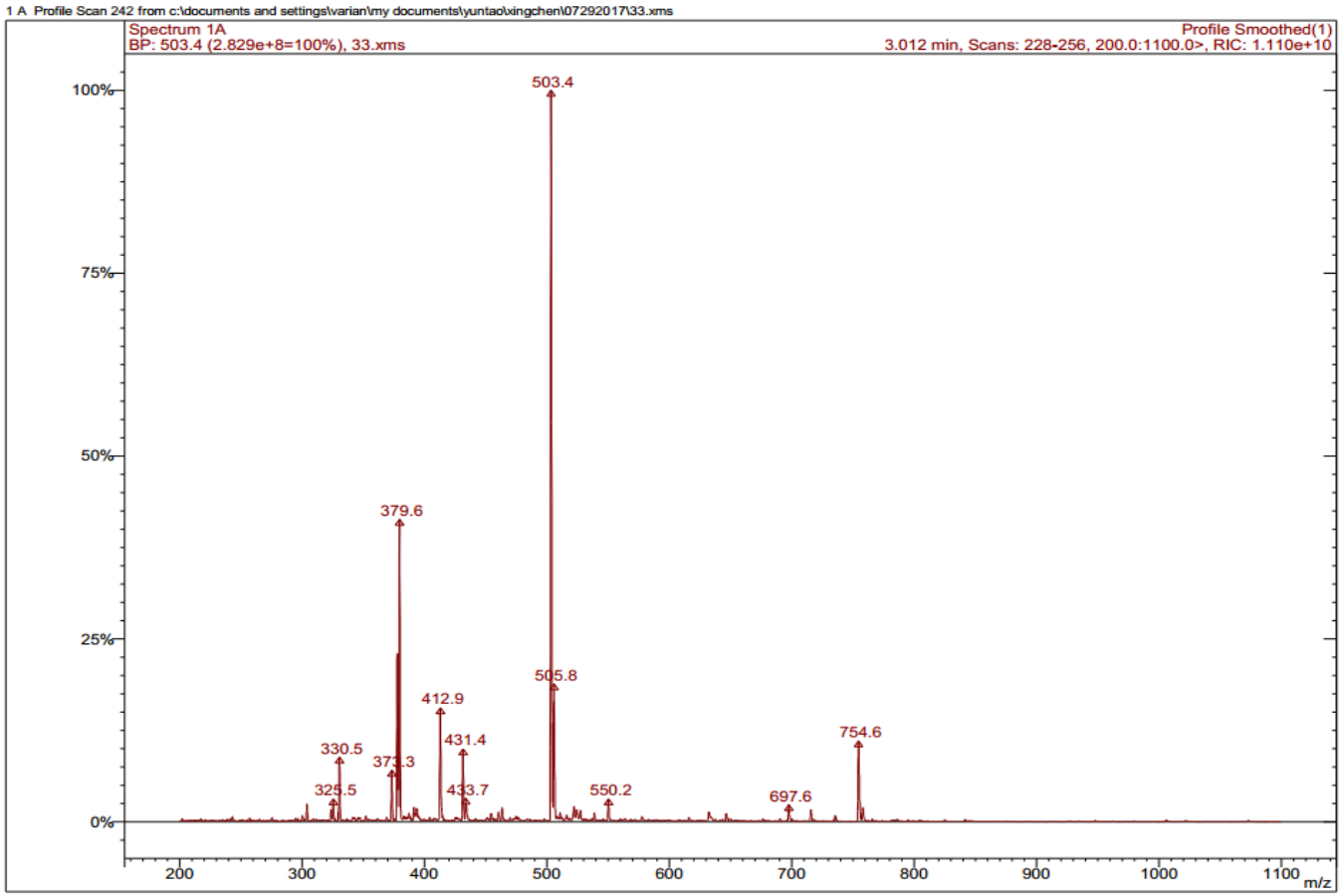

Figure 3.8 ESI-MS spectrum of PDL1-P13-33, MW: (M+3H)3+ 503.4

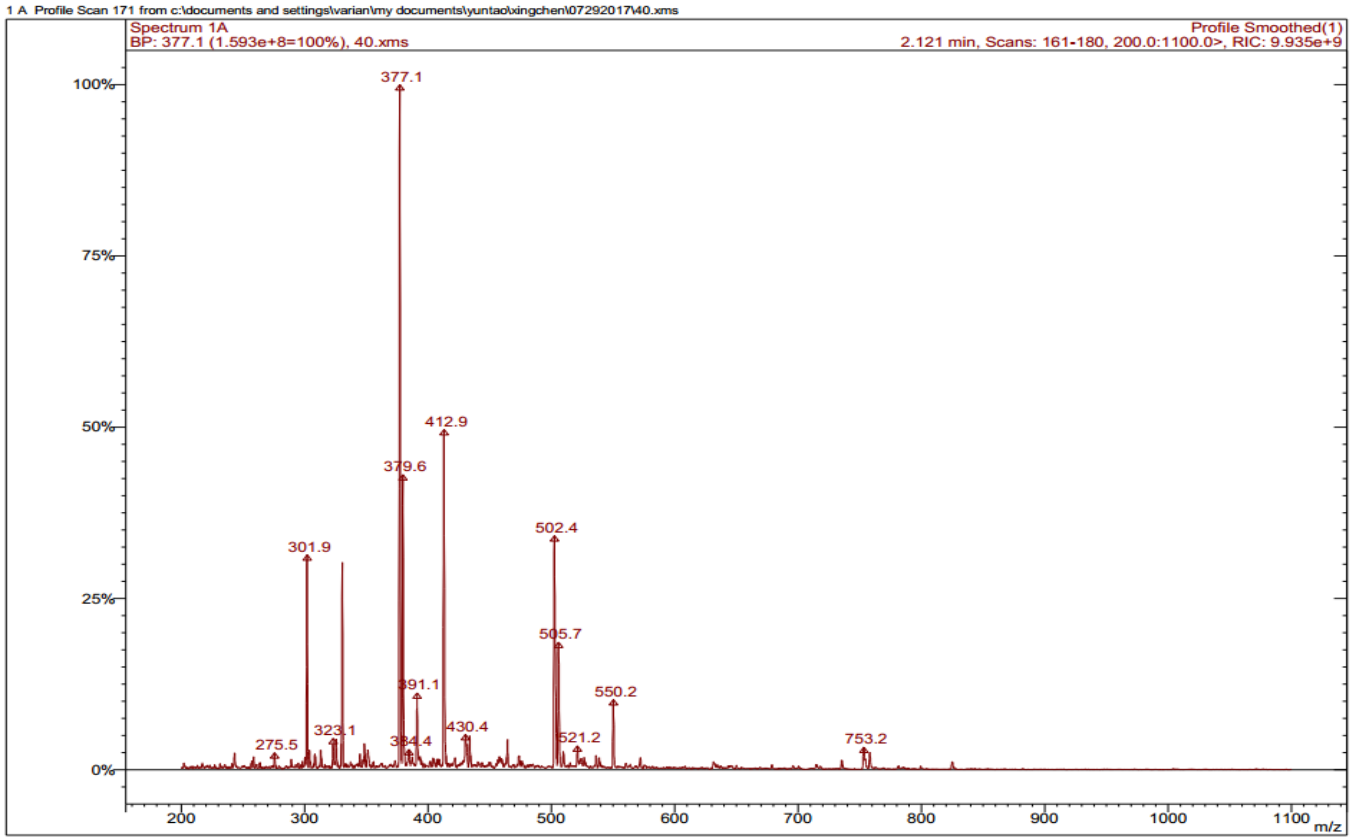

Figure 3.9 ESI-MS spectrum of PDL1-P13-40, MW: (M+3H)3+ 502.4

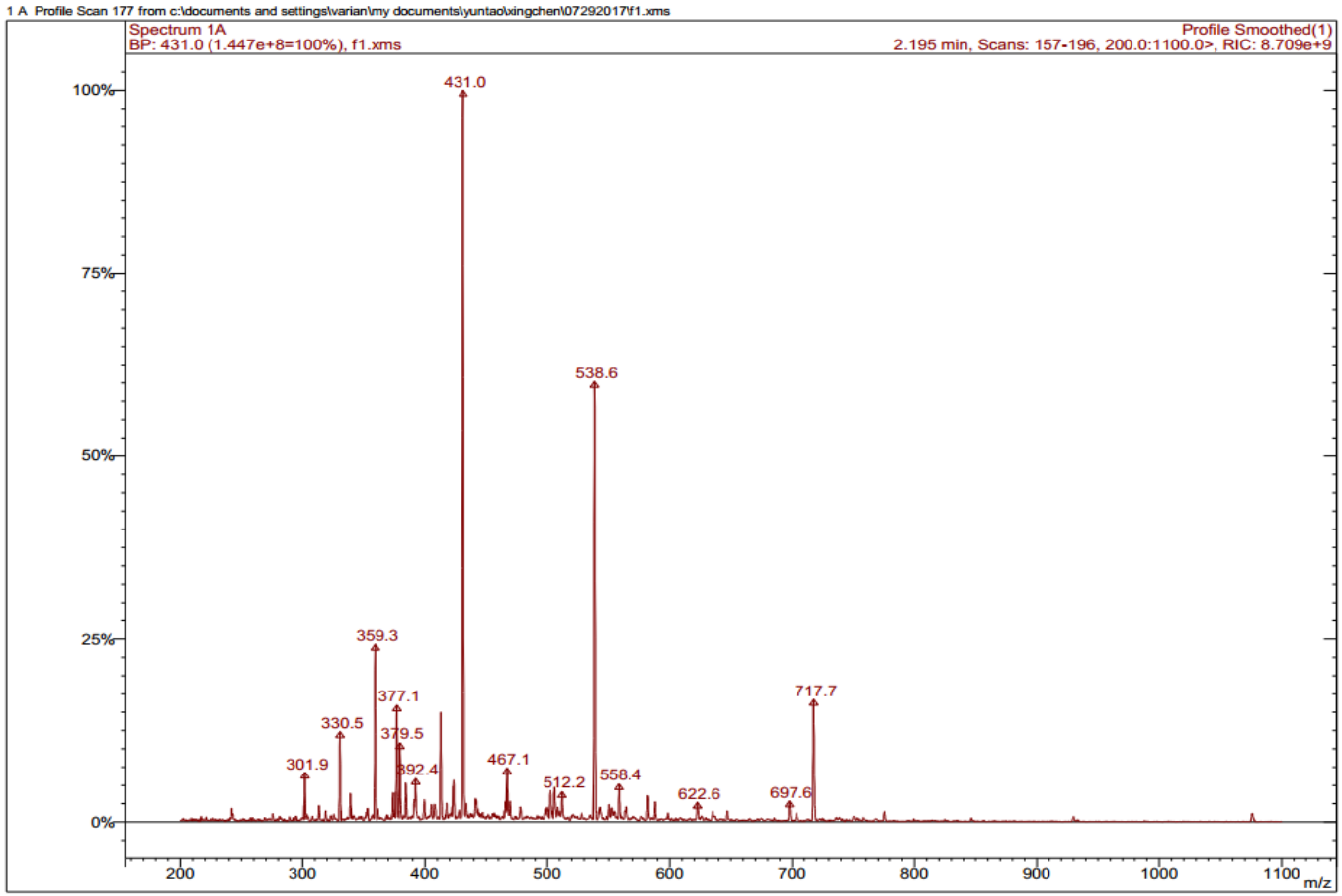

Figure 3.10 ESI-MS spectrum of FITC-PDL1-P13-01, MW: (M+3H)3+ 717.7

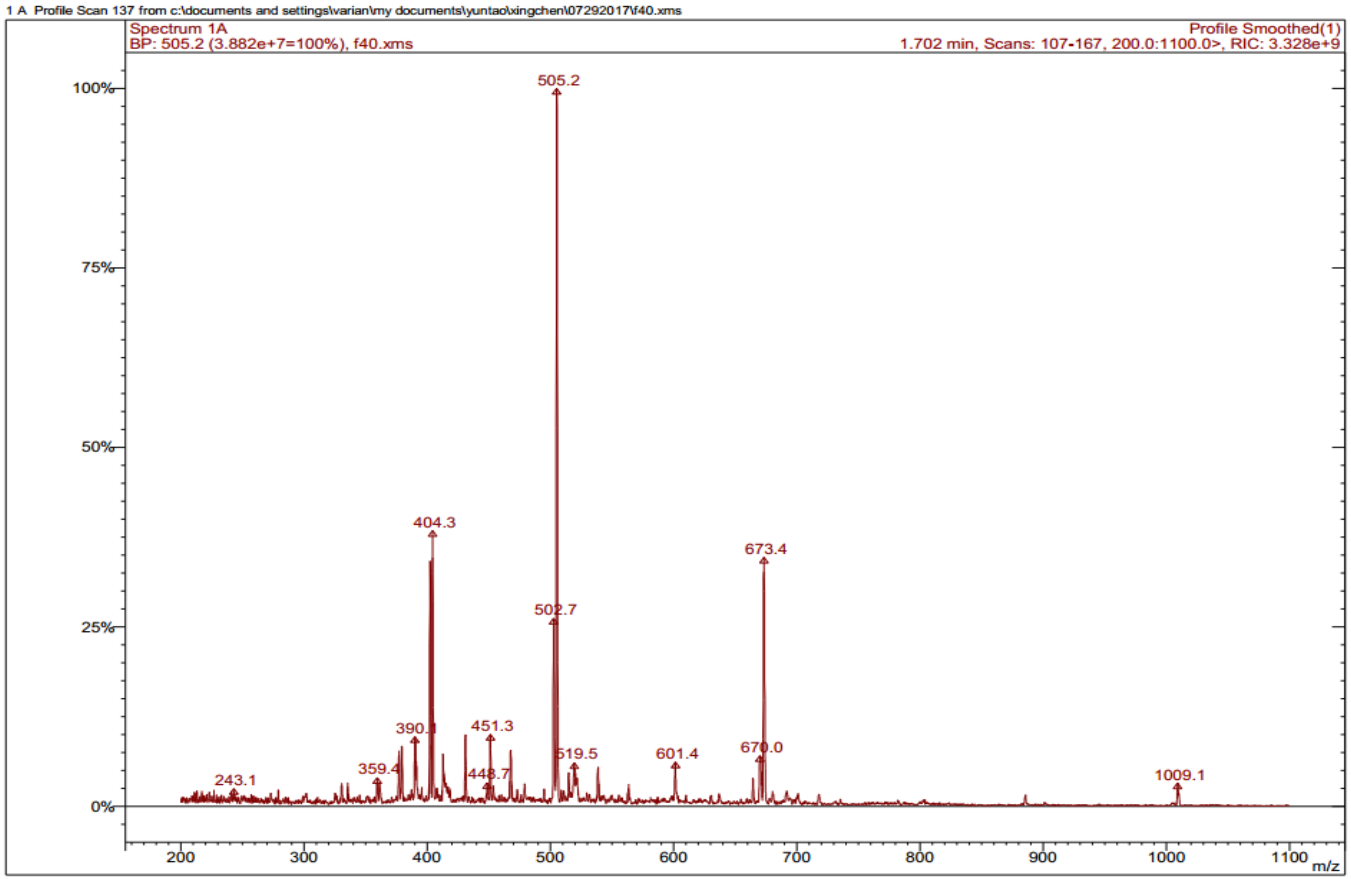

Figure 3.11 ESI-MS spectrum of FITC-PDL1-P13-28, MW: (M+3H)3+ 673.4

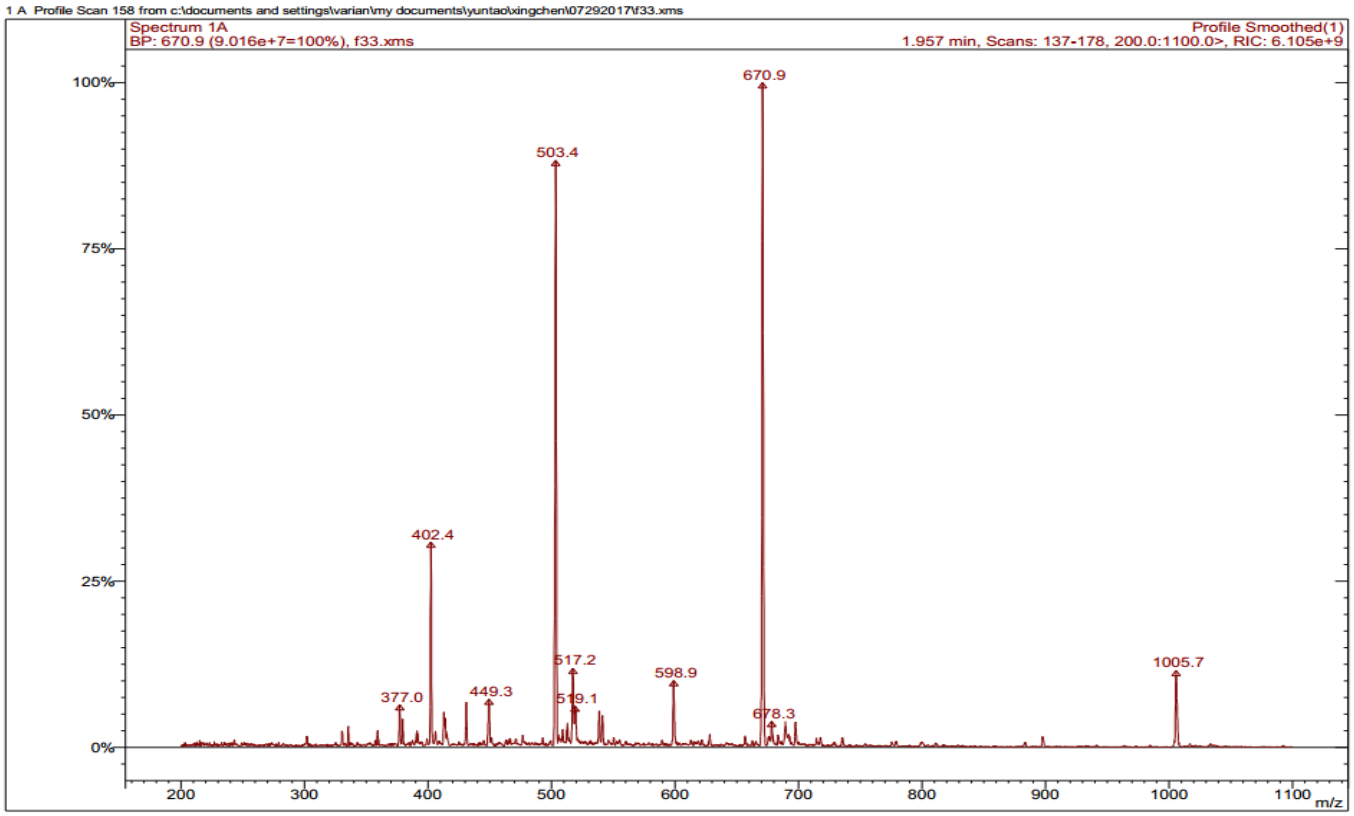

Figure 3.12 ESI-MS spectrum of FITC-PDL1-P13-33, MW: (M+3H)3+ 670.9

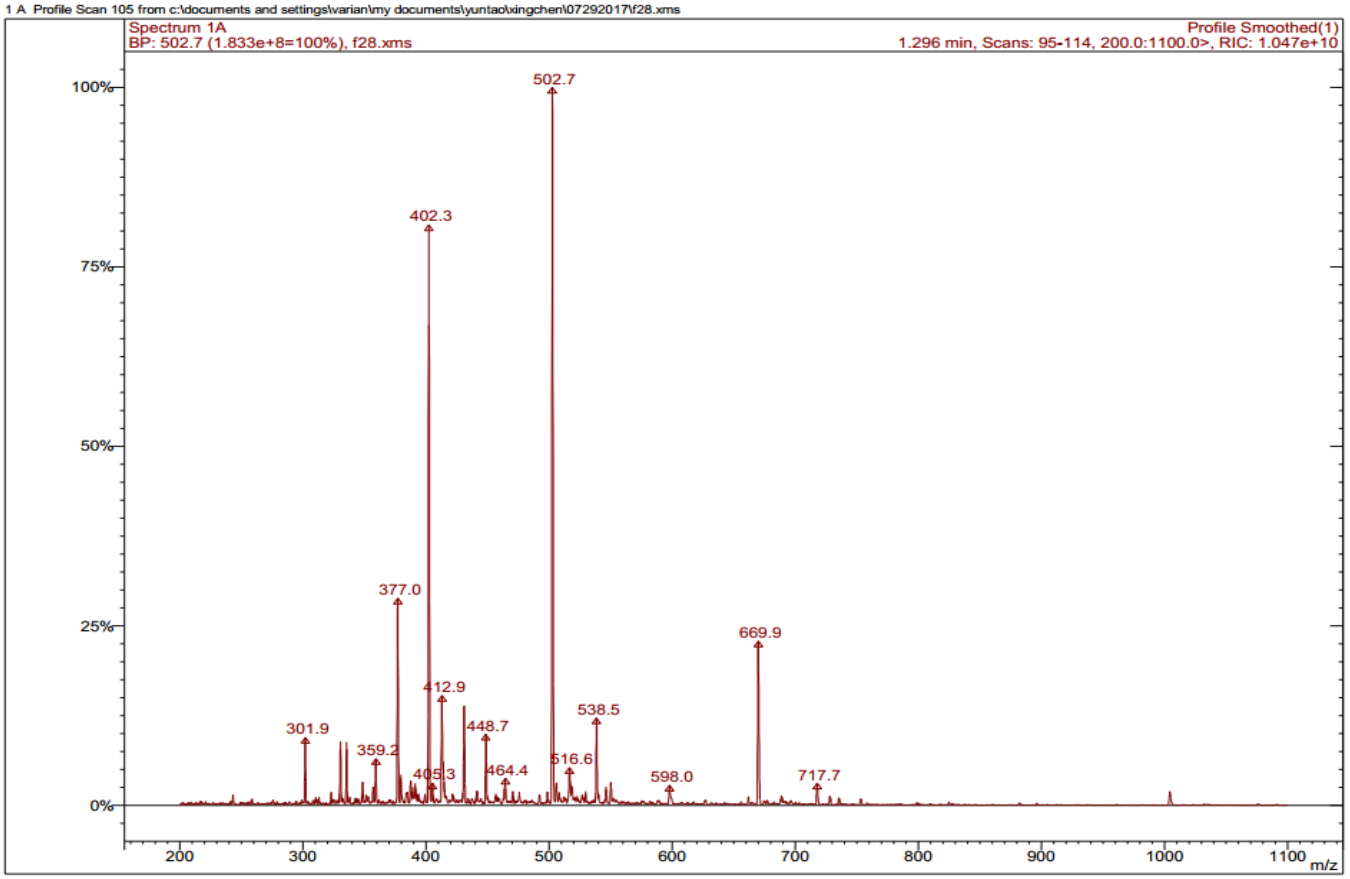

Figure 3.13 ESI-MS spectrum of FITC-PDL1-P13-40, MW: (M+3H)3+ 669.9

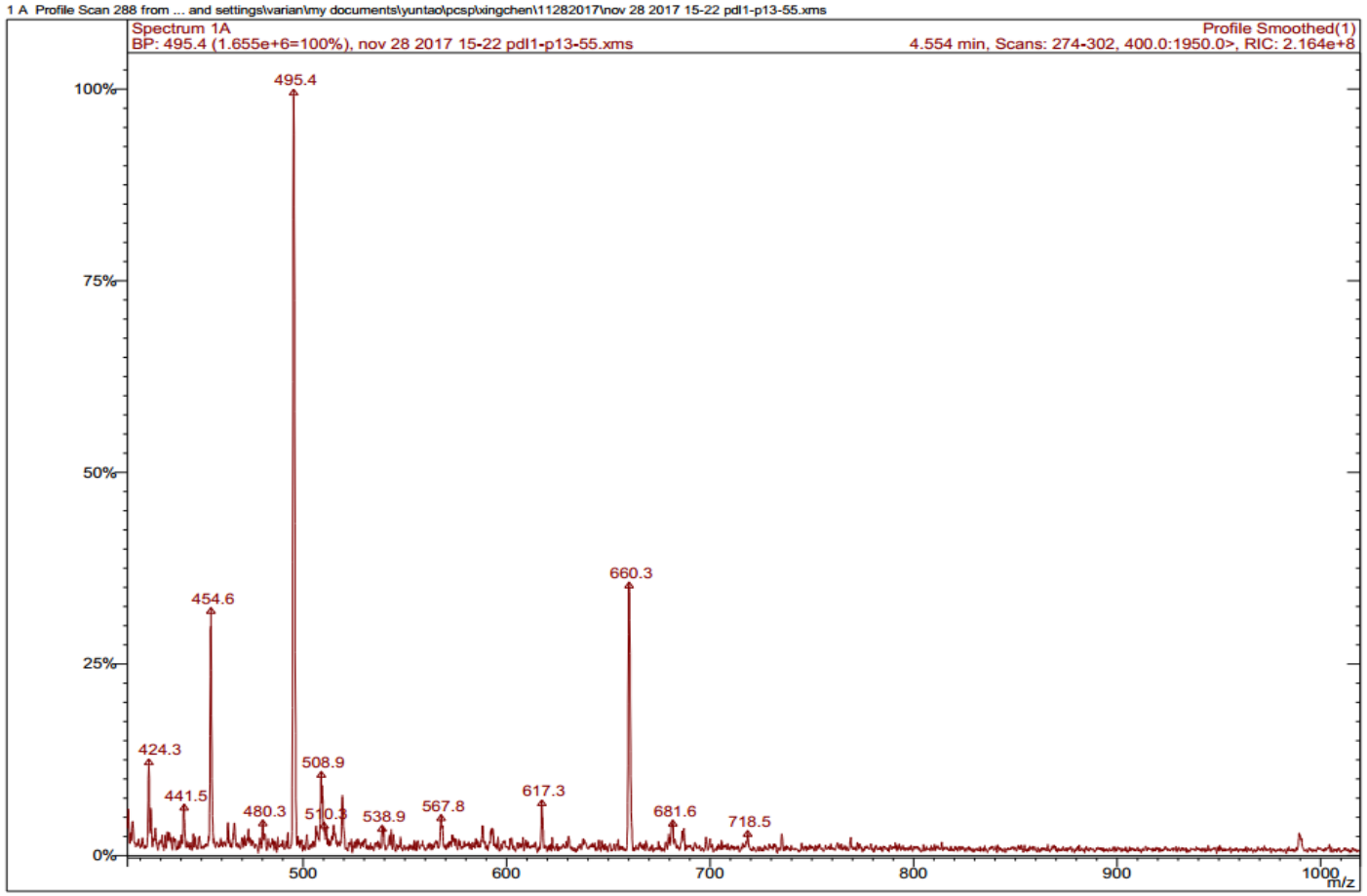

Figure 3.14 ESI-MS spectrum of FITC-PDL1-P13-55, MW: (M+3H)3+ 660.3

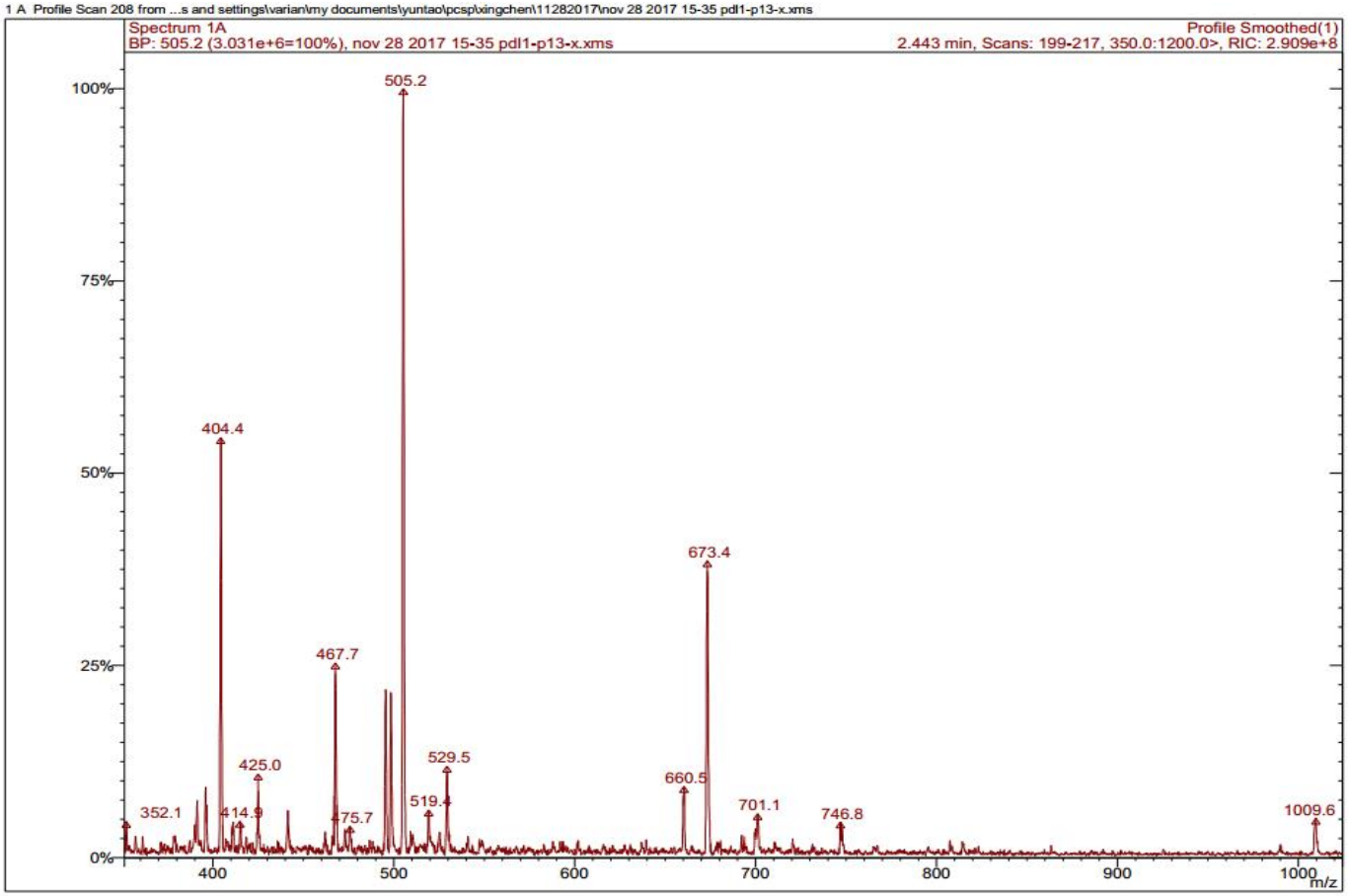

Figure 3.15 ESI-MS spectrum of FITC-PDL1-P13-X, MW: (M+3H)3+ 673.4

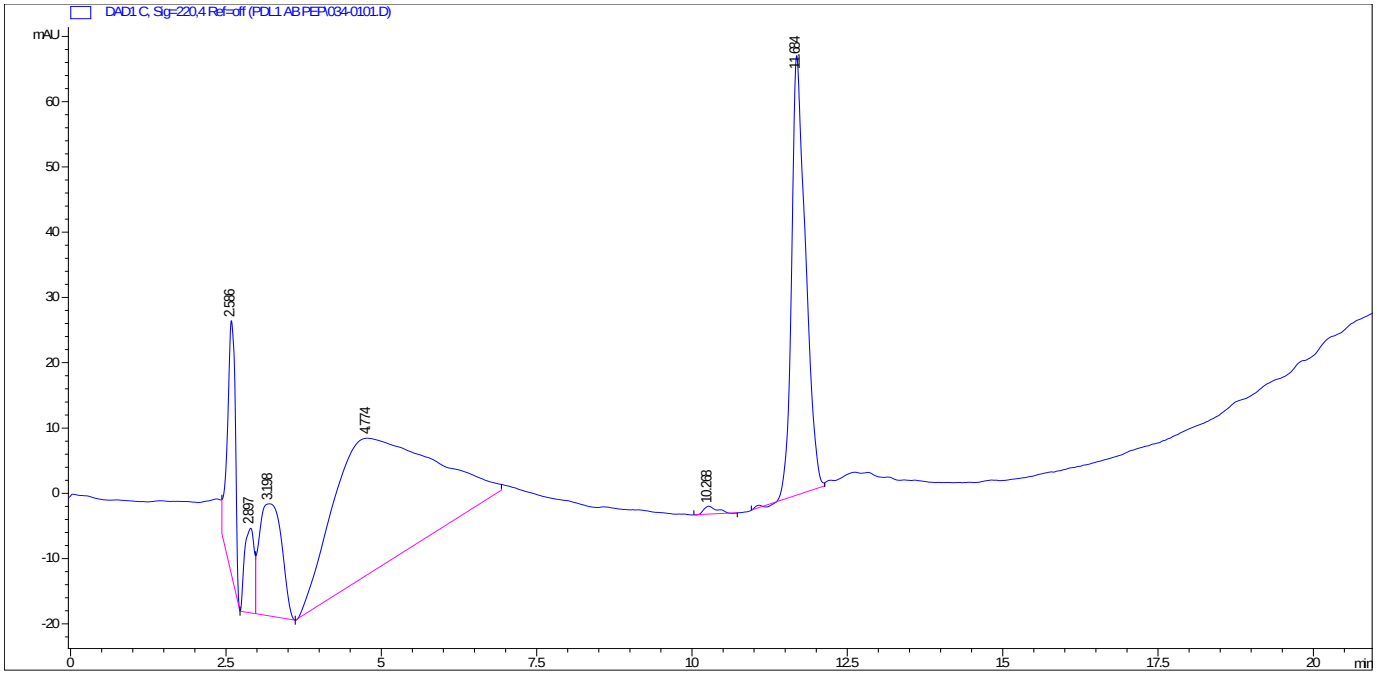

Figure 3.16 HPLC chromatogram of PDL1-01-25MER

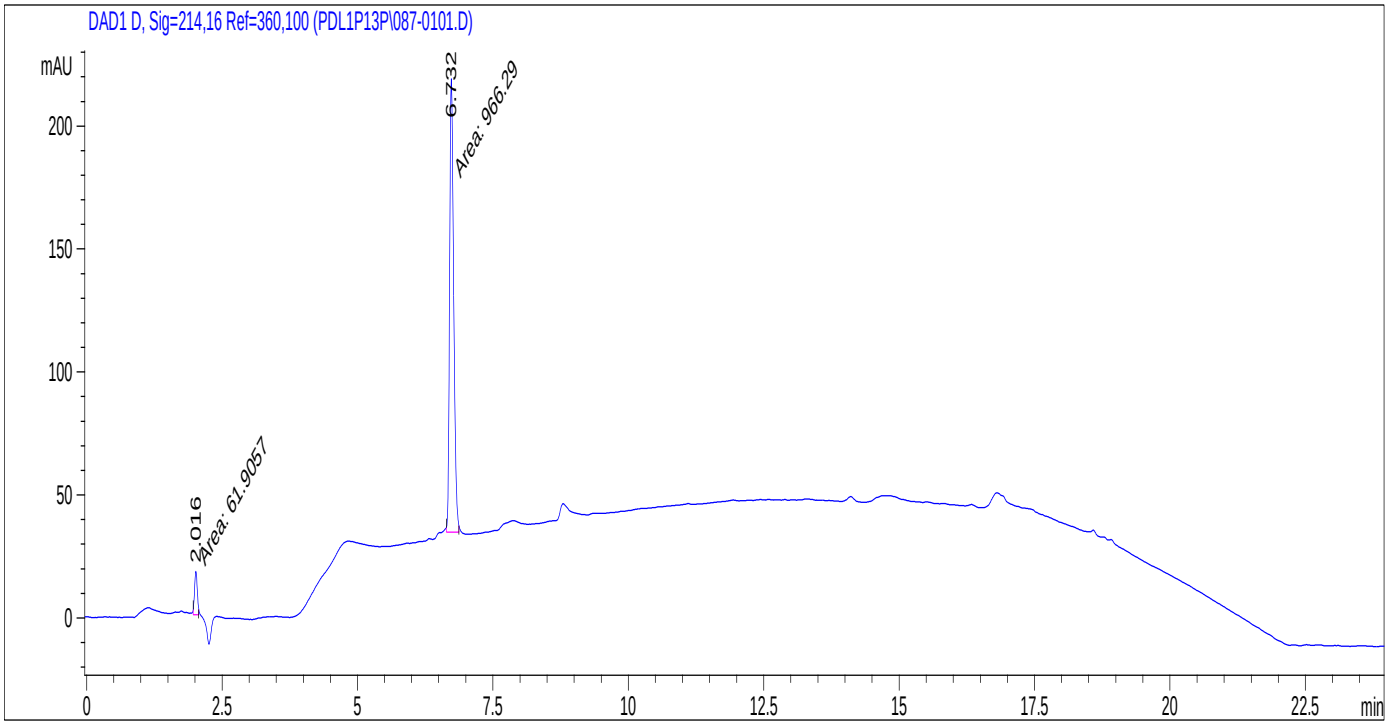

Figure 3.17 HPLC chromatogram of PDL1-06-13MER

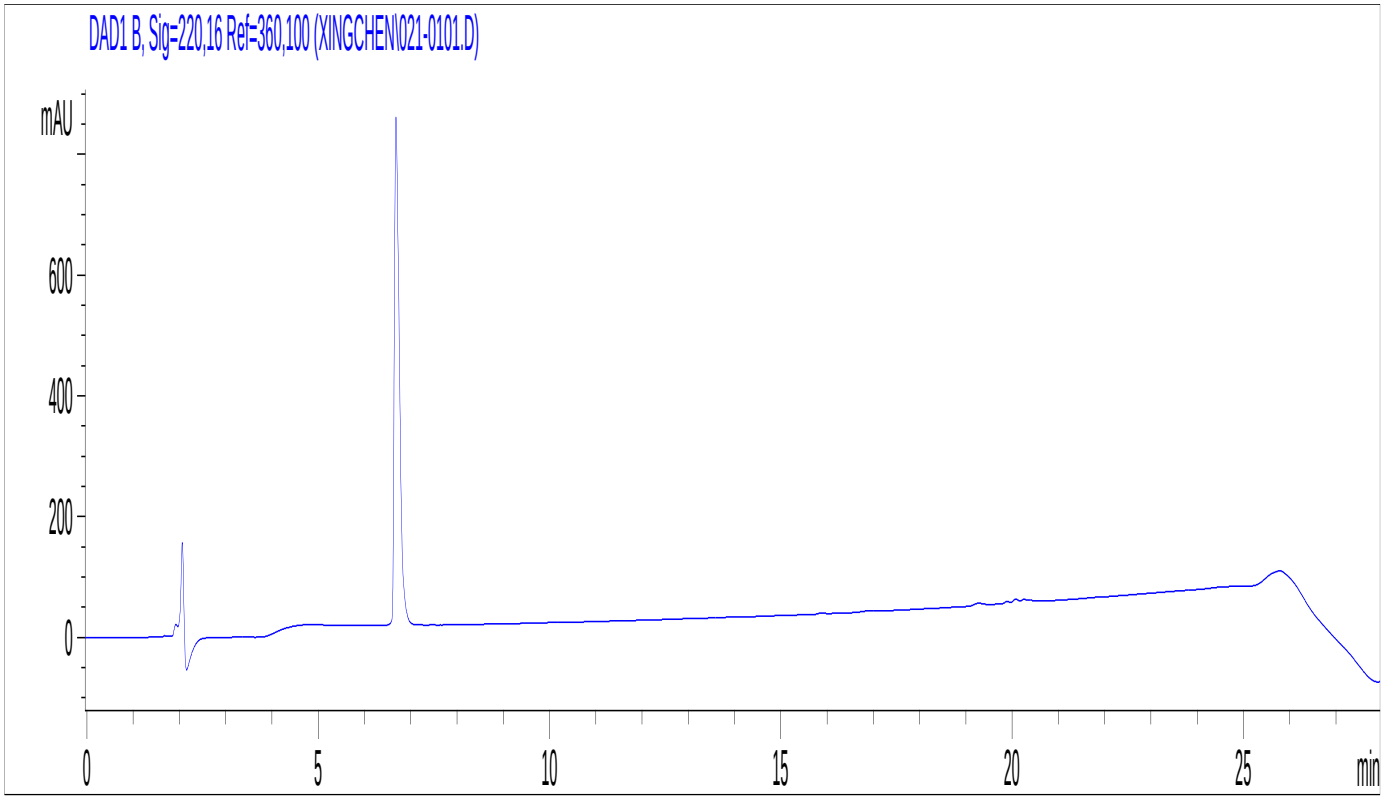

Figure 3.18 HPLC chromatogram of PDL1-P13-01

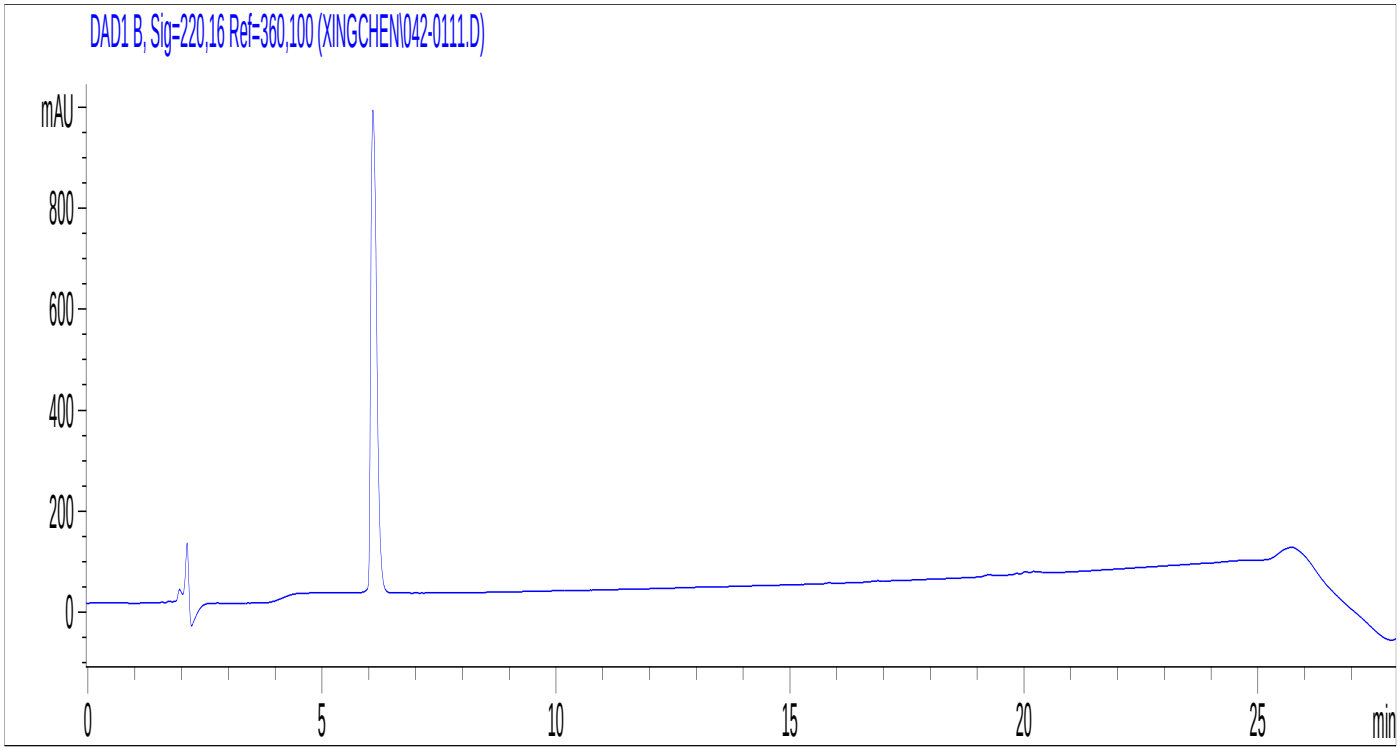

Figure 3.19 HPLC chromatogram of PDL1-P13-28

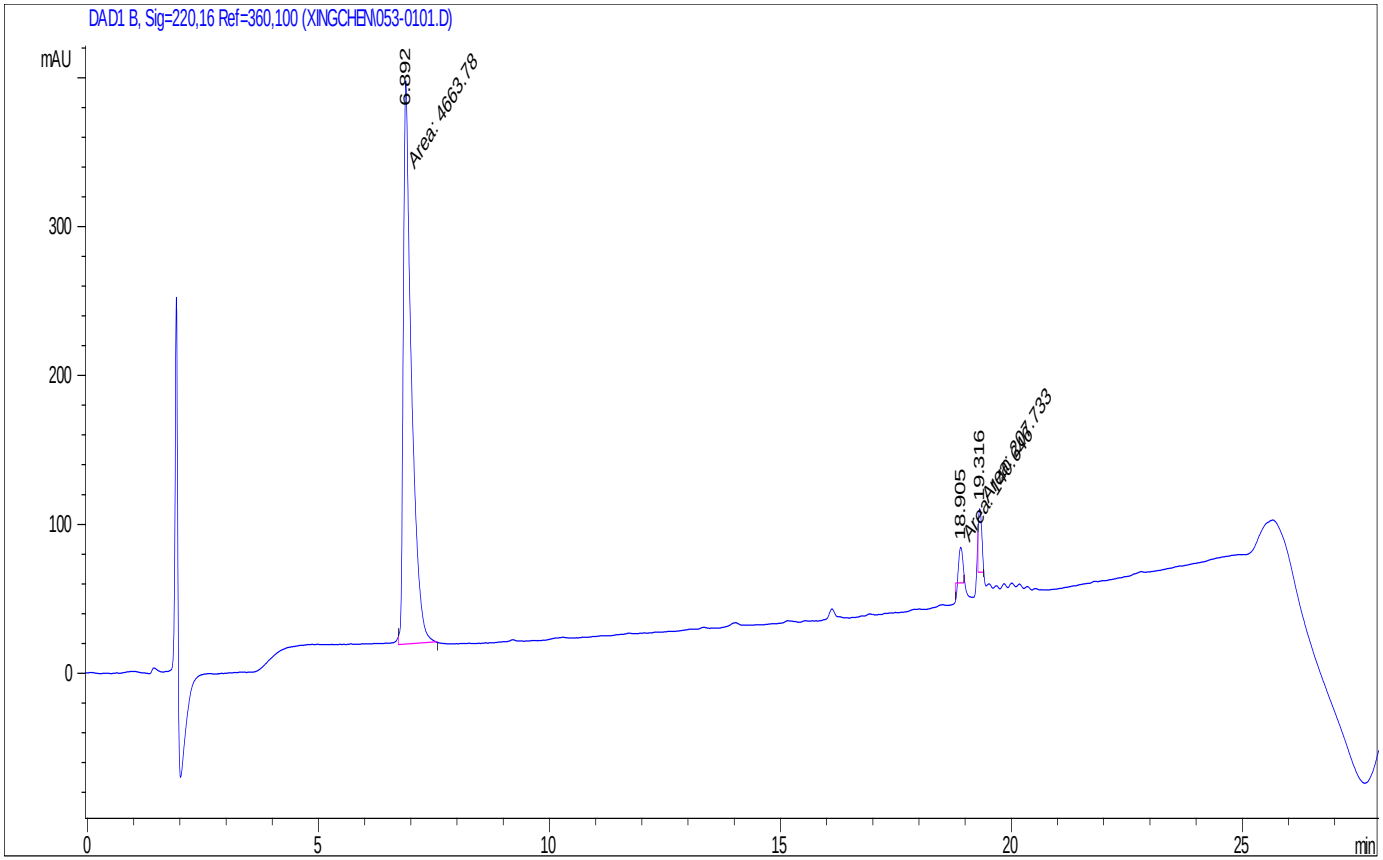

Figure 3.20 HPLC chromatogram of PDL1-P13-33

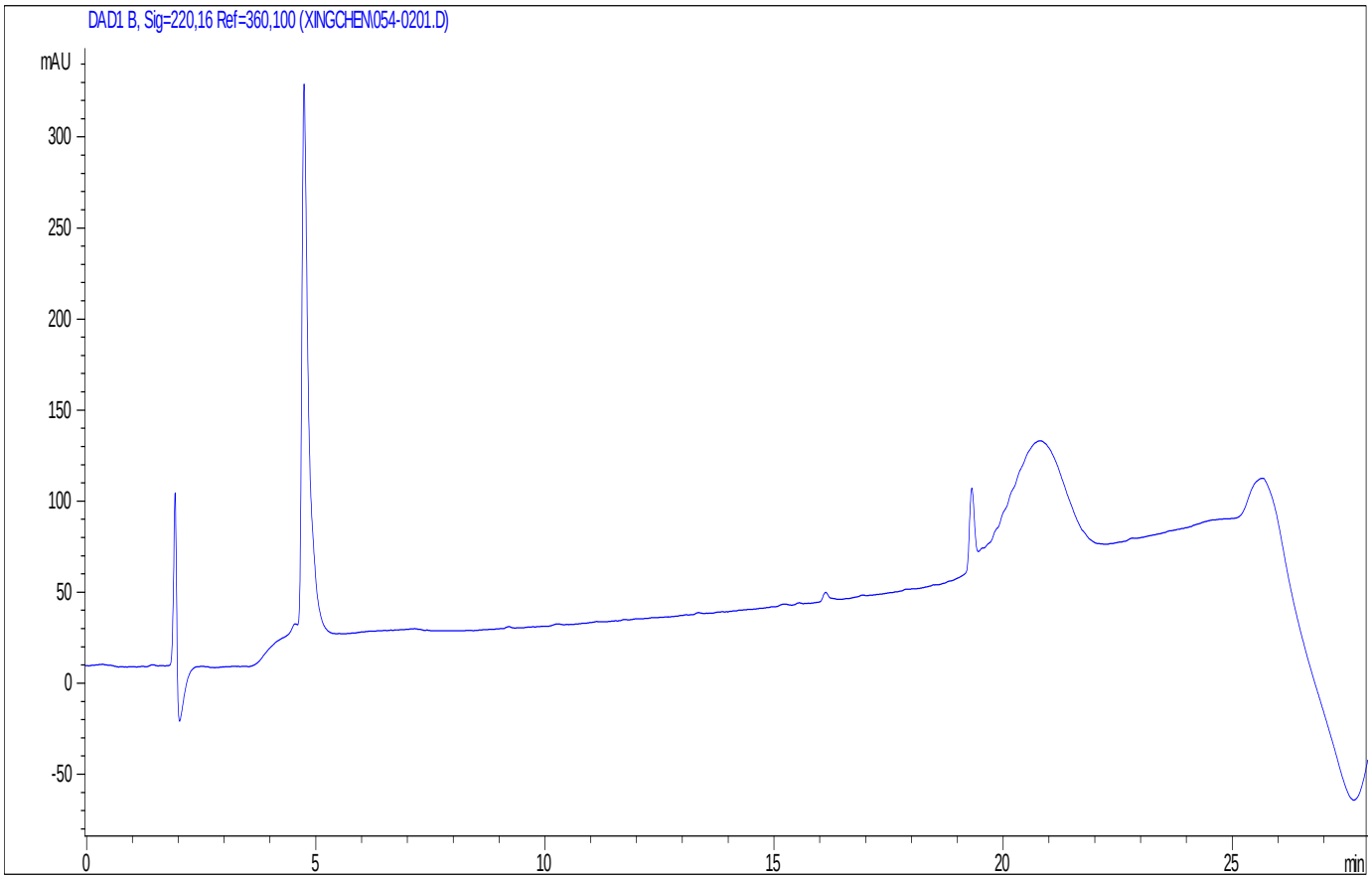

Figure 3.21 HPLC chromatogram of PDL1-P13-40

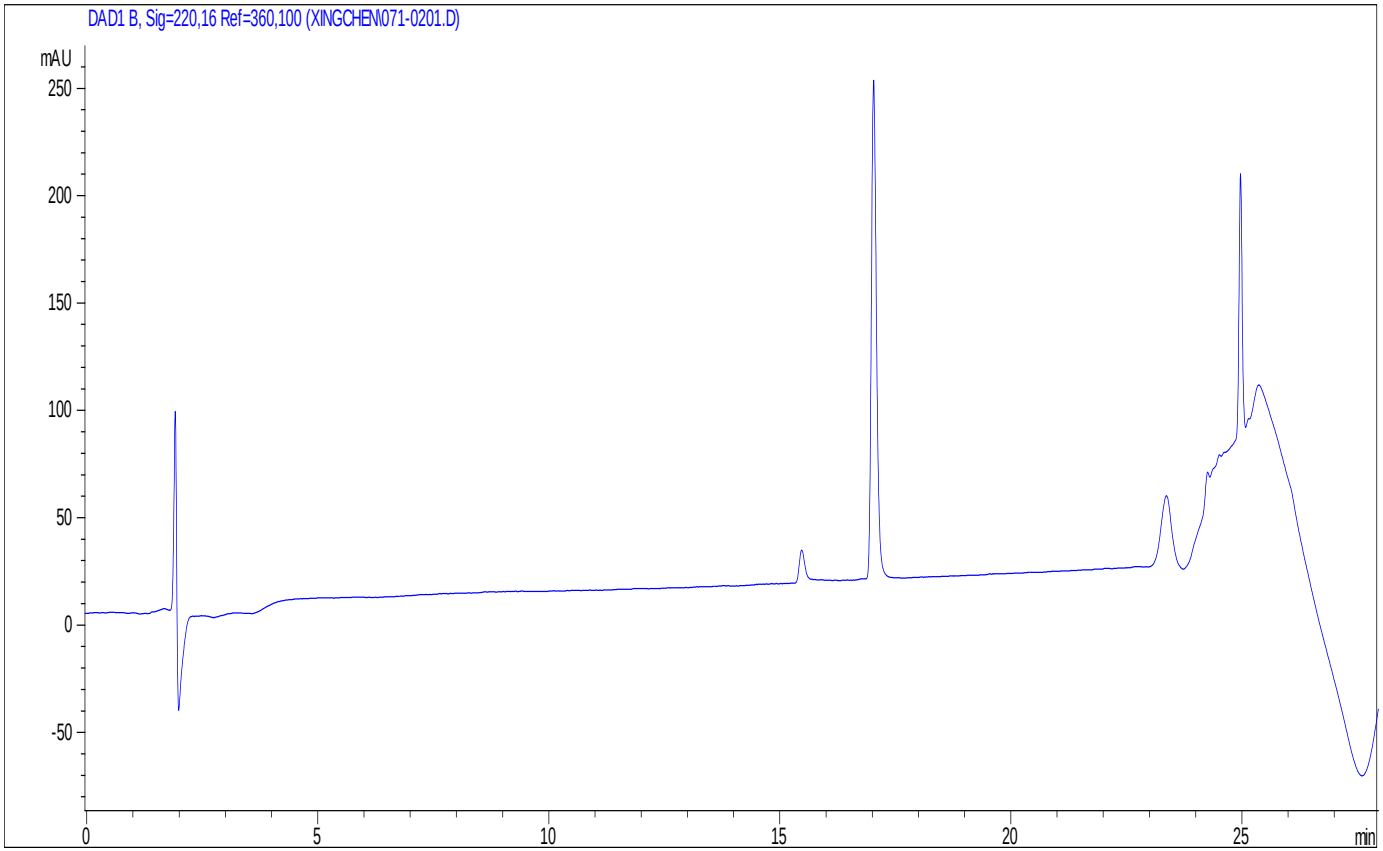

Figure 3.22 HPLC chromatogram of FITC-PDL1-P13-01

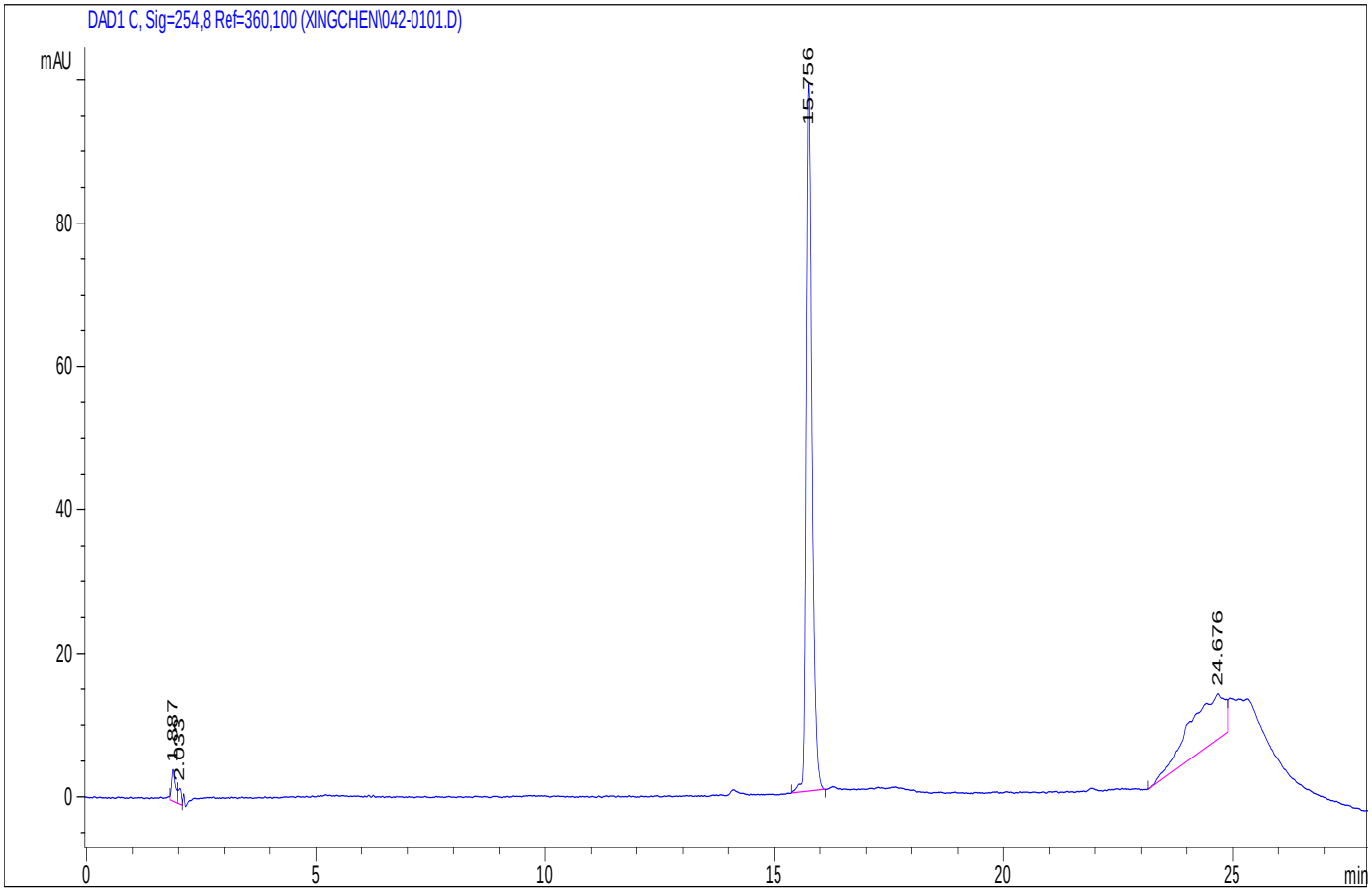

Figure 3.23 HPLC chromatogram of FITC-PDL1-P13-28

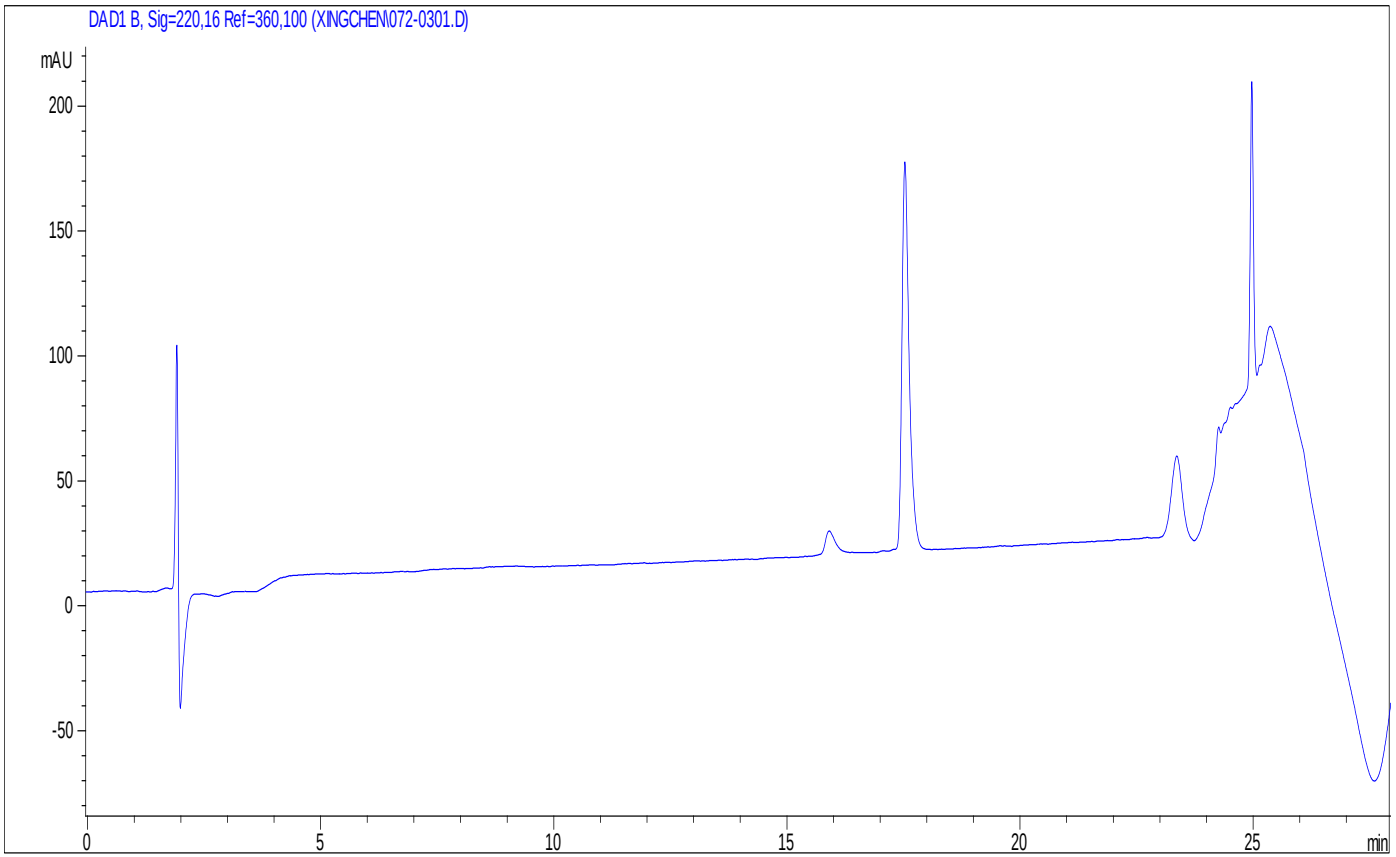

Figure 3.24 HPLC chromatogram of FITC-PDL1-P13-33

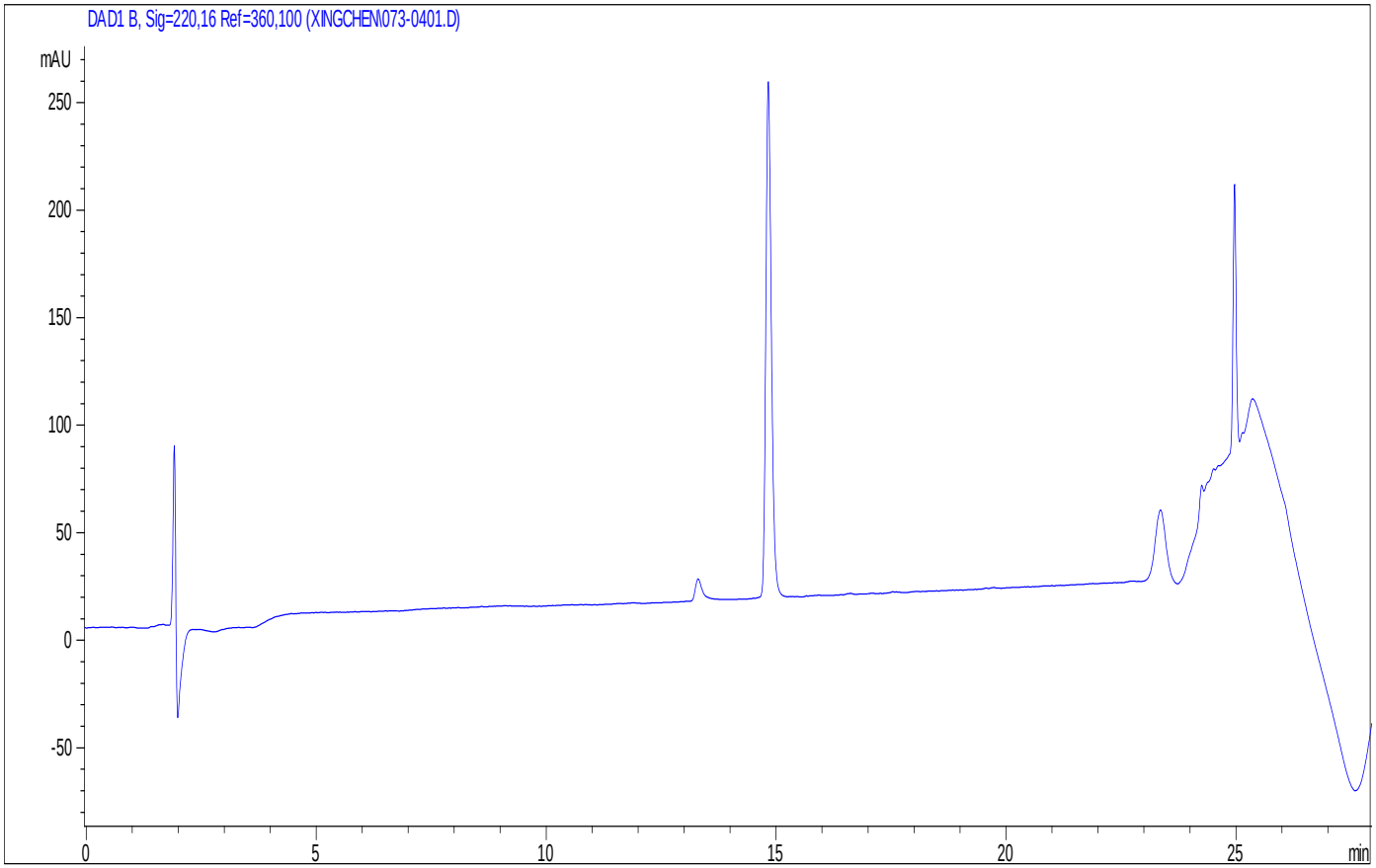

Figure 3.25 HPLC chromatogram of FITC-PDL1-P13-40

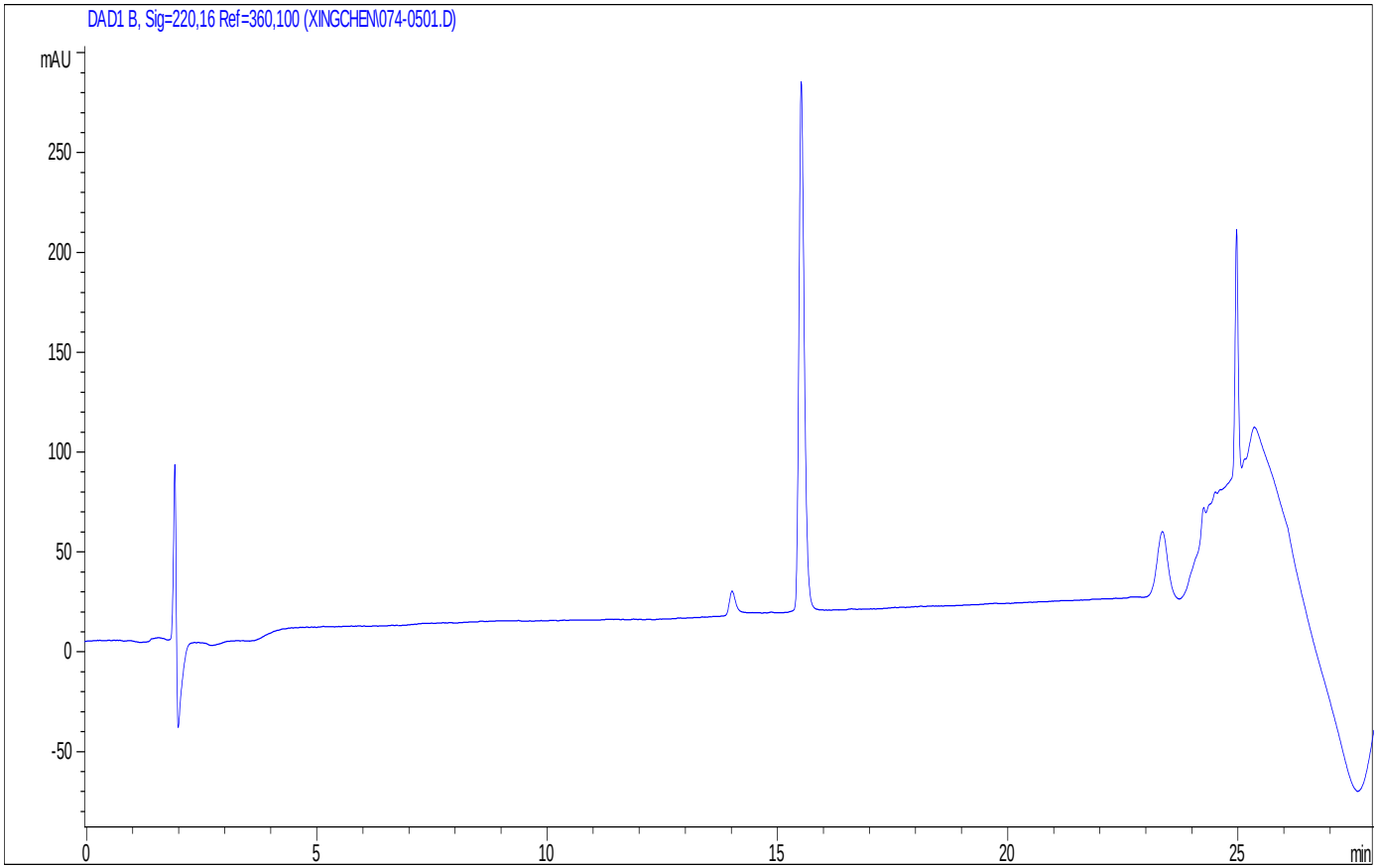

Figure 3.26 HPLC chromatogram of FITC-PDL1-P13-55

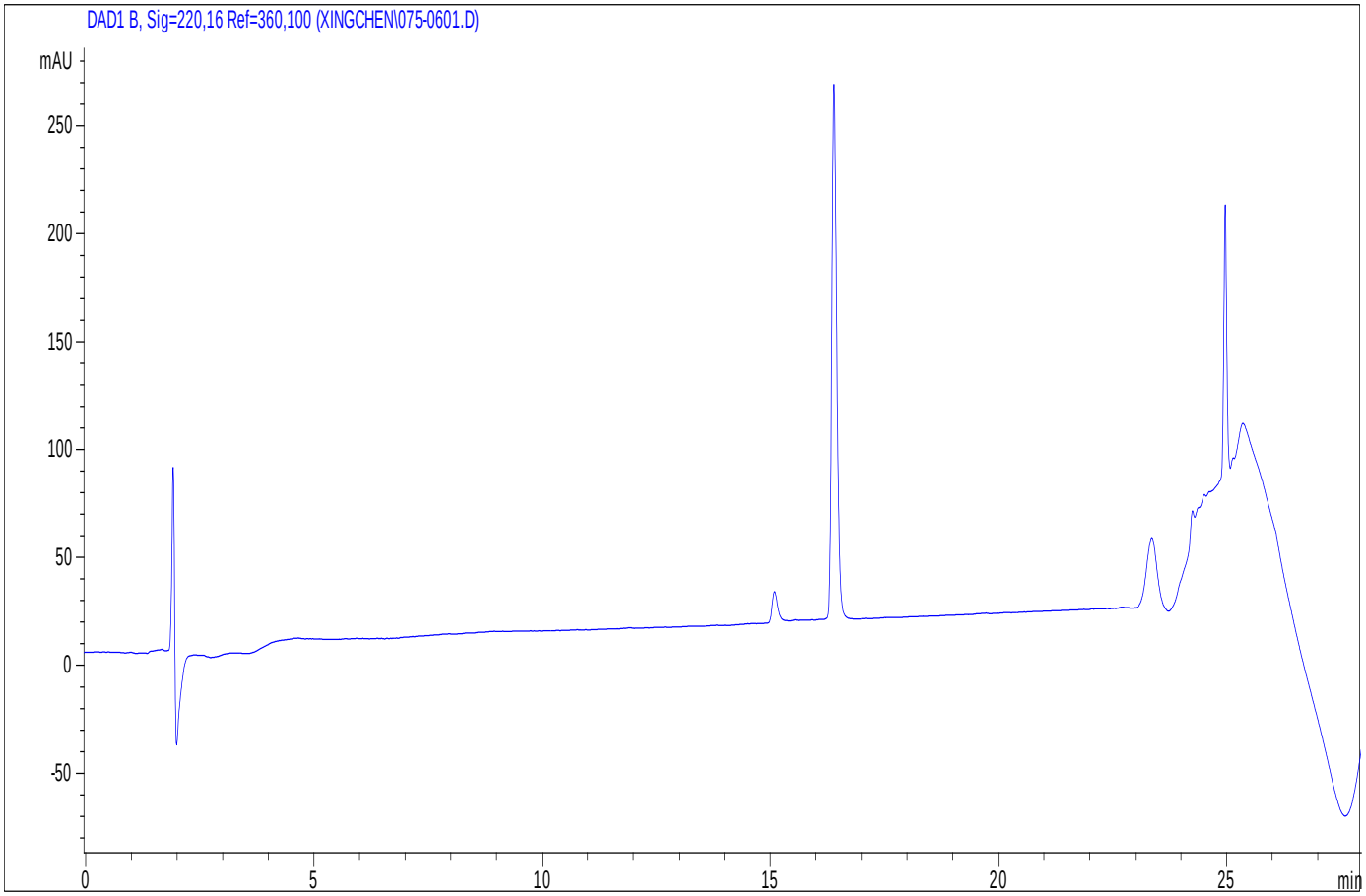

Figure 3.27 HPLC chromatogram of FITC-PDL1-P13-X

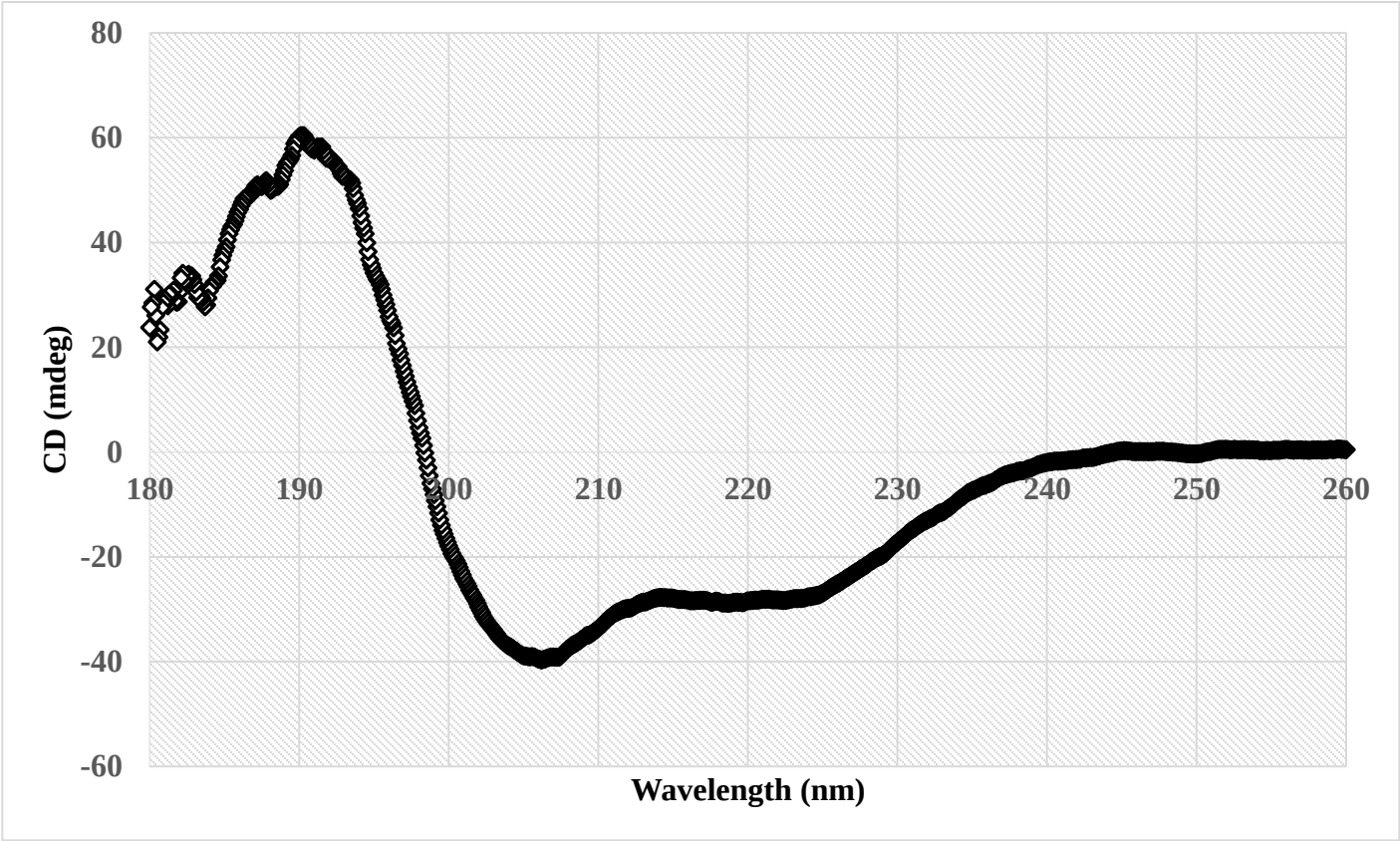

Figure 3.28 CD spectrum of PDL1-01-25MER peptide

Chapter 4: *In Vitro* Binding Specificity, Affinity of Peptides to PDL1

4.1 Introduction

In the different areas of biomedicine, binding studies are significant and meaningful for biomolecules. The increasing attention to the antibodies results in the development of those binding methods. Specificity and affinity are the most important properties in binding studies.

The binding specificity is one of the significant parameters of an antibody. For a biomolecule, it is probable that there is not only one site to bind with, referred to as non-specific binding, and is the reason why drugs have side effects. It is unacceptable if a ligand doesn't bind to its designated receptor. Therefore, it is necessary to focus on the binding specificity studies.

Cell culture experiment is widely performed in binding specificity studies. The expression for the interested protein on the cell is provided, and cancer cells are known to overexpress certain receptors as compared to normal cells. Additionally, it is also convenient to observe the biological activities with other molecules on the cells [114].

PD-L1 protein is found that overexpress on different cancer cells. *In vitro*, cellular uptake studies with fluorophore associated imaging methods are widely used to determine the binding specificity studies to PD-L1 in the lab. After incubating with cells, the FITC labeled peptides can be detected and analyzed based on their localization and visualization by using confocal laser scanning microscopy. Confocal microscopy is

known to provide images with a better resolution and reduced background signal [115]. FITC conjugated peptides are used to check the binding specificity in confocal microscopy experiments.

Different from cell binding studies, determination of the binding affinity is important as well. The binding affinity between a ligand and a receptor is widely determined by the equilibrium dissociation constant (K_D). A high affinity means a strong binding which comes with a small K_D. There are many solutions such as cell-based binding assays with FITC labeled peptides to find K_D values in the receptor-ligand system. Additionally, competition assays with unlabeled and labeled peptides can be employed to obtain the binding constant. However, it is difficult to find the accurate mount of proteins on the cells performed in the experiments and this leads to inaccurate results of binding affinity. What's more, some properties of the peptides can be changed when peptides are labeled with different agents, which means the function of these labeled agents is also unpredictable.

There are many immunoassays such as Surface Plasmon Resonance (SPR), enzyme-linked immunosorbent assays (ELISA), and radioimmunoassay (RIA) for binding affinity studies. Surface Plasmon Resonance (SPR) is one of the quantitative approaches to observe real-time binding activity. SPR is an efficient label-free method that can be performed to calculate the equilibrium dissociation constant between two biomolecules in real time [116,117]. When an analyte binds to the target protein, there will be a change in the refractive index, resulting in the alteration in the resonance angle in SPR. The molecule that is flown over and that binds to the immobilized target on a

gold sensor chip is referred to as an analyte [118,119]. The real-time binding information can be obtained in SPR when it compares with fluorescent polarization study that is performed with the fluorescent probe for a relative binding constant.

The binding specificity studies were performed by cellular uptake studies using two different cell lines including PD-L1 positive cell line, MDA-MB-231, and control cell lines, MCF-7. MDA-MB-231 is a breast cancer cell line known to express PD-L1 at a high level, and MCF-7 is also a breast cancer line used as a control for binding specificity studies [120]. After labeling with FITC, it is easy to determine whether they can bind specifically to PD-L1 positive cells and observe the visualization and location of the peptides by using confocal microscopy. Binding affinity can be determined by the affinity constant and response sensorgram using SPR in a real-time approach.

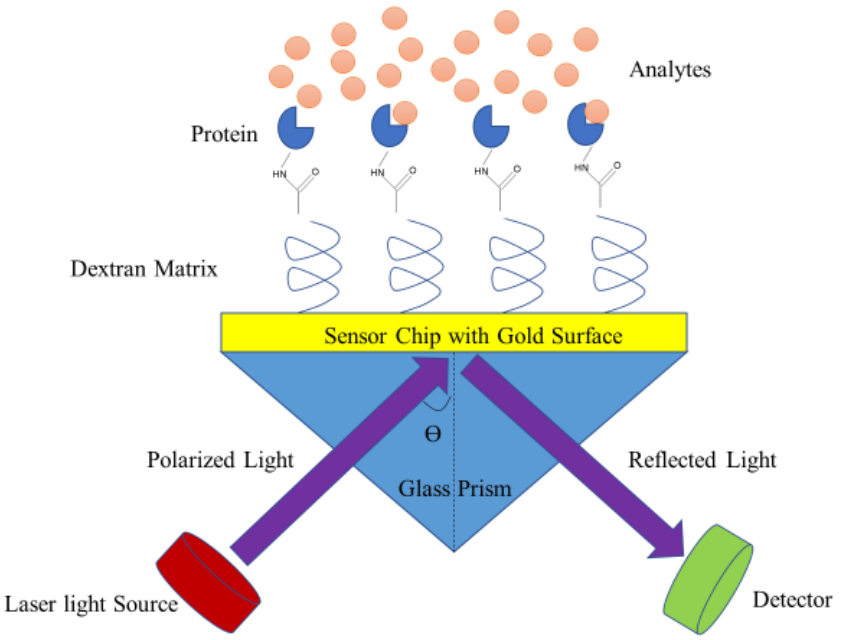

Figure 4.1 A typical SPR set up.

A typical SPR set up is shown here in Figure 4.1. It has a light source, a prism, a golden chip, a flow channel, and a detector. The light source provides polarized light for the system. The prism can reflect the polarized light to different angles based on the binding conditions between the analytes and protein. The molecules immobilized in the golden chip and solution of analytes are injected in the flow channel. All the polarized light comes to the detector and becomes an SPR sensorgram.

The light generated by the light source can hit the top of the sensor golden chip and prism. When analytes flow through the flow channel and bind to the target protein, there will be a shift in the refractive index of the sensor chip. The detector can collect

the reflected light with the different angles caused by these changes in real time and the data can be shown in a sensorgram.

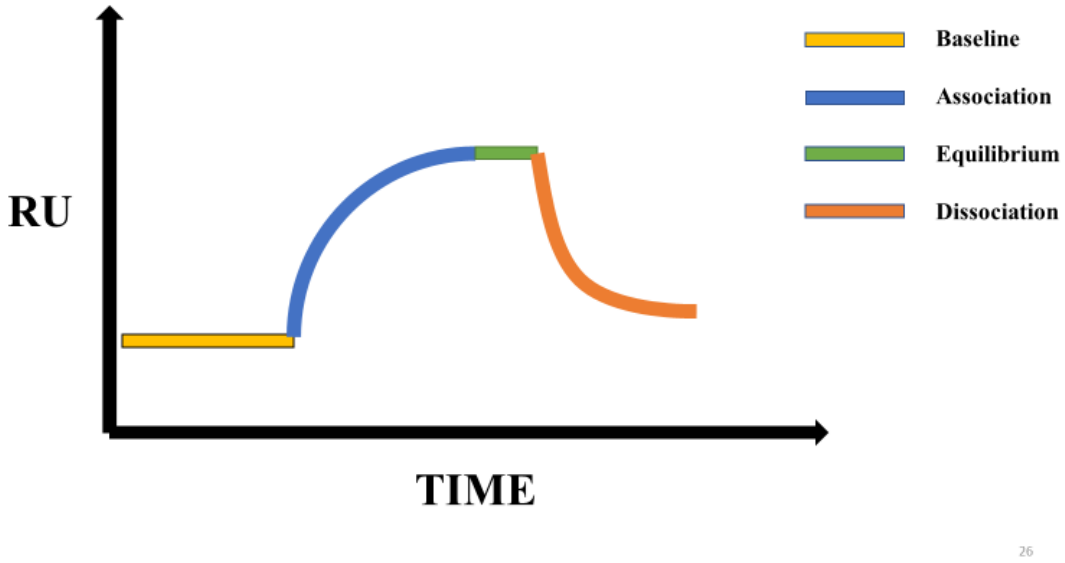

Figure 4.2 A typical sensorgram from SPR.

A typical sensorgram is shown here in Figure 4.2. It has three main phases, the association phase, the equilibrium phase, and the dissociation phase. In the association phase, an increase in the SPR response signal is detected when the analyte starts to bind the immobilized protein. In the steady state, the binding sites become saturated and the response is unchanged for several seconds. This phase is called the equilibrium phase. After the equilibrium phase, a decrease in SPR response is observed which means the analyte starts dissociating. This final phase is termed as the dissociation phase.

4.2 Materials

PD-L1 positive cells MDA-MB-231 and the control cell MCF-7 were purchased from ATCC (Manassas, VA, USA). The cells were cultured in Dulbecco's modified eagle's medium (DMEM) with 4.5g/L glucose, L-glutamine, and sodium pyruvate from Cellgro, Mediatech Inc (Manassas, VA, USA). Penicillin-Streptomycin was also obtained from Cellgro, Mediatech Inc. (Manassas, VA, USA). Trypsin: EDTA was bought from GEMINI (West Sacramento, CA, USA). Phosphate Buffered Saline (PBS) pH 7.2, hyclone Fetal Bovine Serum (FBS) was purchased from Thermo Scientific (Logan, UT, USA). Human PDL-1 Protein was purchased from Sino Biological Inc. (Beijing, China). All microscopy supplies were purchased from VWR (USA). Cell culture supplies were purchased from Santa Cruz Biotechnology Inc. (TX, USA) and Cellgro, Mediatech Inc. (Manassas, VA, USA).

Alexa fluor 594 wheat germ agglutinin and Slow fade gold mounting medium were purchased from Invitrogen (Carlsbad, CA, USA). Phosphate buffered saline, pH 7.4, contains TWEEN® 20, dry powder, N-ethyl-N'-(3-dimethylaminopropyl) carbodiimide (EDC), N-hydroxysuccinimide (NHS), Ethanolamine (EA), Glycine, and Bovine serum albumin (BSA) were purchased from Sigma-Aldrich (St. Louis, MO, USA). All chemicals and solvents were used without further purification.

4.3 Methods

4.3.1 Cell culture. DMEM was used as the cell culture media to which 10% FBS and 1% penicillin-streptomycin (5000 I.U./mL) were added and then refrigerated. MDA-MB-231 and MCF-7 cells were incubated in a T75 flask in the prepared cell culture media at 37˚C and 5% CO2 and were subcultured when the cells reach 80% confluency. Additionally, cells were frozen in the recovery freezing media (DMEM with 5% DMSO) and stored in a nitrogen tank for future experiments.

4.3.2 Confocal microscopy studies. MDA-MB-231 and MCF-7 cells were grown in T75 flasks at 37˚C and 5% CO2. 2× 105 cells were seeded on coverslips placed inside six well-cultured plates when the confluency reached about 80%. The experiment was carried out after 24 hours of attachment. After the medium was removed, the cells were washed twice with PBS and serum-free media.

FITC labeled peptides and control peptide were dissolved and diluted in serum-free DMEM with 1% dimethyl sulfoxide (DMSO). The final solutions of all peptides at the concentration of 20μM were added to the six well-cultured plates.

After incubating for 25 minutes at 37˚C, the cells were washed twice with PBS and then treated with a solution of Alexa Fluor 594 wheat germ agglutinin in PBS at 2.5 μg/mL for 10 minutes to stain the cell plasma membrane. After that, cells were washed twice with PBS and then fixed by 4% paraformaldehyde solution prepared in PBS for 15 minutes. Then, a final wash of distilled water was performed after washing PBS twice. The coverslips with the fixed cells were covered on the microscopic slides with a drop of the mounting medium (slow fade gold). The cells were imaged on an inverted Leica

DMIRE2 confocal laser scanning microscope (Leica Biosystems Richmond Inc, Richmond, USA) with Yokogawa CSU-X1 confocal scanner unit at 64x magnification and oil immersion (Yokogawa Electric Corporation, Japan). The FITC labeled peptides were observed under the 491 nm channel, and the cell plasma membrane stained by Alexa Fluor 594 fluorescence was visualized under the 561 nm channel.

A semiquantitative method of fluorescence intensity for peptides with salt bridge function was performed based on the cell images from confocal microscopy studies. The mean fluorescence intensity of ten cells in different cell images was determined and calculated from ImageJ.

4.3.3 Binding affinity studies using SPR. The binding affinity of peptides was calculated by the Dual Channel SPR Spectrometer SPR7000DC (Reichert Technologies, New York, USA) in SPR studies. N-(3-Dimethylaminopropyl)-N'-ethylcarbodiimide hydrochloride (EDC) and N-hydroxysuccinimide (NHS) were employed to activate the Carboxymethyl Dextran Hydrogel Surface Sensor Chip (Reichert Technologies, New York, USA) under the running buffer of phosphate buffered saline with 0.05% Tween 20 (pH7.4) that was degassed before using at room temperature. Then, ethanolamine (EA) pH 8.5 was injected to block unreactive sites for eight minutes at a rate of 10µL/min. Human PD-L1 protein (25µg/ml) and bovine serum albumin (BSA, 20µg/ml) were used as the control and were diluted and immobilized by flowing them over the left channel of the activated chip in 10 mM sodium acetate buffer pH 4.5. The real-time binding response for peptides (PDL1-01-25MER, PDL1-06-13MER, PDL1-P13-1, PDL1-P13-28, PDL1-P13-33, PDL1-P13-40) over PD-L1 were observed at an injection speed of 25µL/min in the SPR software. PDL1-P13-28 was also injected with BSA protein. Additionally, 10 mM glycine (pH 2.5) in PBST can be performed to regenerate the bound surface of the activated chips[193]. The sensorgrams from SPR were all analyzed using the Scrubber 2® software (BioLogic Software Pty Ltd, Australia) in the terms of zeroed, aligned, referenced, and blanked. The association rate (ka), dissociation rate (kd), and dissociation constant (KD) were also determined by using the Scrubber 2® software global in a 1:1 Lagmurian interaction model.

4.4 Results and discussion

Three generations of peptides against PD-L1 protein were designed based on the Knob-Socket model. After screening in MOE and the AutoDock Vina software, top peptides with lower energy were selected based on the docking results. Lower binding energy and more interaction sites with PD-L1 were also observed in the peptides designed in salt bridge function from MOE and the AutoDock Vina docking results. Experiments were performed to validate the docking results from the computational modeling method and test the binding specificity and affinity of the designed peptides.

The affinity of the designed peptides to PD-L1 protein was determined in SPR studies. Response sensorgrams of three generations of peptides with PD-L1 collected from SPR studies are shown in Figure 4.3-4.9. All response sensorgrams were obtained from the Scrubber software.

No binding responses for α-helix and over-packed peptides were observed in SPR sensorgram which suggested peptides designed in α-helix and over-packed method were not feasible. A reasonable explanation is the original α-helix design may have broken due to the improper position of knobs in the PD-L1 Knob-Socket receptor frame pattern and the low ratio of alpha-helical structure, resulting in the loss of knobs fit into their sockets for α-helix peptides. Additionally, due to the limited space, it is too congested for over-packed peptides to bind to the PD-L1 protein.

When compared with the first and second generations of peptides which designed in α-helix and over-packed method, the third generation of peptides designed with the new binding information, salt bridge, had a much higher binding response. For PDL1-04-25MER and PDL1-06-13MER, they have no response based on the

sensorgram, while PDL1-P13-1, PDL1-P13-28, PDL1-P13-33, and PDL1-P13-40 had a response unit around 15. The SPR results of the response for third generation peptides toward the BSA protein is shown in Figure 4.9. From the results, we can find that peptides showed no binding to BSA protein, which means those designed peptides have a binding specificity. These data are a clear evidence that the third generations of peptides with salt bridge function can bind to the PD-L1 protein. However, K_D values can't be obtained since there was only a slight change when the concentrations of peptides increased. Though affinity of peptides against PD-L1 can't be calculated, the binding between peptides and PD-L1 was further verified using the cell uptake experiments.

The *in vitro* binding specificity of peptides to the PD-L1 positive cancer cells was determined in confocal microscopy studies. In confocal microscopy studies, significant fluorescence was detected on the cellular surfaces of MDA-MB-231, while no fluorescence was detected on MCF-7 cells from cell images (Figures 4.11-4.16) after incubation with 20 μM of FITC labeled peptides solution, which indicates that FITC conjugated peptides can bind to MDA-MB-231 but not to MCF-7 cells. On the contrary, no significant fluorescence was observed from both the two cell lines after incubation with FITC labeled control peptide with a scrambled sequence PDL1-P13-X solution. A plausible explanation is the knob and socket pairs may have broken, resulting in the loss of knobs fit into their sockets. To preserve the binding specificity, the peptide with different amino acids as knobs on the sequence should fit the right sockets on the PD-L1 protein.

The result of the significant fluorescence of MDA-MB-231 can be explained by the specific interaction between PD-L1 and designed peptides, which was consistent with the SPR results shown above.

To determine the visualization and localization of the cell, the cell plasma membrane was marked by the Alexa Flour 594 dye in the confocal microscopy studies. First, free FITC was used to see whether it can go inside the cell lines, and in Figure 4.10 results showed that free FITC can go inside both the two cell lines as a small molecule. In Figures 4.11-4.16, peptides showed internalization by cells instead of binding on the cell surface. The internalization of peptides can be attributed to receptor-mediated endocytosis upon binding onto the PD-L1 protein. Additionally, peptides are much smaller when compared with antibodies, and as a result, it is much easier for peptides to internalize into cells. Results from the confocal microscopy studies suggested that the peptides with salt bridge function can bind to the PD-L1 positive cell lines but not to the control cell lines.

A semiquantitative method of fluorescence intensity for peptides with salt bridge function was performed based on the cell images from confocal microscopy studies. The mean fluorescence intensity of ten cells in cell images for different peptides designed in salt bridge function was shown in Figure 4.17. There is a significant difference in fluorescence intensity between PD-L1 positive cell line and control cell line for peptides designed in salt bridge function, while a tiny difference for the FITC labeled control peptide with a scrambled sequence PDL1-P13-X. AutoDock Vina was used to perform a second screening for the selected peptides from the MOE software. From the Figure 2.9,

we can determine that only PDL1-P13-55 can bind to the designed part of the target protein. The PDL1-P13-55 with the lowest binding energy, which can bind to the designed part of the target protein based on the docking results from Vina, had a higher fluorescence intensity, when compared with the other five peptides in the figure, which indicates the potential of binding ability against PD-L1 Protein.

The *in vitro* binding specificity of peptides towards PD-L1 was determined in the confocal microscopy and SPR studies. Results showed that the peptides with salt bridge function based on the Knob-Socket model and molecular interaction can bind to PD-L1 protein while α-helix and over-packed peptides can’t bind to the PD-L1 protein.

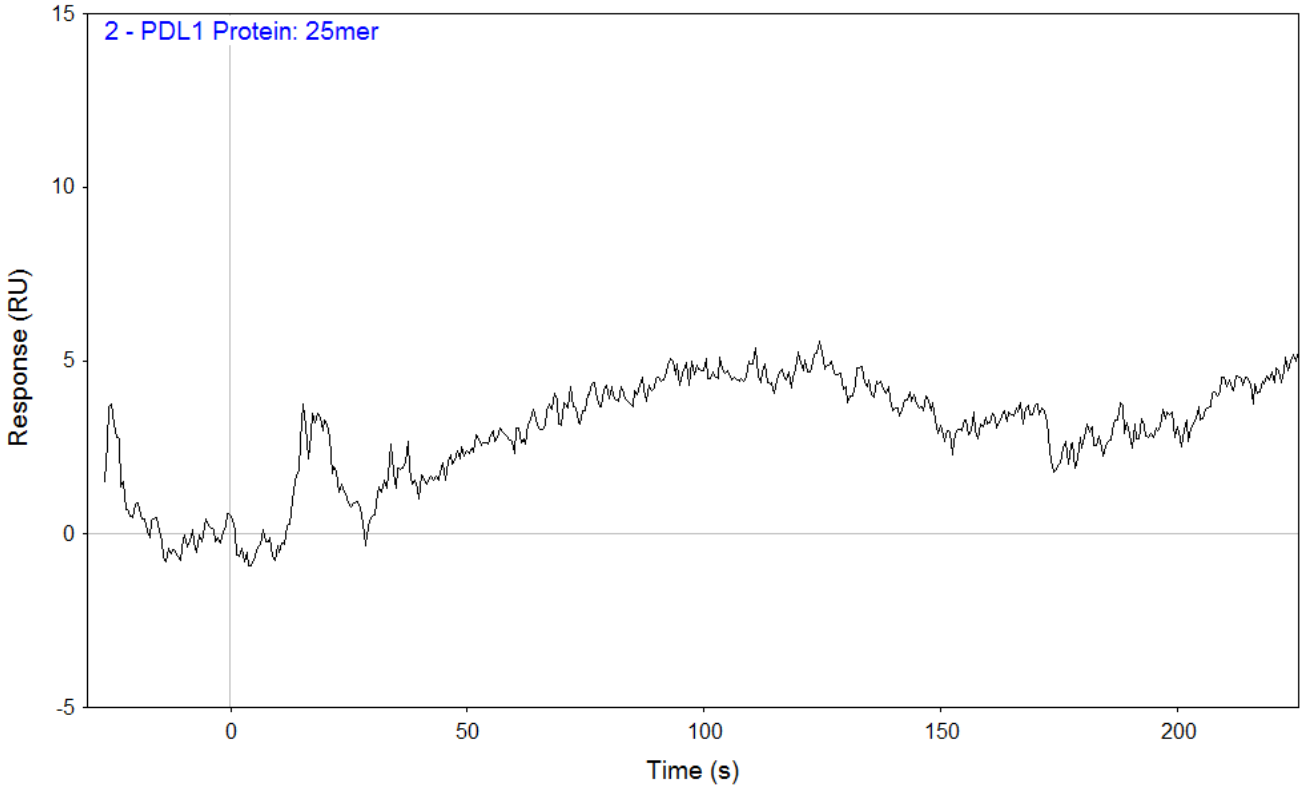

Figure 4.3 SPR response of PDL1-01-25MER

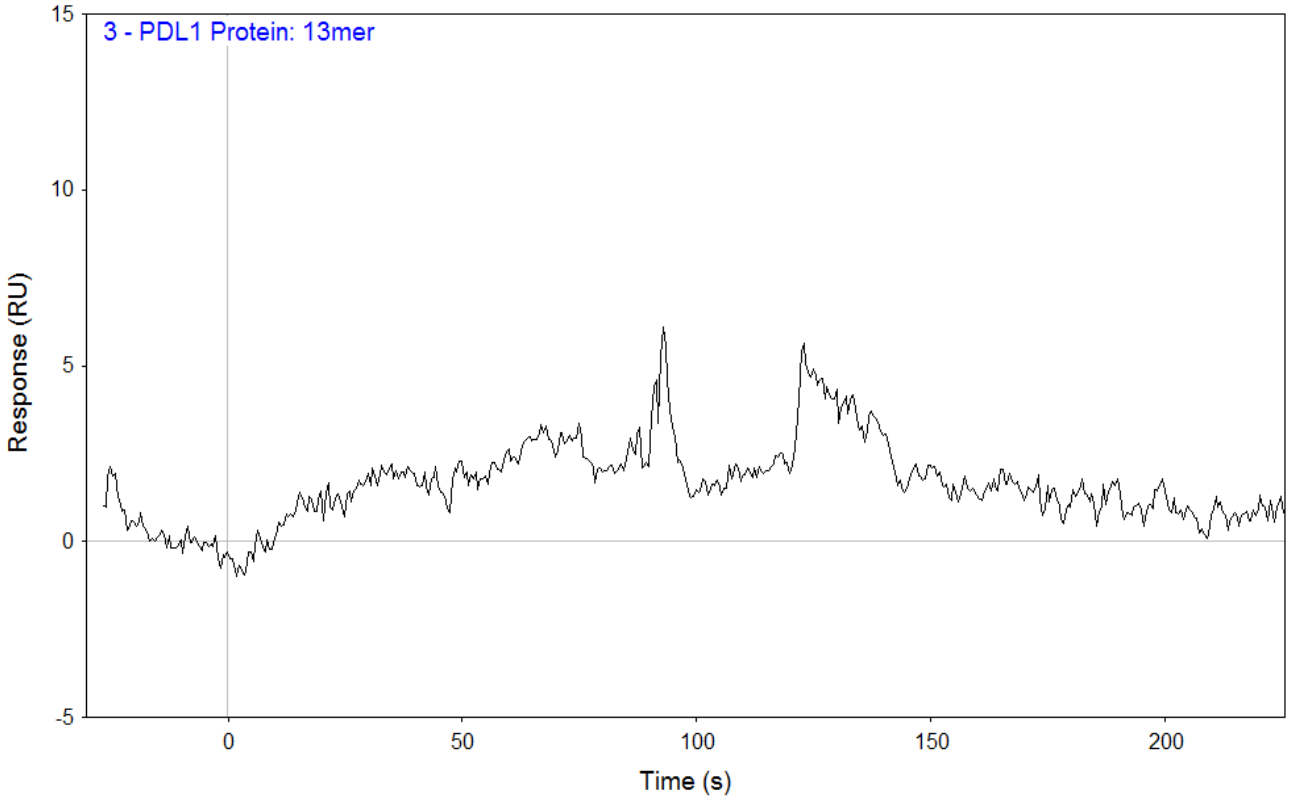

Figure 4.4 SPR response of PDL1-06-13MER

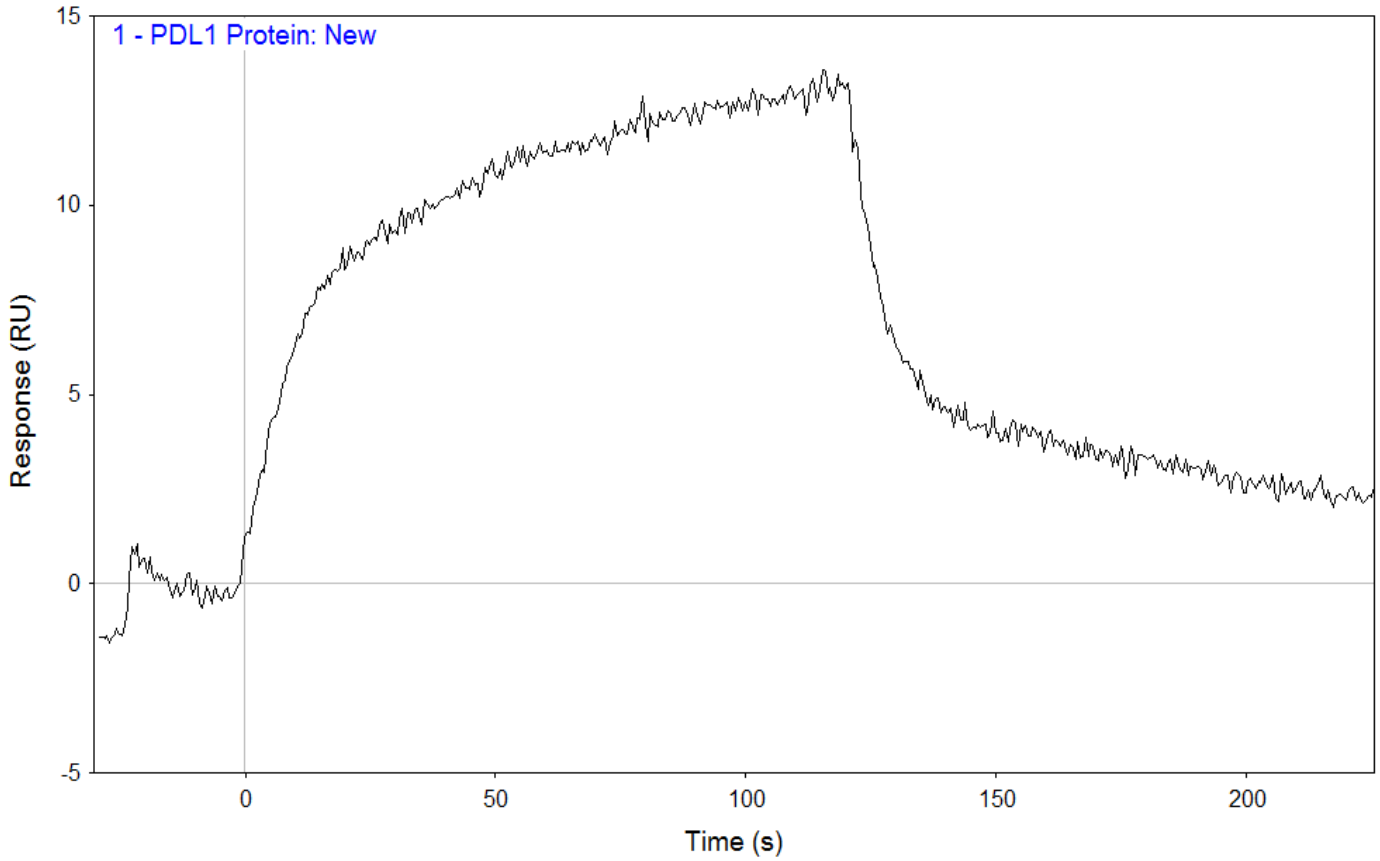

Figure 4.5 SPR response of PDL1-P13-40

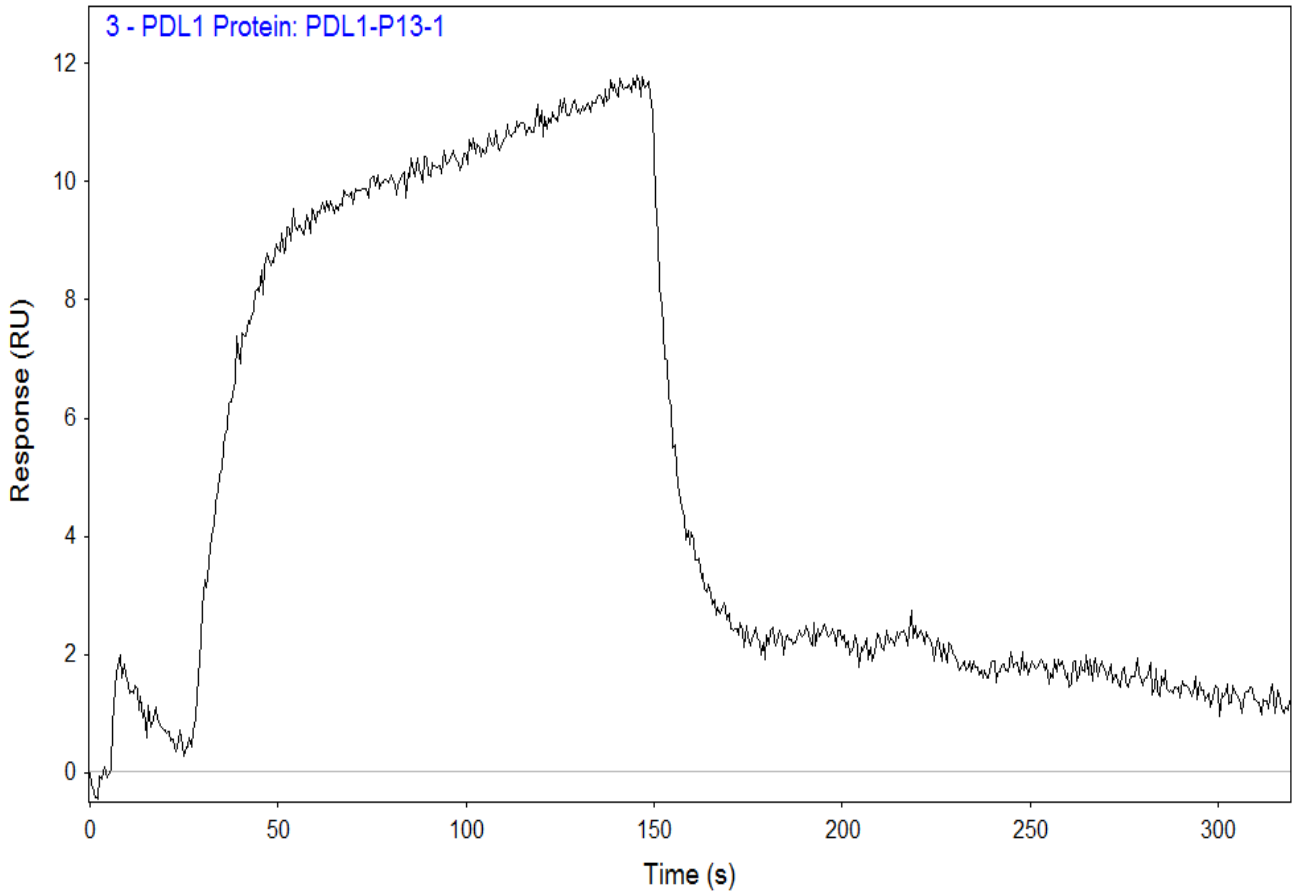

Figure 4.6 SPR response of PDL1-P13-01

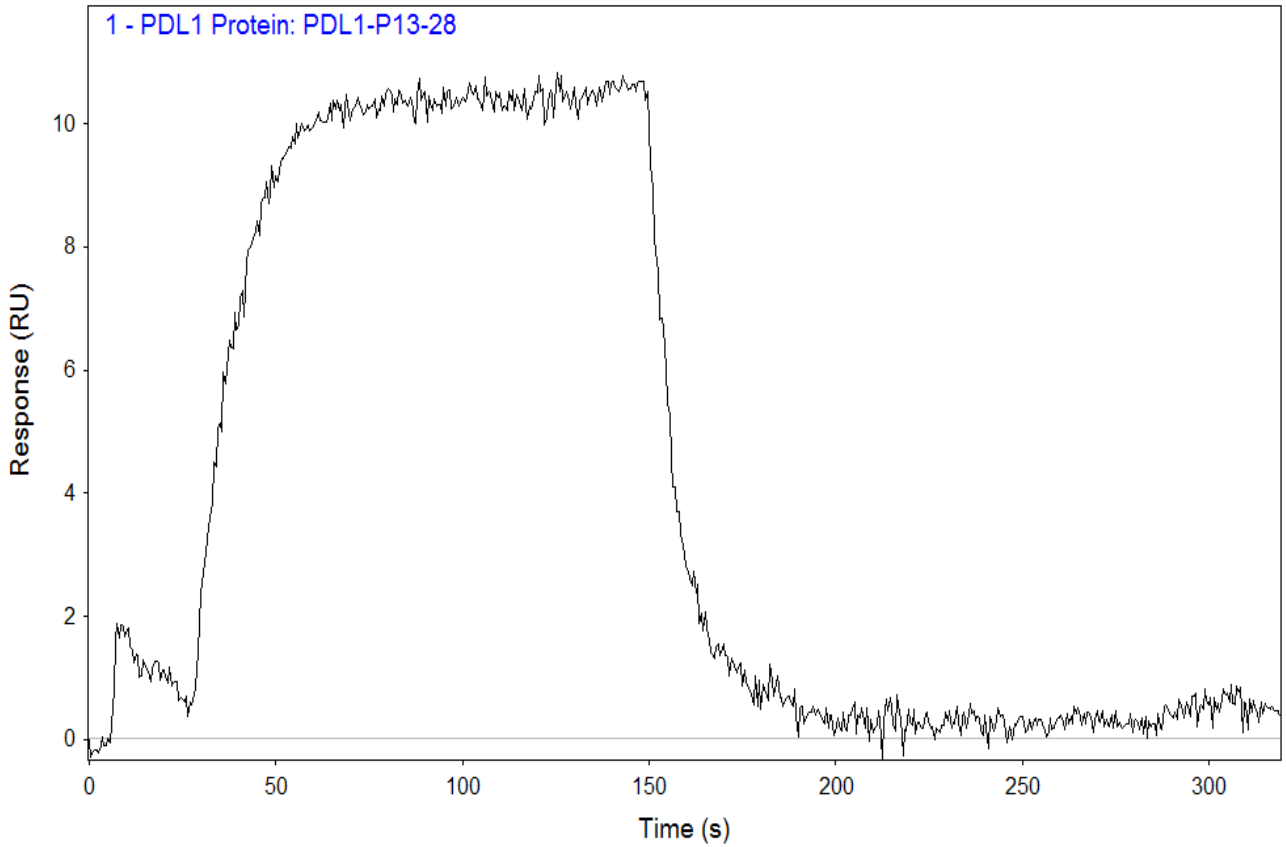

Figure 4.7 SPR response of PDL1-P13-28

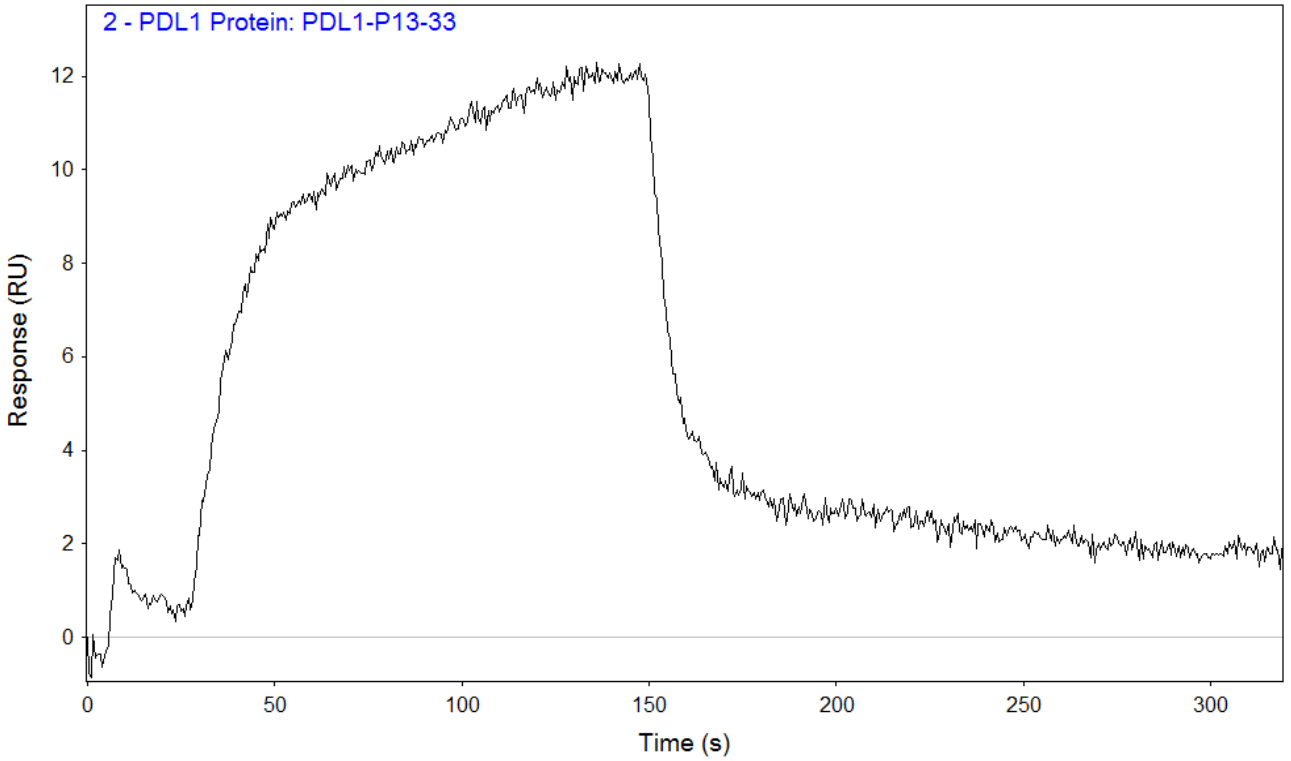

Figure 4.8 SPR response of PDL1-P13-33

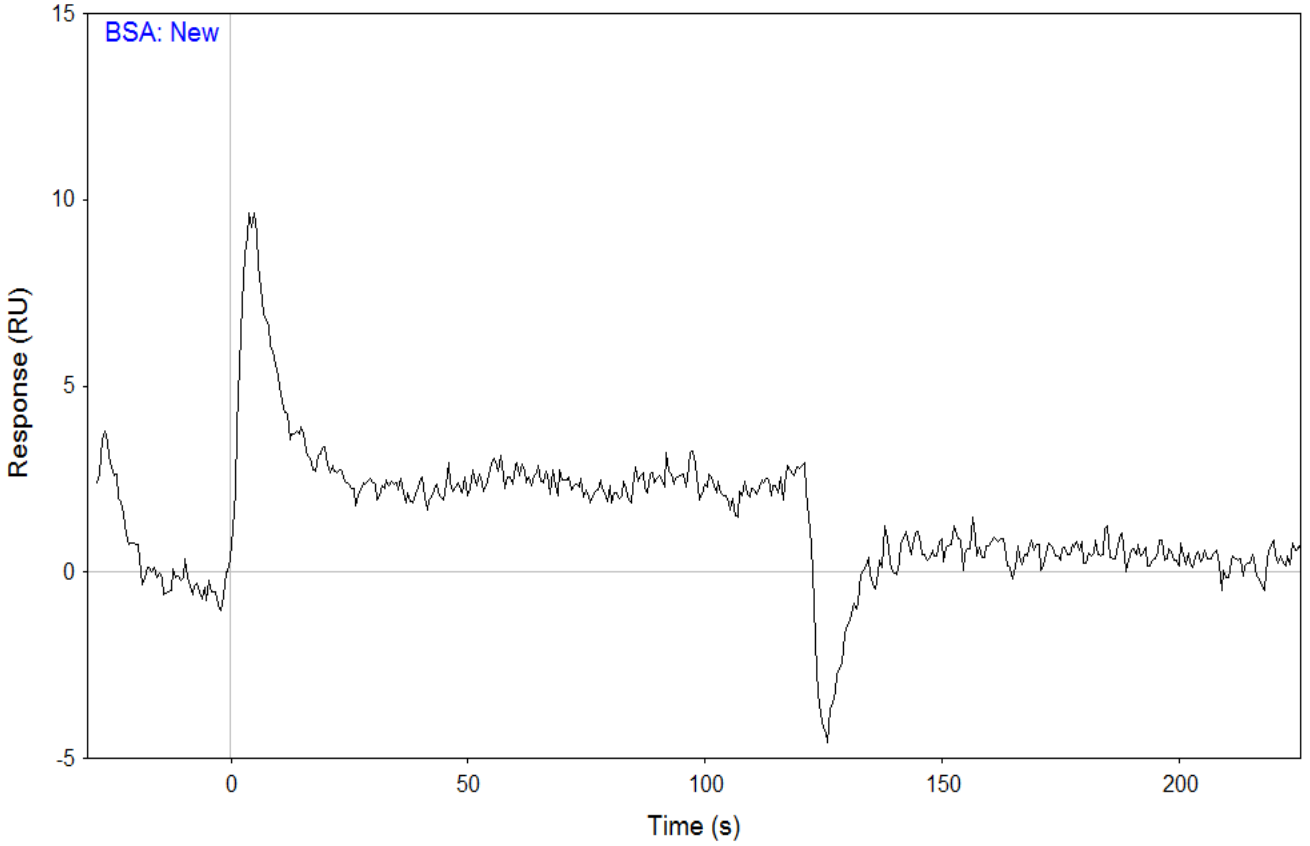

Figure 4.9 SPR response of PDL1-P13-40 against BSA

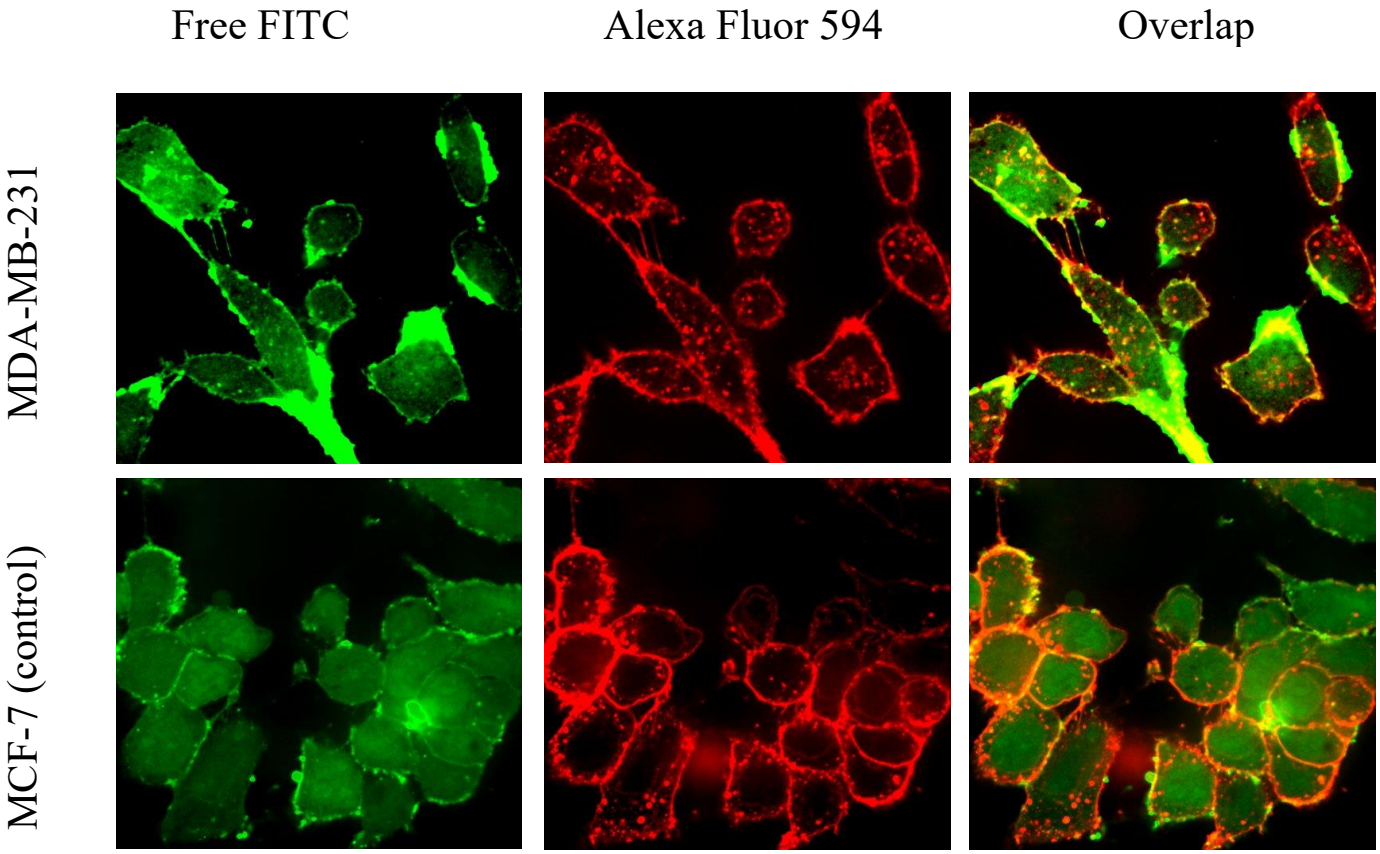

Figure 4.10 Evaluation of binding specificity of Free FITC to MDA-MB-231 and MCF-7 cells as conformed by confocal microscopy.

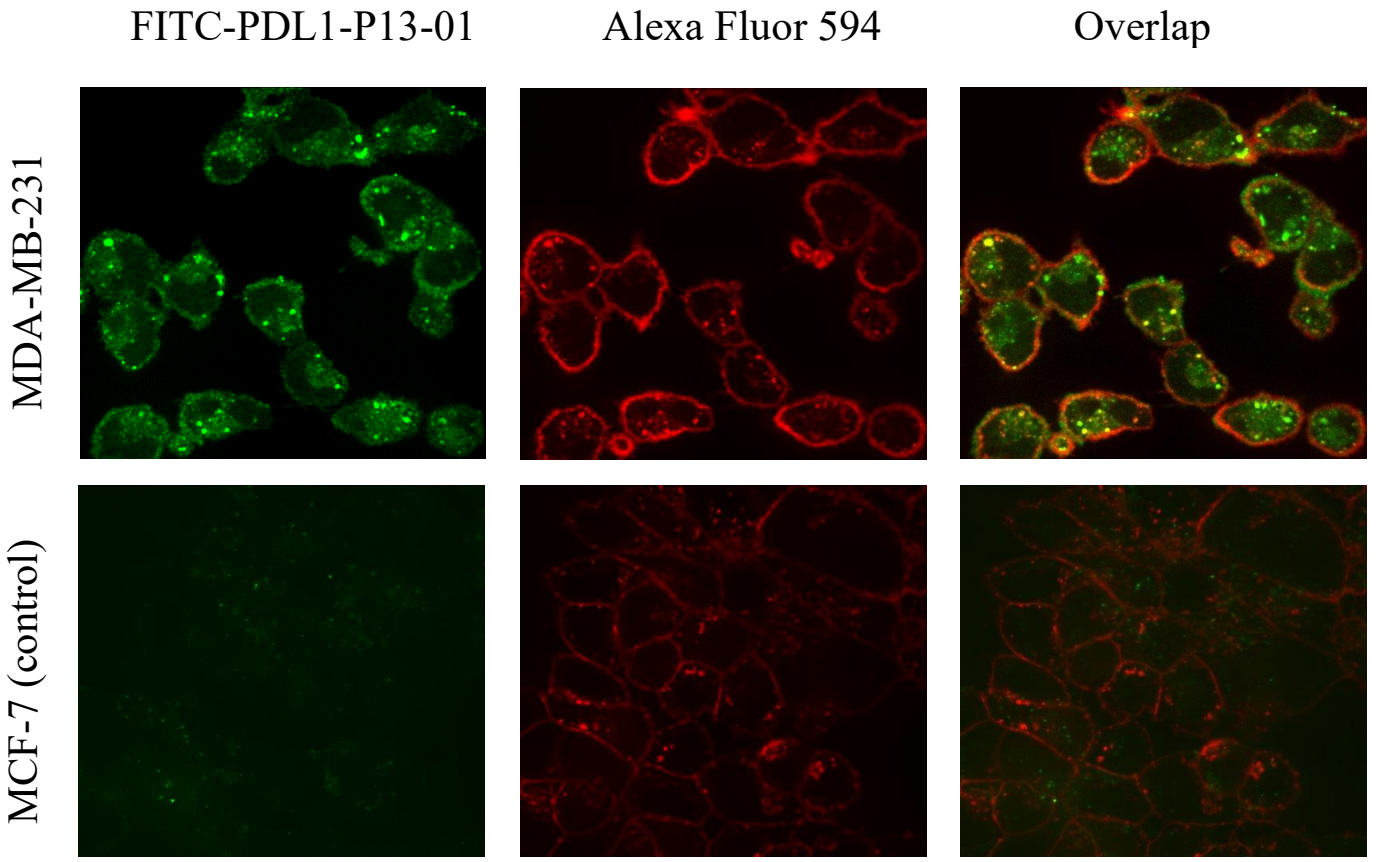

Figure 4.11 Evaluation of binding specificity of FITC-PDL1-P13-01 to MDA-MB-231 and MCF-7 cells as conformed by confocal microscopy.

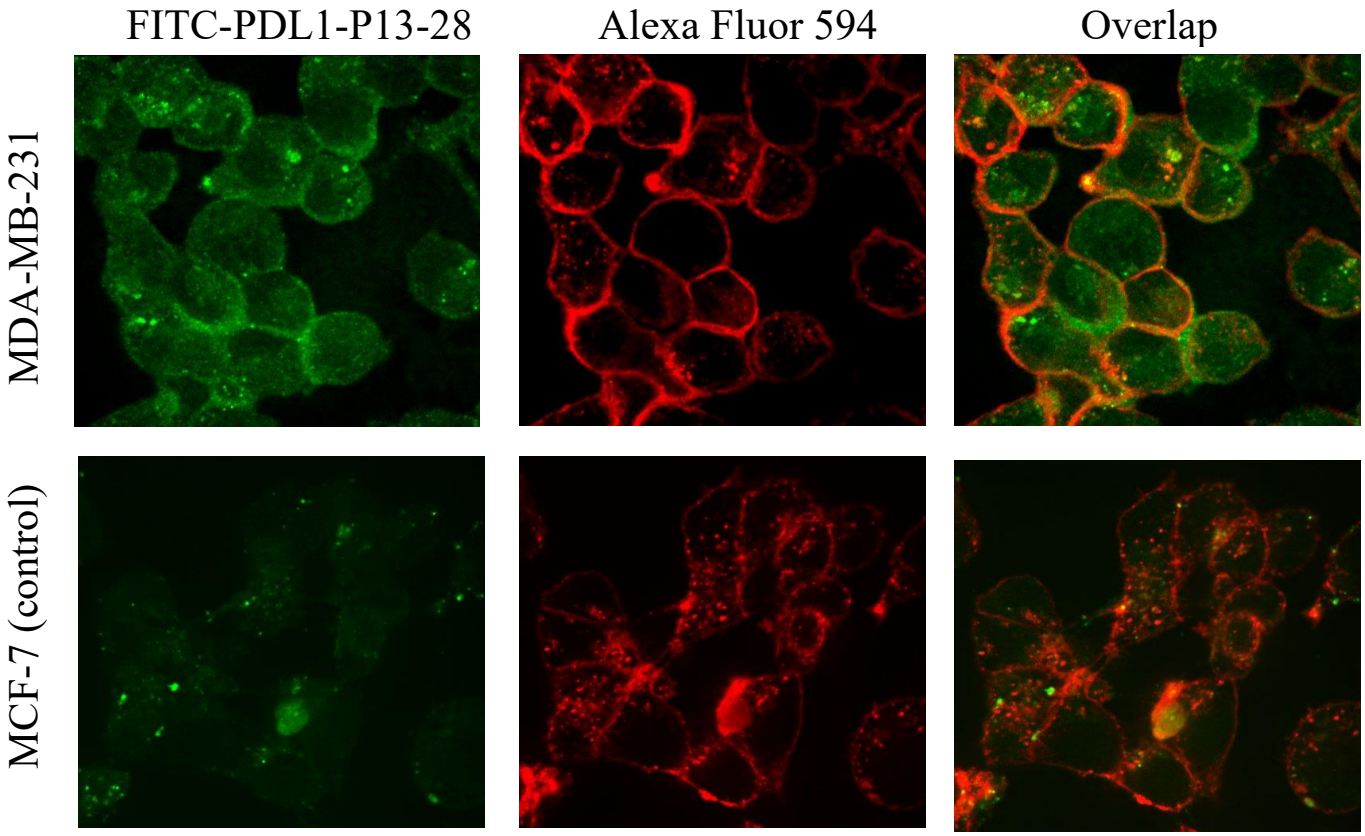

Figure 4.12 Evaluation of binding specificity of FITC-PDL1-P13-28 to MDA-MB-231 and MCF-7 cells as conformed by confocal microscopy.

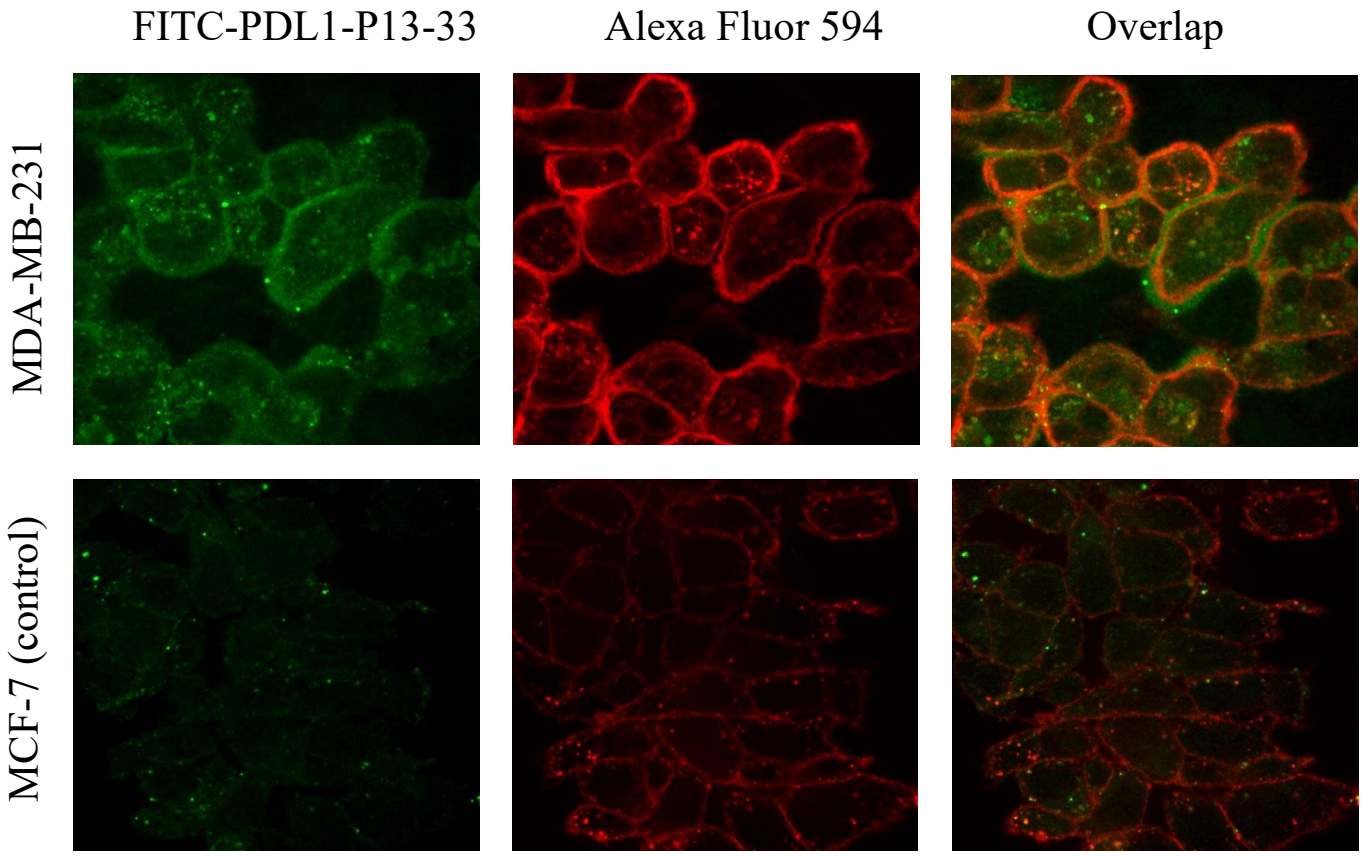

Figure 4.13 Evaluation of binding specificity of FITC-PDL1-P13-33 to MDA-MB-231 and MCF-7 cells as conformed by confocal microscopy.

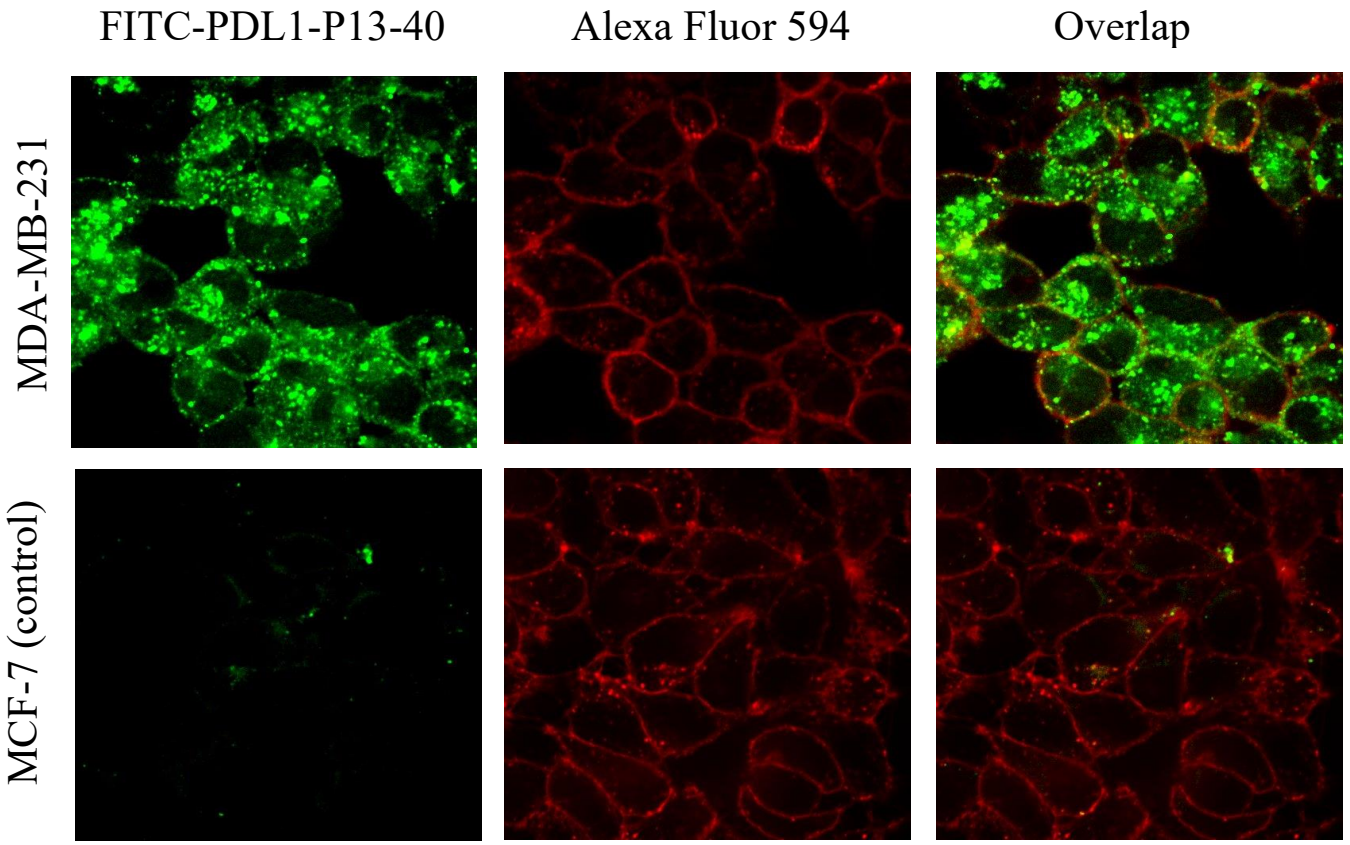

Figure 4.14 Evaluation of binding specificity of FITC-PDL1-P13-40 to MDA-MB-231 and MCF-7 cells as conformed by confocal microscopy.

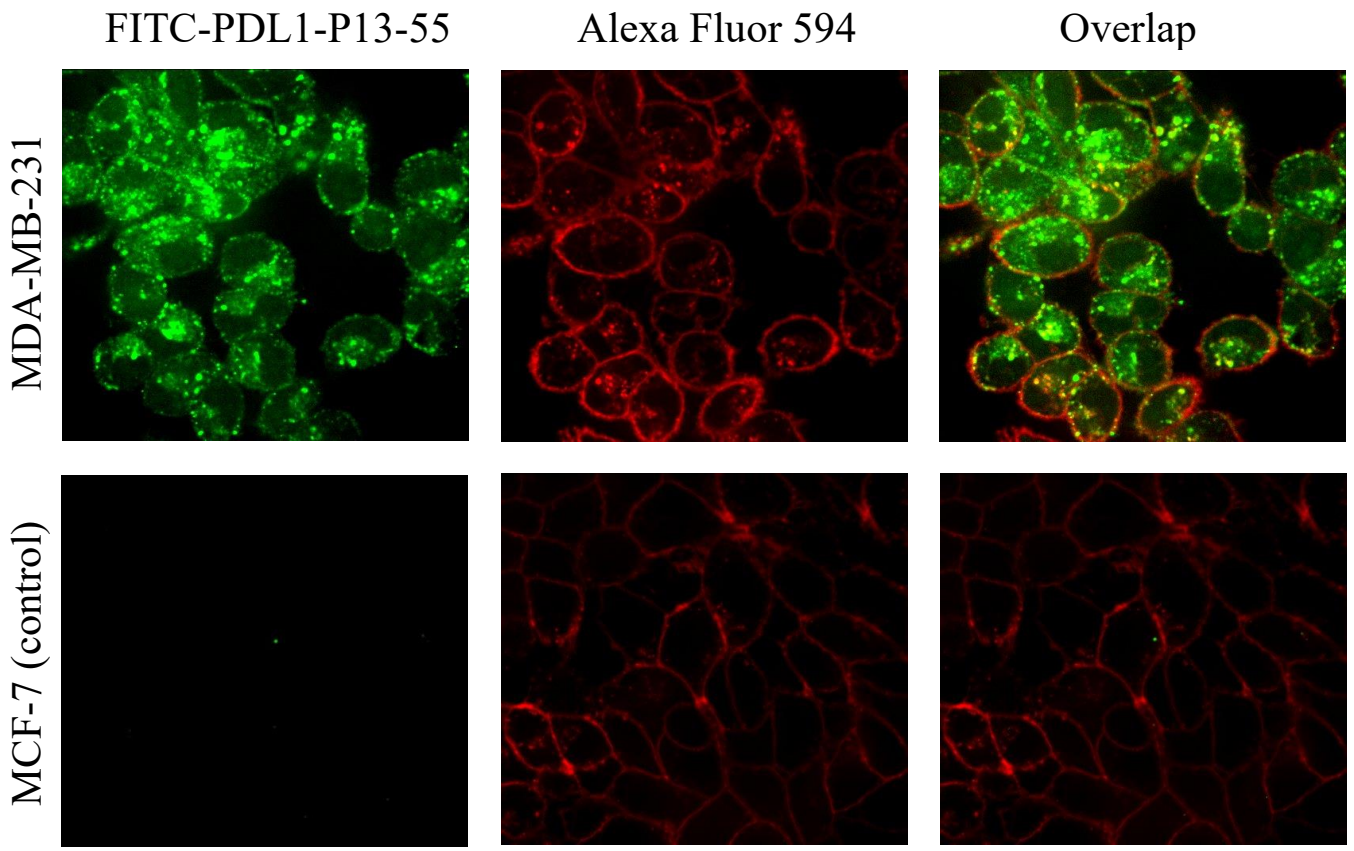

Figure 4.15 Evaluation of binding specificity of FITC-PDL1-P13-55 to MDA-MB-231 and MCF-7 cells as conformed by confocal microscopy.

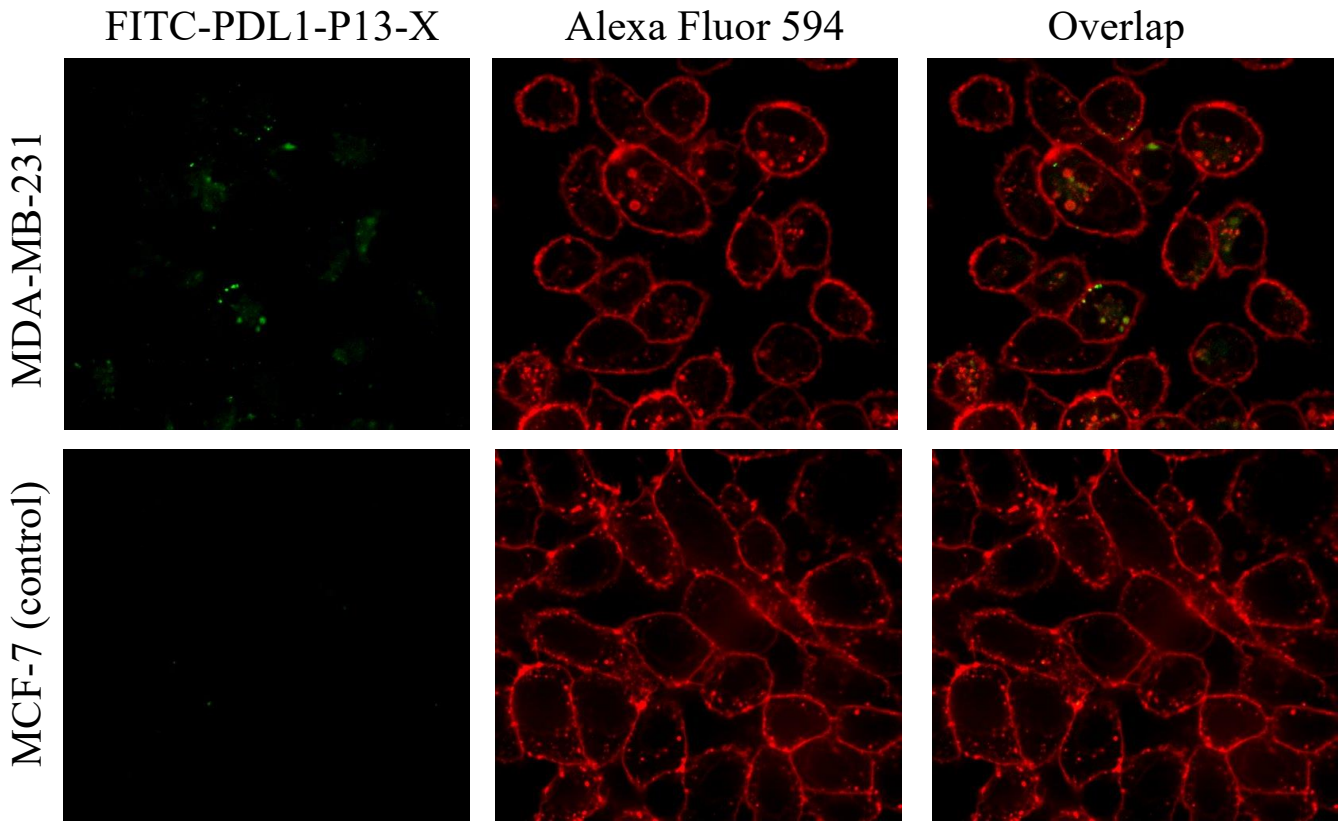

Figure 4.16 Evaluation of binding specificity of FITC-PDL1-P13-X (control) to MDA-MB-231 and MCF-7 cells as conformed by confocal microscopy.

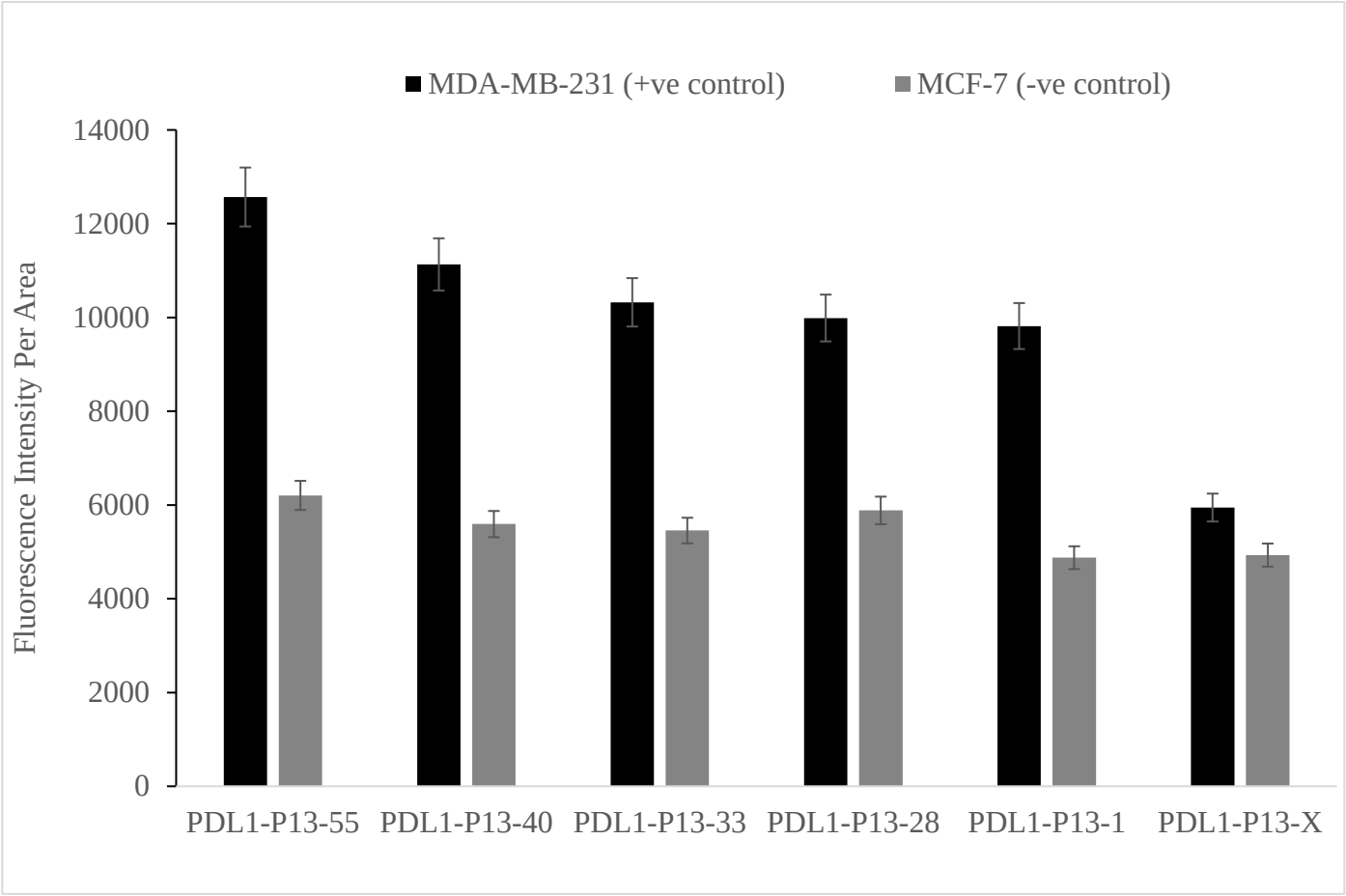

Figure 4.17 Fluorescence intensity for different peptides designed in salt bridge function

Chapter 5: Summary and Conclusions

Programmed death-ligand 1 (PD-L1) is a type 1 transmembrane protein that has been reported to play a vital role in mediating suppressed immunity. The interaction between PD-L1 and PD-1 delivers a negative signal that reduces the proliferation of these T cells. Specific antibodies, peptides, and small molecules are developed by scientists to bind with PD-L1. Antibodies that can block the Programmed death-ligand 1 (PD-L1) on tumor cells have shown to alleviate cancer-induced immunosuppression. While antibodies have a great potential in various therapeutic uses, many drawbacks such as high cost of production, huge molecular size, and poor permeability impose restrictions on the extensive use of full-length antibodies. Compared to antibodies, peptides that selectively bind to PD-L1 have advantages in solubility, permeability, and immunogenicity. The phage display technique or the computational screen of a large library of thousands of candidates are used to develop antibody alternatives. However, all these approaches are tedious, labor-intensive, and time-consuming due to their trial-and-error nature.

In this study, it is hypothesized that rationally designed peptides based on PD-L1-PD1 molecular interactions and the Knob-Socket computational model can bind to PD-L1. Peptides against PD-L1 were designed based on the interaction between PD-L1 and PD-1 without involving massive experimental screening trials. Sequences of these

peptides were obtained from the core amino acids in the binding surface between the PD-L1-PD1 complex by using the Knob-Socket model and further docked in MOE and Vina. The 2D map of peptides against PD-L1 with binding sites was obtained based on the Knob-Socket model. Three generations of peptides, α-helix, over-packed, and new peptides with the salt bridge function were designed and synthesized by using the Solid Phase Synthesis method (SPPS). The top 20% peptides were selected based on the binding energy simulated by MOE and AutoDock Vina before the binding affinity and specificity experiment. Peptide PDL1-P13-55 can bind to the right position which is designed to be bound based on the docking studies. The salt bridge function peptides with a lower binding energy and with a more number of interactions showed the binding preference against the PD-L1 protein, based on the docking results from MOE and AutoDock Vina. The binding between the designed peptides and PD-L1 was verified in vitro binding affinity and specificity experiments. The Surface Plasmon Resonance (SPR) technique was performed to determine the binding affinity of all the designed peptides. Only peptides with the salt bridge function have a high response while the α-helix and over-packed peptides have no response on SPR sensorgrams. The confocal microscopic studies using different cell lines showed that third generations of peptides with salt bridge function bind specifically to PD-L1 positive cell line, MDA-MB-231, but not to PD-L1 control cell line, MCF-7. The salt bridge function peptides with a lower binding energy and with a more number of interactions selected based on the docking results from MOE and AutoDock Vina showed good binding specificity

towards PD-L1, which was confirmed based on the binding responses from SPR and the fluorescence intensity from confocal microscopic studies.

In conclusion, peptides against PD-L1 designed rationally by the Knob-Socket model and the molecular interaction between the PD-L1-PD1 complex showed good binding specificity towards PD-L1, demonstrating the feasibility of this model in the design of binding ligands for targeting delivery.

In the future, novel peptides can be used as a biomarker for the detection of PD-L1 in various studies. The novel peptides can also be conducted as a targeting moiety of a peptide drug conjugate in PD-L1 positive cancers therapy. Cellular cytotoxicity studies can be performed to evaluate the potential of novel peptides to be used as targeting moiety of anticancer drugs.

REFERENCES

1. Zhu, D., Boylan, J., Xu, S., Riggs, J., Shi, T., & Wurmser, A., et al. (2017). Methods of treating a cancer using substituted pyrrolopyrimidine compounds, compositions thereof.
2. Available from: https://en.wikipedia.org/wiki/Cancer#cite_note-WHO2014-2.
3. MJLind. (2008). Principles of cytotoxic chemotherapy. *Medicine. 36* (1): 19–23.
4. Chari, R. V. J., Miller, M. L., & Widdison, W. C. (2014). Antibody–drug conjugates: an emerging concept in cancer therapy. *Angewandte Chemie International Edition, 53*(15), 3796.
5. Danhier F, Feron, O., & Préat, V. (2010). To exploit, the tumor, microenvironment : passive, and active, tumor, targeting, of nanocarriers, for anti-cancer, drug, delivery. *Journal of Controlled Release Official Journal of the Controlled Release Society, 148*(2), 135-46.
6. Haley, B., & Frenkel, E. (2008). Nanoparticles for drug delivery in cancer treatment. *Urologic Oncology Seminars & Original Investigations, 26*(1), 57-64.
7. Syn, N. L., Teng, M., Mok, T., & Soo, R. A. (2017). De-novo and acquired resistance to immune checkpoint targeting. *Lancet Oncology, 18*(12), e731.
8. Korneev, K. V., Atretkhany, K. N., Drutskaya, M. S., Grivennikov, S. I., Kuprash, D. V., & Nedospasov, S. A. (2017). Tlr-signaling and proinflammatory cytokines as drivers of tumorigenesis. *Cytokine, 89*, 127.

9. Woof, J. M., & Burton, D. R. (2004). Human antibody-fc receptor interactions illuminated by crystal structures. *Nature Reviews Immunology, 4*(2), 89-99.

10. Natsume, A., Niwa, R., & Satoh, M. (2009). Improving effector functions of antibodies for cancer treatment: enhancing adcc and cdc. *Drug Design Development & Therapy, 3*(3), 7-16.

11. Strome, S. E., Sausville, E. A., & Mann, D. (2007). A mechanistic perspective of monoclonal antibodies in cancer therapy beyond target-related effects. *Oncologist, 12*(9), 1084-95.

12. Fagarasan, S., & Honjo, T. (2003). Intestinal iga synthesis: regulation of front-line body defences. *Nature Reviews Immunology, 3*(1), 63.

13. Brandtzaeg, P., & Pabst, R. (2004). Let's go mucosal: communication on slippery ground. *Trends in Immunology, 25*(11), 570.

14. Macpherson, A. J., & Slack, E. (2007). The functional interactions of commensal bacteria with intestinal secretory iga. *Current Opinion in Gastroenterology, 23*(6), 673.

15. Jr, R. G., Rowe, D. S., Bradley, J., Waldmann, T. A., & Fahey, J. L. (1966). Metabolism of human immunoglobulin d (igd). *Journal of Clinical Investigation, 45*(9), 1467.

16. Geysen, H. M., Tainer, J. A., Rodda, S. J., Mason, T. J., Alexander, H., & Getzoff, E. D., et al. (1987). Chemistry of antibody binding to a protein.*Science, 235*(4793), 1184.

17. Klaus J. Erb. (2007). Helminths, allergic disorders and ige-mediated immune responses: where do we stand?. *European Journal of Immunology, 37*(5), 1170-3.

18. Fitzsimmons, C. M., Mcbeath, R., Joseph, S., Jones, F. M., Walter, K., & Hoffmann, K. F., et al. (2007). Factors affecting human ige and igg responses to allergen-like schistosoma mansoni antigens: molecular structure and patterns of in vivo exposure. *International Archives of Allergy & Immunology, 142*(1), 40.

19. Watanabe, N., Bruschi, F., & Korenaga, M. (2005). Ige: a question of protective immunity in trichinella spiralis infection. *Trends in Parasitology,21*(4), 175-8.

20. Pfister, K., Turner, K., Currie, A., Hall, E., & Jarrett, E. E. (1983). Ige production in rat fascioliasis. *Parasite Immunology, 5*(6), 587-593.

21. Koshland, D. E. (1958). Application of a theory of enzyme specificity to protein synthesis. *Proceedings of the National Academy of Sciences of the United States of America, 44*(2), 98.

22. Mifflin, H. (2000). *The American Heritage Dictionary of the English Language*. Houghton Mifflin.

23. Alberts, B.; Johnson, A.; Lewis, J.; Walter, P.; Raff, M.; Roberts, K. (2002). Molecular biology of the cell (4th ed). *Journal of Biological Education*, 45-47.

24. Lei, Z., & Gang, R. (2012). Ipet and fetr: experimental approach for studying molecular structure dynamics by cryo-electron tomography of a single-molecule structure. *Plos One, 7*(1), e30249.

25. Junqueira, L. C. U., & Carneiro, J. (2005). *Basic histology : text & atlas*. Lange Medical Books / McGraw-Hill.

26. Oda, M., Kozono, H., Morii, H., & Azuma, T. (2003). Evidence of allosteric conformational changes in the antibody constant region upon antigen binding. *International Immunology, 15*(3), 417.

27. Getzoff, E. D., Tainer, J. A., Lerner, R. A., & Geysen, H. M. (1988). The chemistry and mechanism of antibody binding to protein antigens.*Advances in Immunology, 43*(43), 1.

28. Goldberg, R. J. (2002). A theory of antibody—antigen reactions. i. theory for reactions of multivalent antigen with bivalent and univalent antibody2. *Journal of the American Chemical Society, 74*(22), 5715-5725.

29. Sahimi, & Muhammad. (1994). *Applications of percolation theory*. Taylor & Francis.

30. Spiers, J. A. (1958). Goldberg's theory of antigen-antibody reactions in vitro. *Immunology, 1*(2), 89-102.

31. Nezlin, R., & Ghetie, V. (2004). Interactions of immunoglobulins outside the antigen-combining site. *Advances in Immunology, 82*, 155.

32. Sagawa, T., Oda, M., Morii, H., Takizawa, H., Kozono, H., & Azuma, T. (2005). Conformational changes in the antibody constant domains upon hapten-binding. *Molecular Immunology, 42*(1), 9-18.

33. Manivel, V., Sahoo, N. C., Salunke, D. M., & Rao, K. V. S. (2000). Maturation of an antibody response is governed by modulations in flexibility of the antigen-combining site. *Immunity, 13*(5), 611.

34. James, L. C., & Tawfik, D. S. (2003). The specificity of cross-reactivity: promiscuous antibody binding involves specific hydrogen bonds rather than nonspecific hydrophobic stickiness. *Protein Science, 12*(10), 2183.

35. Lo, C. L., Chothia, C., & Janin, J. (1990). The atomic structure of protein-protein recognition sites. *Journal of Biological Chemistry, 265*(27), 16027.

36. Bogan, A. A., & Thorn, K. S. (1998). Anatomy of hot spots in protein interfaces. *Journal of Molecular Biology, 280*(1), 1.

37. Veronique Chitarra, Pedro M. Alzari, Graham A. Bentley, T. Narayana Bhat, Jean-Luc Eisele, & Anne Houdusse. (1993). Three-dimensional structure of a heteroclitic antigen-antibody cross- reaction complex.*Proceedings of the National Academy of Sciences of the United States of America, 90*(16), 7711-5.

38. Harmsen, M. M., & Haard, H. J. D. (2007). Properties, production, and applications of camelid single-domain antibody fragments. *Applied Microbiology & Biotechnology, 77*(1), 13-22.

39. Chothia, C., Lesk, A. M., Tramontano, A., Levitt, M., Smith-Gill, S. J., & Air, G., et al. (1989). Conformations of immunoglobulin hypervariable regions. *Nature, 342*(6252), 877-883.

40. Jones, S., & Thornton, J. M. (1996). Principles of protein-protein interactions. *Proceedings of the National Academy of Sciences of the United States of America, 93*(1), 13-20.

41. 4Th, T. J., Thomas, L. K., & Richeson, N. A. (2010). University of south carolina school of medicine. *Academic Medicine Journal of the Association of American Medical Colleges, 85*(9 Suppl), S528.

42. Von, B. E., & Kitasato, S. (1991). The mechanism of diphtheria immunity and tetanus immunity in animals. *Molecular Immunology, 28*(12), 1319-20.

43. Stabsarzt, B. V., & Kutasati. (1991). Ueber das zustandekommen der diphtherie-immunität und der tetanus-immunität bei thieren ☆. *Molecular Immunology, 28*(12), 1319-1320.

44. Piro, A., Tagarelli, A. G., Lagonia, P., & Quattrone, A. (2008). Paul ehrlich: the nobel prize in physiology or medicine 1908. *International Reviews of Immunology, 27*(1-2), 1-17.

45. Fischer, E. (2010). Einfluss der configuration auf die wirkung der enzyme.*European Journal of Inorganic Chemistry, 27*(3), 2985-2993.

46. Lemieux, R. U., & Spohr, U. (1994). How emil fischer was led to the lock and key concept for enzyme specificity 1. *Advances in Carbohydrate Chemistry & Biochemistry, 50*, 1.

47. Burnet, F. M. (1976). A modification of jerne's theory of antibody production using the concept of clonal selection. *Ca A Cancer Journal for Clinicians, 26*(2), 119-121.

48. Pauling, L. (1940). A theory of the structure and process of formation of antibodies. *Journal of the American Chemical Society, 62*(10), 2643–2657.

49. Porter, R. R. (1959). The hydrolysis of rabbit y-globulin and antibodies with crystalline papain. *Biochemical Journal, 73*(73), 119.

50. Edelman, G. M., Benacerraf, B., Ovary, Z., & Poulik, M. D. (1961). Structural differences among antibodies of different specificities.*Proceedings of the National Academy of Sciences of the United States of America, 47*(11), 1751-1758.

51. Peterson, P. A. (1972). 1972 nobel prize in physiology or medicine. the chemical structure of antibodies. *Lkartidningen, 69*(44), 5069-73.

52. Dan, I., Hochman, J., & Givol, D. (1972). Localization of antibody-combining sites within the variable portions of heavy and light chains.*Proceedings of the National Academy of Sciences of the United States of America, 69*(9), 2659.

53. Köhler, G., & Milstein, C. (1975). Continuous cultures of fused cells secreting antibody of predefined specificity. 1975. *Biotechnology,24*(5517), 524.

54. Binnie, C., Cossar, J. D., & Stewart, D. I. (1997). Heterologous biopharmaceutical protein expression in streptomyces. *Trends in Biotechnology, 15*(8), 315-320.

55. Horwitz, A. H., Chang, C. P., Better, M., Hellstrom, K. E., & Robinson, R. R. (1988). Secretion of functional antibody and fab fragment from yeast cells. *Proceedings of the National Academy of Sciences of the United States of America, 85*(22), 8678-82.

56. Ridder, R., Schmitz, R., Legay, F., & Gram, H. (1995). Generation of rabbit monoclonal antibody fragments from a combinatorial phage display library and their production in the yeast pichia pastoris. *Bio/technology,13*(3), 255.

57. Werner, R. G. (1998). Innovative and economic potential of mammalian cell culture. *Arzneimittel-Forschung, 48*(4), 423.

58. DeYoung, G., (1996) Monoclonal ab processors manufacturers stress costs and productivity. *Genetic Engineering News, 16*(5): p. 8-&.

59. Lipman, N. S., Jackson, L. R., Trudel, L. J., & Weisgarcia, F. (2005). Monoclonal versus polyclonal antibodies: distinguishing characteristics, applications, and information resources. *Ilar Journal, 46*(3), 258.

60. Kleinschmidt-Demasters, B. K. (1997). Immunohistochemistry of Pituitary Adenomas. *Diseases of the Pituitary*. Humana Press.

61. Hansel, T. T., Kropshofer, H., Singer, T., Mitchell, J. A., & George, A. J. (2010). The safety and side effects of monoclonal antibodies. *Nature Reviews Drug Discovery, 9*(4), 325-38.

62. Swartz, M. A. (2001). The physiology of the lymphatic system. *Advanced Drug Delivery Reviews, 50*(1), 3-20.

63. Baselga, J., Norton, L., Albanell, J., Kim, Y. M., & Mendelsohn, J. (1998). Recombinant humanized anti-her2 antibody (herceptin) enhances the antitumor activity of paclitaxel and doxorubicin against her2/neu overexpressing human breast cancer xenografts. Cancer Research,58(13), 2825-31.

64. Diehnelt, C. W., Shah, M., Gupta, N., Belcher, P. E., Greving, M. P., & Stafford, P., et al. (2010). Discovery of high-affinity protein binding ligands – backwards. *Plos One, 5*(5), e10728.

65. Holliger, P., & Hudson, P. J. (2005). Engineered antibody fragments and the rise of single domains. *Nature Biotechnology, 23*(9), 1126-36.

66. Bird, R. E., Hardman, K. D., Jacobson, J. W., Johnson, S., Kaufman, B. M., & Lee, S. M., et al. (1988). Single-chain antigen-binding proteins.*Science, 242*(4877), 423-426.

67. Colcher, D., Bird, R., Roselli, M., Hardman, K. D., Johnson, S., & Pope, S., et al. (1990). In vivo tumor targeting of a recombinant single-chain antigen-binding protein. *J Natl Cancer Inst, 82*(14), 1191-1197.

68. Milenic, D. E., Yokota, T., Filpula, D. R., Finkelman, M. A., Dodd, S. W., & Wood, J. F., et al. (1991). Construction, binding properties, metabolism, and tumor targeting of a single-chain fv derived from the pancarcinoma monoclonal antibody cc49. *Cancer Research, 51*(1), 6363-71.

69. Adams, G. P., Mccartney, J. E., Tai, M. S., Oppermann, H., Huston, J. S., & Bookman, M. A., et al. (1993). Highly specific in vivo tumor targeting by monovalent and divalent forms of 741f8 anti-c-erbb-2 single-chain fv. *Cancer Research, 53*(17), 4026-4034.

70. Huston, J. S., Mudgett-Hunter, M., Tai, M. S., Mccartney, J., Warren, F., & Haber, E., et al. (1991). Protein engineering of single-chain fv analogs and fusion proteins. *Methods in Enzymology, 203*(1), 46.

71. Mallender, W. D., & Jr, V. E. (1994). Construction, expression, and activity of a bivalent bispecific single-chain antibody. *Journal of Biological Chemistry, 269*(1), 199-206.

72. Cumber, A. J., Ward, E. S., Winter, G., Parnell, G. D., & Wawrzynczak, E. J. (1992). Comparative stabilities in vitro and in vivo of a recombinant mouse antibody fvcys fragment and a bisfvcys conjugate. *Journal of Immunology, 149*(1), 120-6.

73. Kipriyanov, S. M., Dübel, S. ,., Breitling, F. ,., Kontermann, R. E., & Little, M. ,. (1994). Recombinant single-chain fv fragments carrying c-terminal cysteine residues: production of bivalent and biotinylated miniantibodies. *Molecular Immunology, 31*(14), 1047-58.

74. Ahmad, Z. A., Yeap, S. K., Ali, A. M., Ho, W. Y., Alitheen, N. B. M., & Hamid, M. (2012). Scfv antibody: principles and clinical application.*Clinical & Developmental Immunology, 2012*(8), 980250.

75. Huston, J. S., Levinson, D., Mudgett-Hunter, M., Tai, M. S., Novotný, J., & Margolies, M. N., et al. (1988). Protein engineering of antibody binding sites: recovery of specific activity in an anti-digoxin single-chain fv analogue produced in escherichia coli. *Proceedings of the National Academy of Sciences of the United States of America, 85*(16), 5879-83.

76. Chaudhary, V. K., Batra, J. K., Gallo, M. G., Willingham, M. C., Fitzgerald, D. J., & Pastan, I. (1990). A rapid method of cloning functional variable-region antibody genes in escherichia coli as single-chain immunotoxins. *Proceedings of*

the National Academy of Sciences of the United States of America, 87(3), 1066-70.

77. Deng, X. K., Nesbit, L. A., & Jr, K. J. M. (2003). Recombinant single-chain variable fragment antibodies directed against clostridium difficile toxin b produced by use of an optimized phage display system. *Clinical & Diagnostic Laboratory Immunology, 10*(4), 587.

78. Clackson, T., Hoogenboom, H. R., Griffiths, A. D., & Winter, G. (1991). Making antibody fragments using phage display libraries. *Nature,352*(6336), 624.

79. Finlay, W. J. J., Shaw, I., Reilly, J. P., & Kane, M. (2006). Generation of high-affinity chicken single-chain fv antibody fragments for measurement of the pseudonitzschia pungens, toxin domoic acid. *Applied & Environmental Microbiology*, *72*(5), 3343-9.

80. Shadidi, M., & Sioud, M. (2001). An anti-leukemic single chain fv antibody selected from a synthetic human phage antibody library.*Biochem Biophys Res Commun, 280*(2), 548-552.

81. Zhang, J. L., Guo, J. J., Zhang, Z. Y., Jing, Y. X., Zhang, L., & Guo, R., et al. (2006). Screening and evaluation of human single-chain fragment variable antibody against hepatitis b virus surface antigen. *Hepatobiliary Pancreat Dis Int 5*(2), 237-241.

82. Raag, R., & Whitlow, M. (1995). Single-chain fvs. *Faseb Journal, 9*(1), 73-80.

83. Tanaka, T., Hasegawa, Y., Saito, M., Ikeda, M., & Kato, N. (2010). Generation of single-chain fvs against detergent-solubilized recombinant antigens with a simple coating procedure. *Journal of Bioscience & Bioengineering, 110*(3), 374.

84. Fan, E., Zhang, Z., Minke, W. E., Zheng, H., & Hol†, W. G. J. (2000). High-affinity pentavalent ligands of escherichia coli heat-labile enterotoxin by modular structure-based design. *Journal of the American Chemical Society, 122*(11), 2663-2664.

85. Koide, A., Abbatiello, S., Rothgery, L., & Koide, S. (2002). Probing protein conformational changes in living cells by using designer binding proteins: application to the estrogen receptor. *Proceedings of the National Academy of Sciences of the United States of America, 99*(3), 1253.

86. Xu, L., Aha, P., Gu, K., Kuimelis, R. G., Kurz, M., & Lam, T., et al. (2002). Directed evolution of high-affinity antibody mimics using mrna display: chemistry & biology. *Chemistry & Biology, 9*(8), 933.

87. Koivunen, E., Arap, W., Rajotte, D., Lahdenranta, J., & Pasqualini, R. (1999). Identification of receptor ligands with phage display peptide libraries. *Journal of Nuclear Medicine Official Publication Society of Nuclear Medicine, 40*(5), 883-8.

88. Gupta, N., Belcher, P. E., Johnston, S. A., & Diehnelt, C. W. (2011). Engineering a synthetic ligand for tumor necrosis factor-alpha.*Bioconjugate Chemistry, 22*(8), 1473.

89. Wang, H., Wang, L., Wang, Y., Jiang, K., & Li, C., et al. (2011). High-affinity peptide against mt1-mmp for in vivo tumor imaging. *Journal of Controlled Release Official Journal of the Controlled Release Society,150*(3), 248.

90. Pasqualini, R., Koivunen, E., & Ruoslahti, E. (1997). Alpha v integrins as receptors for tumor targeting by circulating ligands. *Nature Biotechnology, 15*(6), 542.

91. Williams, B. A., Diehnelt, C. W., Belcher, P., Greving, M., Woodbury, N. W., & Johnston, S. A., et al. (2009). Creating protein affinity reagents by combining peptide ligands on synthetic dna scaffolds. *Journal of the American Chemical Society, 131*(47), 17233-41.

92. Balhorn, R., Hok, S., Burke, P. A., Lightstone, F. C., Cosman, M., & Zemla, A., et al. (2007). Selective high-affinity ligand antibody mimics for cancer diagnosis and therapy: initial application to lymphoma/leukemia.*Clinical Cancer Research An Official Journal of the American Association for Cancer Research, 13*(2), 5621s.

93. Dong, H., Zhu, G., Tamada, K., & Chen, L. (1999). B7-h1, a third member of the b7 family, co-stimulates t-cell proliferation and interleukin-10 secretion. *Nature Medicine, 5*(12), 1365.

94. Chemnitz, J. M., Parry, R. V., Nichols, K. E., June, C. H., & Riley, J. L. (2004). Shp-1 and shp-2 associate with immunoreceptor tyrosine-based switch motif of programmed death 1 upon primary human t cell stimulation, but only receptor ligation prevents t cell activation. *Journal of Immunology, 173*(2), 945-954.

95. Dong, H., Strome, S. E., Salomao, D. R., Tamura, H., Hirano, F., & Flies, D. B., et al. (2002). Tumor-associated b7-h1 promotes t-cell apoptosis: a potential mechanism of immune evasion. *Nature Medicine,8*(8), 793-800.

96. Said, E. A., Dupuy, F. P., Trautmann, L., Zhang, Y., Shi, Y., & Elfar, M., et al. (2010). Programmed death-1-induced interleukin-10 production by monocytes impairs cd4+ t cell activation during hiv infection. *Nature Medicine, 16*(4), 452.

97. Herbst, R. S., Soria, J. C., Kowanetz, M., Fine, G. D., Hamid, O., & Gordon, M. S., et al. (2014). Predictive correlates of response to the anti-pd-l1 antibody mpdl3280a in cancer patients. *Nature, 515*(7528), 563.

98. Velcheti, V., Schalper, K. A., Carvajal, D. E., Anagnostou, V. K., Syrigos, K. N., & Sznol, M., et al. (2014). Programmed death ligand-1 expression in non-small cell lung cancer. *Laboratory investigation; a journal of technical methods and pathology, 94*(1), 107.

99. Brahmer, J. R., & Pardoll, D. M. (2013). Immune checkpoint inhibitors: making immunotherapy a reality for the treatment of lung cancer. *Cancer Immunology Research, 1*(2), 85.

100. Chen, L., & Han, X. (2015). Anti–pd-1/pd-l1 therapy of human cancer: past, present, and future. *Journal of Clinical Investigation, 125*(9), 3384.

101. Elbakri, A., Nelson, P. N., & Abu Odeh, R. O. (2010). The state of antibody therapy. *Human Immunology, 71*(12), 1243.

102. Vanhee, P., Am, V. D. S., Verschueren, E., Serrano, L., Rousseau, F., & Schymkowitz, J. (2011). Computational design of peptide ligands. *Trends in Biotechnology, 29*(5), 231-9.

103. Watt, P. M. (2006). Screening for peptide drugs from the natural repertoire of biodiverse protein folds. *Nature Biotechnology, 24*(2), 177-83.

104. Joo, H., Chavan, A. G., Phan, J., Day, R., & Tsai, J. (2012). An amino acid packing code for α-helical structure and protein design. *Journal of Molecular Biology, 419*(3–4), 234-254.

105. Fellouse, F. A., Barthelemy, P. A., Kelley, R. F., & Sidhu, S. S. (2006). Tyrosine plays a dominant functional role in the paratope of a synthetic antibody derived from a four amino acid code. *Journal of Molecular Biology, 357*(1), 100-114.

106. Amblard, M., Fehrentz, J. A., Martinez, J., & Subra, G. (2005). Fundamentals of modern peptide synthesis. *Cheminform, 298*(10), 3.

107. Isidrollobet, A., Álvarez, M., & Albericio, F. (2009). Amino acid-protecting groups. *Chemical Reviews, 109*(6), 2455-504.

108. Kaiser, E., Colescott, R. L., Bossinger, C. D., & Cook, P. I. (1970). Color test for detection of free terminal amino groups in the solid-phase synthesis of peptides. *Analytical Biochemistry, 34*(2), 595.

109. R. B. Merrifield. (1963). Solid phase peptide synthesis. i. the synthesis of a tetrapeptide. *Journal of the American Chemical Society, 85*(14).

110. Wang, S. S. (1973). Alkoxybenzyl alcohol resin and p-alkoxybenzyloxycarbonylhydrazide resin for solid phase synthesis of protected

peptide fragments. j am chem soc. *Journal of the American Chemical Society, 95*(4), 1328-1333.

111. Fields, G. B., & Noble, R. L. (1990). Solid phase peptide synthesis utilizing 9-fluorenylmethoxycarbonyl amino acids. *Chemical Biology & Drug Design, 35*(3), 161-214.

112. Gan, S. D., & Patel, K. R. (2013). Enzyme immunoassay and enzyme-linked immunosorbent assay. *Journal of Investigative Dermatology,133*(9), E10-E12.

113. Guo, H., Hathaway, H., Royce, M. E., Prossnitz, E. R., & Miao, Y. (2013). Influences of hydrocarbon linkers on the receptor binding affinities of gonadotropin-releasing hormone peptides. *Bioorganic & Medicinal Chemistry Letters, 23*(20), 5484-5487.

114. Nass, N., & Kalinski, T. (2015). Tamoxifen resistance: from cell culture experiments towards novel biomarkers. *Pathology Research & Practice,211*(3), 189.

115. Stadler, C., Hjelmare, M., Neumann, B., Jonasson, K., & Pepperkok, R., et al. (2012). Systematic validation of antibody binding and protein subcellular localization using sirna and confocal microscopy.*Journal of Proteomics, 75*(7), 2236-2251.

116. Cullen, D. C., Brown, R. G., & Lowe, C. R. (1987). Detection of immuno-complex formation via surface plasmon resonance on gold-coated diffraction gratings. *Biosensors, 3*(4), 211-225.

117. Place, J. F., Sutherland, R. M., & Dähne, C. (1985). Opto-electronic immunosensors: a review of optical immunoassay at continuous surfaces. *Biosensors, 1*(4), 321-353.

118. David, A., & Paula, G. (2002). Binding of small peptides to immobilized antibodies: kinetic analysis by surface plasmon resonance. *Current protocols in immunology / edited by John E. Coligan. [et al.], Chapter 18*(1), Unit 18.9.

119. Madeira, A., Vikeved, E., Nilsson, A., Sjögren, B., Andrén, P. E., & Svenningsson, P. (2011). *Identification of protein-protein interactions by surface plasmon resonance followed by mass spectrometry*. *Current Protocols in Protein Science*. John Wiley & Sons, Inc.

120. Beckers, R. K., Selinger, C. I., Vilain, R., Madore, J., Wilmott, J. S., & Harvey, K., et al. (2015). Pdl1 expression in triple-negative breast cancer is associated with tumour-infiltrating lymphocytes and improved outcome. *Histopathology, 48*(1), S146-S147.